ISTANBUL TECHNICAL UNIVERSITY ★ GRADUATE SCHOOL OF SCIENCE ENGINEERING AND TECHNOLOGY

PRODUCTION AND CHARACTERISATION OF BOND COAT ON NICKEL BASED SUPERALLOY

M.Sc. THESIS

Selda NAYİR

Department of Metallurgical and Materials Engineering

Materials Engineering Programme

Thesis Advisor: Associated Prof. Dr. Murat Baydoğan

DECEMBER, 2014

ISTANBUL TECHNICAL UNIVERSITY ★ GRADUATE SCHOOL OF SCIENCE ENGINEERING AND TECHNOLOGY

PRODUCTION AND CHARACTERISATION OF BOND COAT ON NICKEL BASED SUPERALLOY

M.Sc. THESIS

Selda NAYİR
(506101444)

Department of Metallurgical and Materials Engineering

Materials Engineering Programme

Thesis Advisor: Assoc. Prof. Dr. Murat Baydoğan

DECEMBER, 2014

İSTANBUL TEKNİK ÜNİVERSİTESİ ★ FEN BİLİMLERİ ENSTİTÜSÜ

NİKEL ESASLI SÜPERALAŞIM ÜZERİNDE BAĞ KAPLAMASININ OLUŞTURULMASI VE KARAKTERİZASYONU

YÜKSEK LİSANS TEZİ

Selda NAYİR
(506101444)

Metalurji ve Malzeme Mühendisliği Anabilim Dalı

Malzeme Mühendisliği Programı

Tez Danışmanı: Doç. Dr. Murat Baydoğan

ARALIK, 2014

Selda NAYİR, a **M.Sc.** student of ITU **Institute of Science and Technology** student ID **506101444**, successfully defended the **thesis** entitled "**PRODUCTION AND CHARACTERISATION OF BOND COAT ON NICKEL BASED SUPERALLOY** which she prepared after fulfilling the requirements specified in the associated legislations, before the jury whose signatures are below.

Thesis Advisor :	**Assoc. Prof. Dr. Murat Baydogan** İstanbul Technical University	.....
Jury Members :	**Prof. Dr. Huseyin CIMENOGLU** İstanbul Technical University	.....
	Prof. Dr. Ziya Engin ERKMEN Marmara University	.....

Date of Submission : 15 December 2014
Date of Defense : 22 January 2015

To my family,

FOREWORD

I would like to thank Assoc. Prof. Dr. Murat Baydogan and Prof. Dr. Huseyin CIMENOGLU for encouragement, guidance and councelling to achieve to complete my studies and this thesis work. I would also like to thank to Istanbul Technical University Res. Assist. Onur TAZGUL and Faiz MUHAFFEL for helping and guidance to carry out my laboratory studies and my thesis.
Other important persons, considering my thesis term, senior Materials engineers Nilufer Metin and other friends whom I like to give my special thanks for their valuable friendship and support when needed.
Finally, I would like to express my special appreciation to my familiy for their continued support, endless encouragement, and patience.

December 2014

Selda NAYİR
(Materials Engineer)

TABLE OF CONTENTS

Page

ABBREVIATION

IGT **:** Industrial Gas Turbine
DS **:** Directionally solidified
SX **:** Single crystal
PH **:** Precipitation Hardened
ODS **:** Oxide dispersion strengthening
IN718 : Inconel 718
IN713 **:** Inconel 713
IN706 **:** Inconel 706
IN909 **:** Inconel 909
IN625 **:** Inconel 625
U700 **:** Udimet 700
U720 **:** Udimet 720
TCP **:** Topologically closed packed
TBC **:** Thermal Barrier Coating
BC **:** Bond coating
TGO **:** Thermally grown oxide
$\mathbf{D_{Ni}}$ **:** Nickel diffusivity
$\mathbf{D_{Al}}$ **:** Aluminum diffusivity
CVD **:** Chemical Vapor Deposition
CGDS **:** Cold Gas Dynamic Spray
HVOF **:** High Velocity Oxygen Fuel
LPPS **:** Low Pressure Plasma Spray

LIST OF TABLES

Page

LIST OF FIGURES

Page

PRODUCTION AND CHARACTERISATION OF BOND COAT ON NICKEL BASED SUPERALLOY

SUMMARY

The gas turbine produced energy is directly related the operating temperature therefore higher operating temperatures is required for energy production. The requirements need higher temperature capability materials and associated technologies such as improved oxidation and environmental coatings. Therefore, for elevated temperature application, Nickel-base superalloys are the best choice and they have become the standard for industrial gas turbines hot gas path components such as buckets, nozzles, and shrouds.

Even though the base material provide great features for this kind of application the component has surface damage caused by oxidation and hot corrosions shortened the service life. Therefore, the blade protection is essential, and the solutions lead the protective coating layer of the turbine blades.

For protection of the hot gas path component and better working condition of turbine, the coating must meet the engine operating condition requirements. It must withstand hot corrosion, oxidation, and erosion and static and alternate stresses applied to the blade surface; to this end the coating must have the requisite combination of strength and ductility. Besides, it must show good stability and not degrade the blade material mechanical properties.

In the light of previous information, the thesis focus on the production of aluminide coating on the nickel based superalloys, Inconel 718 (IN718) by cold gas dynamic spray coating method. The method is promising technique because its working temperature relatively low when compares with the thermal barrier coatings methods.

The main action of the study is examining the diffusion behavior of cold sprayed aluminum, nickel and other constituent elements of superalloy and understanding the formation of diffusion zones. Accordingly, some part of the specimens is coated only with unalloyed aluminum and remaining parts are coated with unalloyed aluminum and nickel separate steps (First Al is coated on substrate than Ni is coted on Al surface). In both sample groups, Al activity is higher than Ni (Al diffusion rate higher than Ni-$D_{Al}>D_{Ni}$), because of being in elemental state. Especially, only Al coated and annealed at higher temperature (700°C, 850°C, 900°C for 24h- 950°C, and 1000°C, 1050°C for 1 h) samples clearly show three layered coatings and roughly name of these layers are, from surface to substrate, refractory element precipitates, NiAl, and Carbide layers. The multilayered coating is also called as "inward diffusion coatings" because of the high diffusion rate of Al than Ni ($D_{Al}>D_{Ni}$).

The samples that are coated only Al and annealed at 500°C, 600°C for 24h, represent the basic formation of Al_3Ni and Al_3Ni_2 intermetallic that are the production of first

interaction of Al and Ni below the 640°C (Melting temperature of Al). Moreover,this is a result of predominant inward diffusion of aluminum from the aluminum layer, which causes the coating layer to grow into the substrate starting from its surface.

The standard three layered (multilayered) structure is formed at specimens that are annealed at 700°C, 850°C, 900°C, 950°C, 1000°C,1050°C. The first zone of the multilayer is outer zone that includes refractory elements precipitates (α-Cr, Fe) in the AlNi matrix and that is formed by dominant diffusion of Al (inward diffusion) throughout to the substrate. In addition, AlNi phase is hyper stoichiometric (NiAl containing greater than 50 Al %at.). Second zone (middle zone) is formed by both inward and outward diffusion of Al and Ni that creates uniform AlNi phases (hypo stoichiometric AlNi- Al <50 % at.). Finally, third zone, created by only outward diffusion of Ni and the reduction of Ni in this region causes the precipitation of the various elements originally present in solid solution in the superalloy in the form of several complex precipitates. These are some carbides (MC, M23C6) and refractor elements' phases (σ-Cr, Fe). Consequently, higher activity of Al leads to the complex structure of multilayered coating and at each layer, different diffusion.

Aluminum has very high activity and content in the first zone. It causes the lack of sufficient solubility of certain substrate elements like Cr, Ti, Mo in the zone.

In the scope of the thesis, outwardly diffused microstructre can not be produced due to the high activity of aluminum. On the other hand, the second and third zone could be given as an example for that kind of structure.

The different annealing time and temperature (700°C, 850°C, 900°C, 950°C, 1000°C,1050°C) do not make any change in the microstructure except distinct thickness for the zones

The first and third zones are mechanically weak and brittle due to the formation of refractory precipitates and carbides; they should be eliminated from the coating by additional processes or changing the composition of coating powders.

The both aluminum and nickel coated samples are annealed at 850°C, 900°C for 24h, 950°C, 1000°C, and 1050°C for 1h. The similar three-layered structure is observed between aluminum-substrate, and aluminum–nickel. However, in the middle zone, porous and cracked type area is produced. The structure is formed due to high activity of aluminum, because aluminum is completely consumed before creating a diffusional bond between substrate-aluminum and aluminum-nickel. Therefore,nickel coating on the aluminum does not meet the requirement of diffusional coating.

The diffusion activities of elements and created phases are supported by characterization test results of X-ray diffraction (XRD), scanning electron microscope (SEM), and energy dispersive spectroscopy (EDS)

The Al coated samples are subjected to hardness test to measure the hardness of each zone. According to results, the first and third zone value is highest because of refractory precipitates and carbides.

NİKEL ESASLI SÜPERALAŞIM ÜZERİNDE BAĞ KAPLAMASININ OLUŞTURULMASI VE KARAKTERİZASYONU

ÖZET

Gaz türbinleri, teknolojinin birçok alanında, enerji üretiminde kullanılmak üzere tasarlanmış ve enerji ihtiyacıyla doğru orantılı olarak gelişimleri devam etmiştir. Türbin içerisindeki çalışma ortam sıcaklığının günden güne artırılması ve aşındırıcı atmosfer, bu ortamda çalışabilecek, dayanıklı bıçak ve kaplamalara olan gereksinimini de artırmaktadır. Bu sebeple gaz türbinlerinde kaydedilecek yeni teknolojik gelişmeler, bu türbinlerin önemli parçaları olan bıçak, kanatçık (vane) gibi elemanlarında yapılacak olan gelişmelere birebir bağlıdır.

Türbin motoru içerisine beslenen gaz, türbin disklerinin daha hızlı dönmesini dolayısıyla uçak üzerinde itme gücü (thrust) oluşmasını sağlar. Beslenen gaz sebebiyle türbin parçalarının yüksek sıcaklık (1090°C'yi aşan sıcaklıklar) ve basınca maruz kalır ve bu elemanlar üzerinde erozyon, oksidasyon, korozyon ve termal yorulma çatlakları gibi hasarlara yol açıp parçaların servis sürelerinin kısalmasına neden olur. Bu aşındırıcı etkilerden parçaları korumak için çevreye-dirençli kaplamalar (environment-resistant coating) ve termal bariyer kaplamalar kullanılır.

Yüzey kaplamalarında üzerinde yapılan çalışmalar sonucu, yüksek oksidasyon direnci, nikel esaslı süper alaşımlara uygulandığında kararlı bir yapı sergilemesi ve diğer mekanik ve fiziksel özellikleri sebebiyle difüzyon alüminat (aluminides) kaplamalar en çok tercih edilen kaplama tipi olmuştur. Aluminat difüzyon kaplamaları, türbinin sıcak bölümlerinde kullanılan nikel esaslı olan bıçakların yüzeylerinde kullanılıp yüksek sıcaklıkta meydana gelen oksidasyon ve korozyona karşı bıçakları korurlar. Bu kaplamalar, yüksek sıcaklıklarda (900°C'nin üstünde) koruyucu ve yavaş yavaş büyüyen oksit (Al_2O_3) filmleri oluşturma özelliklerine sahiptirler. Bu sebeple Al_2O_3için bir bakıma rezervuar görevi üstlenirler.

Süperalaşımlar üzerine uygulanan difüzyon aluminat kaplamaları, içe doğru (inward) ve dışa doğru (outward) difüzyon süreçleri sonucu oluşan mikroyapılara göre sınıflandırılmıştır. İçe doğru difüzyon, alüminyum aktivitesinin nikel aktivitesinden daha yüksek olduğu durumlarda meydana gelip alüminyum uygulandığı yüzeyden süperalaşımın içine doğru olan difüzyon hızı, nikelin süperalaşımdan kaplamaya doğru olan hızından daha yüksektir. Alüminyumun yüksek aktivitesi sonucu, en dış yüzeyde kırılgan yapıda δNi_2Al_3 oluşur. Aluminuymun yüksek difüzyonu sırasında bir kısım nikelde difüzyona uğrayarak δNi_2Al_3 hemen altında β-NiAl arametalik (intermetallic) fazı oluşur. Bu tür bir kaplama, hem kırılgan hem de düşük erime sıcaklığına sahip olup, kırılgan δNi2Al3 fazını daha az kırılgan yapıda olan ve alüminyum miktarınca zengin βNiAl (Al >50 at. %) fazına dönüştürmek için ek bir ısıl işleme ihtiyaç vardır.

Dışa doğru difüzyon, alüminyum aktivitesinin nikel aktivitesinden düşük olduğu yüksek sıcaklık işlemlerinde (980-1090°C) gerçekleşir. İçe doğru difüzyonla oluşan kaplama ile karşılaştırıldığında, altlık bünyesinde bulunan refrakter elementler daha yavaş bir şekilde altlıktan kaplamaya doğru difüzyona uğrar ve burada oluşan NiAl fazı içerisinde alüminyum miktarı düşüktür (hypostoichiometry -Al <50 **at.** %). Bu sebeple daha sünek yapıda bir kaplama elde edilir. Bu kaplamanın tipik yapısı, dış kısımda NiAl fazı içeren bir kuşak (zone), altta ise refrakter metallerin (W, Mo, Ta gibi), nikelin oranının azalması nedeniyle oluşturduğu, karbürler ile σ-(Cr,Fe) fazı gibi kırılgan yapılar yer alır.

Difüzyon alüminat kaplamaları geniş bir uygulama alanı yakalamasına rağmen, farklı türdeki türbin bıçağı çalışma koşullarına uyarlanamamaları, her türden bıçağın kompozisyonuna uygun olarak hazırlanabilecek yeni tip kaplamanın zorunluluğunu beraberinde getirmiştir. Elektron-ışın, elektrik-ark plazma metotlarının geliştirilmesi, farklı türdeki bıçaklar üzerine uygulanabilen ve örtü (overlay) tabakaların geliştirilmesini hızlandırmıştır. Difüzyon alüminat kaplamanın aksine örtü kaplama, kompozisyonunu, kalınlığını ve fiziksel-kimyasal- mekanik özelliklerini kontrol edebilen ve motor türlerine göre opsiyonları mevcuttur.

Örtü kaplama, difüzyon kaplamanın modifiye edilmiş bir versiyonu olup, kaplama içerisinde bulunan yüksek alüminyum oranının kırılganlığı artırması sebebiyle, kaplama içerisinde ki alüminyum miktarının düşürülüp daha sünek bir yapıda kaplama oluşturulur. Örtü kaplama, önceden alaşımlandırıldığı için, altlıktan kendisine olacak difüzyona ihtiyaç duymayıp, içindeki alaşımlarla, hem mikroyapısı kontrol edilir hem de altlığa doğru olan difüzyonlarla, altlığa yapışmasını sağlanır.

Termal bariyer kaplamanın (TBC) örtü kaplamaya daha iyi yapışması sağlayıp altlığı oksidasyon ve termal etkilere karşı daha iyi korumak maksadıyla örtü kaplama ve TBC arasına ince bir flaş kaplama (flash coat) uygulaması da yapılabilir.
Örtü kaplamalar yüzeye termal kaplama yöntemleriyle; vakum plasma spray (VPS),düşük basınçlı plazma sprey (LPPS) ya da yüksek hızlı oksy-fuel (HVOF) yöntemleriyle uygulana gelmiştir. VPS ve LPPS yöntemiyle yüzeyde biriktirilen kaplamada bazı erimemiş tanecikler kalabilmektedir. Özellikle HVOF yöntemiyle yapılan kaplamada, önemli miktarda mikro boyutta porozite ve oksitlerin varlığı birbirine bağlı yollar oluşturmaktadır.

Dolayısıyla, yüksek sıcaklık ve oksidasyon uygulamalarında yüksek oksitlenme hızı ve altlığın korozyona uğraması kaçınılmaz hale gelmektedir. Fakat soğuk püskürtme yöntemiyle (cold spray coating), gözenek ve oksit barındırmayan üstün oksidasyon direnci özelliğine sahip kaplamalar geliştirilmektedir.
Soğuk püskürtme yöntemiyle, ince tanecikli yapıdaki tozlar 500-1000m/s, süpersonik inert gaz jetleriyle kaplama yapılacak yüzeye çarparak beslenir. Çarpma sırasında oluşan plastik deformasyon ile atlık ve kapla arasında yoğun ve güçlü bir bağ oluşturulur**.**

Yukarıdaki bilgiler ışığında çalışma konusunun temel amacı, nikel esaslı süperalaşım malzemesi üzerinde soğuk püskürtme yöntemiyle aluminat kaplama oluşturmaktır. Hernekadar, güncel kaplamalar içinde bağ kaplama yönelimi örtü tipi kaplama olmasına rağmen, çalışma esnasında aluminat difüzyon kaplama incelenmiştir.

Çalışma temel olarak, püskürtülen toz tipine göre, iki tip kaplamayı esas almıştır. İlk tip kaplamada sadece aluminyum altlık üzerine püskürtülmüş ve hazırlanan numuneler 500°C, 600°C, 700°C, 850°C ve 900°C'lerde 24 saat, 950°C, 1000°C ve

1050°C ise 1 saat olmak üzere atmosfer kontrolü olmayan fırında, havada, tavlanmıştır. Tavlanan numuneler, gerekli metalografik işlemlere tabi tutulduktan sonra X-ışını difraktometresi ile x-ışını desenleri elde edilmiştir.

İkinci kaplamada ise altlık öncelikle Alüminyumla kaplanıp ardından üzerine Nikel püskürtülmüştür. Bu numuneler ise 850°C ve 900°C'lerde 24 saat, 950°C, 1000°C ve 1050°C ise 1 saat olmak üzere havada tavlanmıştır. Tavlana numunelere benzer şekilde uygun metalografik işlemlerden geçirilip X-ışını difraktometresi ile x-ışını desenleri elde edilmiştir.

İlgili numune grupları, Taramalı Elektron Mikroskobu (SEM) ve Enerji dağınımlı x-ışınları çözümleyicisi (EDS) incelemelerine tabi tutularak elde edilen x-ışını desenleri yorumlanmıştır. Buna göre 500°C ve 600°C'de 24 saat tavlanan numunelere beklendiği üzere, kaplama ile tabaka arasında dıştan içe doğru, Al_3Ni, Al_3Ni_2 tabakaları oluşmuştur. 500°C'de tavlanan numunede alüminyumun tamamen tüketilmediği göze çarpmıştır, 600°C'de ise alüminyumun büyük bir kısmının, oluşan fazlar tarafından tüketildiği fark edilmiştir. Oluşan fazlar ve çalışılan sıcaklık, alüminyumun altlık içine doğru olan difüzyonuna kanıt niteliğindedir.

700°C, 850°C ve 900°C'de 24 saat tavlana numunelerde AlNi fazı kendini, kaplama içerisindeki yoğunluğunu artırarak göstermiştir. Bu sıcaklıklarda oluşturulan kaplamanın en temel özelliği ayırt edilir şekilde üç tabakadan oluşmasıdır. Kaplamanın dış yüzeyinden içe doğru, ilk kuşak Cr, Fe gibi refrakter elementlerinin çökeltilerini (α-Cr,Fe precipitates) içermekte olup matris AlNi yada Al_3Ni_2 fazlarından oluşmaktadır ve bu kuşak alüminyumun içe doğru difüzyonun (inward diffusion) en önemli kanıtıdır. Orta kuşakta ise yekpare AlNi fazı göze çarpmakta olup diğer refrakter elementler katı çözelti içerisinde çözünmüş durumdadır. Bu kuşağın oluşumunda hem alüminyumun içe doğru (inward) hem de Nikelin dışa doğru (outward) difüzyonu söz konusu olduğu için yekpare AlNi fazı elde edilmiştir. En alt kuşak ise Nikelin dışa doğru dizfuzyonu nedeniyle oluştuğu için nikelce fakirdir bu sebeple Nikel içerisinde daha fazla çözünemeyen refrakter elementler (Ti, Nb) karbür (MC, M23C6), diğer elementler ise σ-(Cr, Mo) fazını yaparak mekanik olarak zayıf bir katman oluştururlar.

Bu üç kuşak, enerji dağınımlı x-ışınları çözümleyicisine (EDS) göre incelendiğinde şunlar elde edilmiştir. Alüminyumun aktivitesinin çok yüksek olması sebebiyle alüminyumun difuzyon hızı (D_{Al}) Nikelin hızından (D_{Ni}) daha yüksektir. Bu sebeple atlık içine difüze olurken Cr, Fe gibi bazı elementlerin alfa fazı oluşturarak bu kısımda çökelmesine neden olur. Bunun sebebi ayrıca, Buradaki AlNi fazının alüminyum açısından doygunluk seviyesinde olması ve bu sebeple bu elementleri içinde çözememesidir. Ara kuşağın oluşumunda hem alüminyumun hem de nikelin difüzyonu bunu sağlamaktadır, bu sebeple iç kuşak (alt kuşak) nikelce fakir krom ve diğer elementlerce zengindir. Bu iç kuşakta da nikelin difüzyonu, kromun daha fazla nikel içinde çözünmemesine neden olur ve krom çökelir. Ayrıca bu kısımda, nikelin azalması sebebiyle biriken Titanyum, Niyobyum, Molibden gibi elementler karbür yaparak başka fazlara dönüşür. Bu karbürler ve sigma fazı alt kuşağı, çökelen refrakter elementeler ise üst kuşağı, mekanik olarak zayıf kırılgan yapıya büründürür. Bu tür kuşaklar ise kaplama içerisinde tercih edilmemektedirler.

950°C, 1000°C ve 1050°C ise 1 saat tavlanan numunelerde de kaplama kalınlığının değişmesi dışında, 900°C tavlanan numune ile benzer mikro yapı elde edilmiştir. Bu sıcaklıkların denenmesinin sebebi hem AlNi'yi daha kısa süre oluşturmak hem de

mikro yapıda olması muhtemel değişimleri daha kısa sıcaklık aralıklarında gözlemleyip doğru çıkarımlar elde etmektir.

Alüminyumla kaplanıp ardından üzerine Nikel püskürtülen ver 850°C, 900°C'lerde 24 saat, 950°C, 1000°C ve 1050°C ise 1 saat tavlanan numunelerde, alüminyumla altlık arasında, yukarıdaki numunelerde oluşan benzer üç kuşaklı yapı elde edilmiştir. Nikel ile alüminyum arasında aluminat fazlar oluşmasına rağmen bu iki oluşum arasında (Al-altlık ve Al-Ni) boşluklu ve mekanik olarak zayıf bir bölge meydana gelmiştir. Bunun sebebi, aktivitesi hayli yüksek olan alüminyumun altlık ve nikele doğru hızla giderek arada gerekli bağı oluşturamadan tükenmesi ve belirgin şekilde iki ayrı bölgenin oluşmasıdır. Bu sebeple alüminyum üzerine uygulanan nikel, mekanik özellik açısından uygun bir kaplama türü değildir.

Çalışmanın son uygulaması olarak, kaplama içerisinde oluşan üç kuşaklı yapının sertliklerini belirmek amacıyla sertlik testi uygulanmıştır. Buna göre, üst ve alt kuşakların sertlikleri, içlerinde bulunan refrakter çökeltileri ve karbürler sebebiyle yüksek çıkmıştır.

1 INTRODUCTION

Gas turbines are internal combustion engine that burn gas gaseous and liquid fuel. It delivers the energy of this combustion by means of thrust, in aircraft engine. Moreover, the energy is contributed by rotating shaft that provides electricity via a generator or mechanical power for driving compressors or ship propulsion. [1]

Higher operating temperature of the gas turbine has a primary effect on the amount of energy is produced. Higher operating temperatures need higher temperature capability materials and associated technologies such as improved oxidation and environmental coatings. Nickel base superalloys are the best choice for elevated temperature application and they have become the standard for industrial gas turbines hot gas path components such as buckets, nozzles, and shrouds. [2]

Blade is one of the hot gas path component and has surface damage caused by oxidation and hot corrosions shortened the service life. Therefore, the blade protection is essential. The solution of the surface deterioration is sought during the decades, and solutions lead the protective coating layer of the turbine blades. [3]

Research point out the protective coating and it begins with the diffusion coating has a remarkable properties such as high oxidation resistance, high stability when deposited on nickel superalloys, and favorable combination physical and mechanical features.The coating type is main protective layer for decades. However, new generation engines with increased inlet gas temperatures resulted also shortening the surface life of the coatings due to low ductility of the diffusion coatings and high stress generated in cooled blades. The failure of the diffusion coating make the requirement of new type of protective layer and after evolution of the layer it result in ceramic coating for thermal protection. Under the ceramic layer, metallic coating is applied on the substrate for oxidation and corrosion resistance and they become a standard for hot gas path parts.

The study is mainly related the first coating layer of the blade (metallic bond coat) to investigate the diffusional bond coating behaviors of aluminum and nickel powders

applied by cold gas dynamic spray technique (CGDS) on nickel base superalloys Inconel 718 (IN718). Powder applied samples are heated at different annealing temperature that are higher and lower than the certain temperature 640°C (melting temperature of the aluminum). Furthermore, the diffusional behavior of sample microstructure is examined by X-ray diffractometry (XRD), scanning electron microscope (SEM), and energy dispersive X-ray spectroscopy (EDS). Finally, the hardness test is applied to the samples to measure the hardness of each coating layer.

The litreature part of the study firstly examines the basic properties of gas turbine, blades then go through to superalloys and their important types. After, the most important coatings types and their application techniques will be discussed. The last section will be evaluated prior art studies that are similar to the thesis experiment to make clarify the diffusion mechanism and layers of the coatings.

1.1 Gas Turbine

The gas turbine is a power plant produces a great amount of energy depending on its size and weight. It is an internal combustion engine that burns gaseous or liquid fuel and delivers the energy of this combustion either by means of thrust, in an aircraft jet engine; or by means of a rotating shaft . Turbine provides electricity via a generator, or mechanical power for driving compressors. [4]

The working condition of turbines is very aggressive because of high operating temperature and pressure is created by compression and combustion sections.

Basic sketch of gas turbine engine sections are displayed in Figure 1 and are a compressor section, a combustor section and a turbine section. During operation, air is pressurized in the compressor section and is mixed with fuel and burned in the combustor section to generate hot combustion gases.

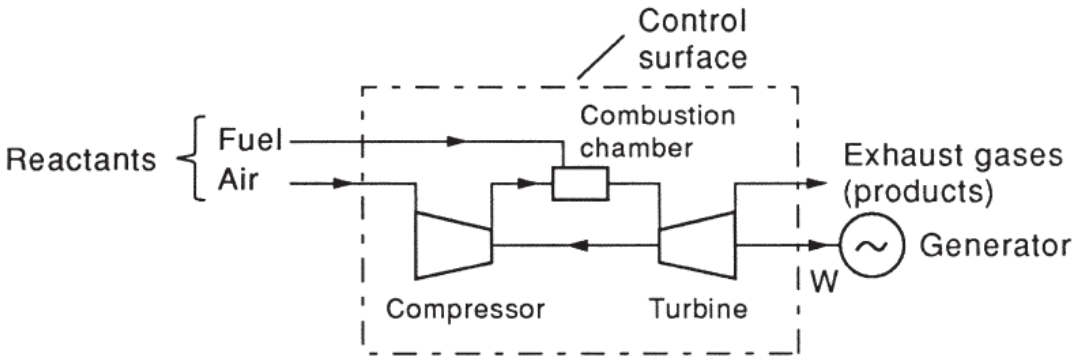

Figure 1.1 : Open circuit gas turbine plant **[5]**

The hot combustion gases are transferred through the turbine section, which extracts energy from the hot combustion gases to power the compressor section and other gas turbine engine loads. [6]

Compressed air is mixed with fuel and ignited to create thrust for propulsion in combustion section. The heated air could lead temperature to 1650°C in the turbine section, and component temperature could well reach 1090°C. [2]

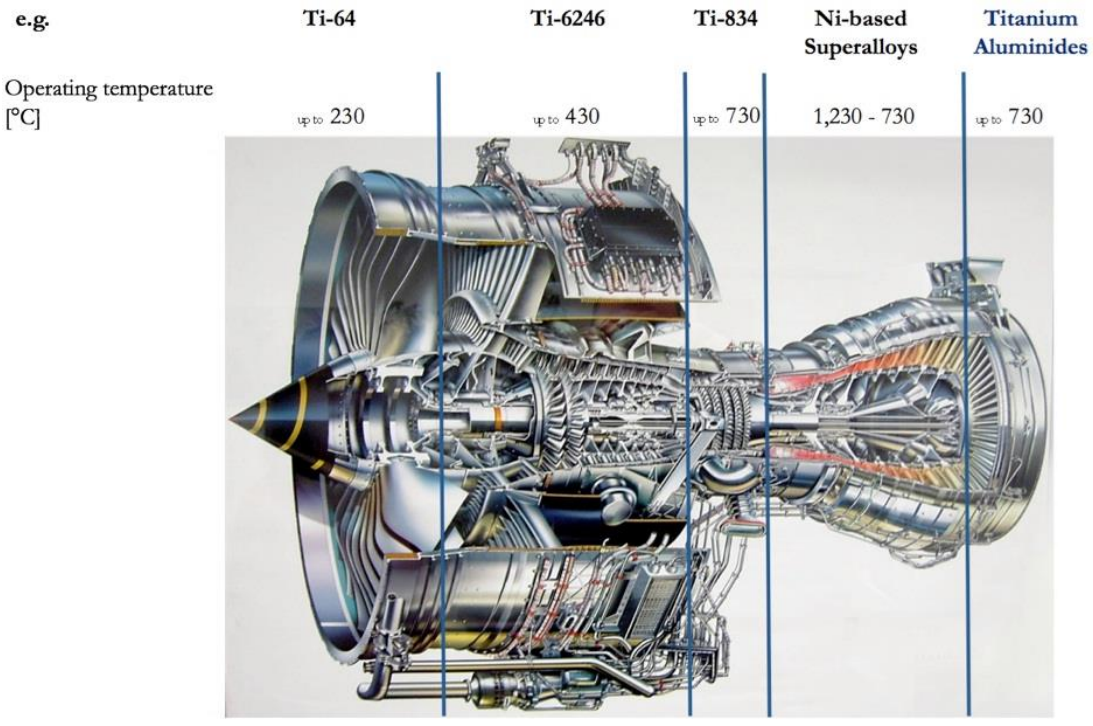

Figure 1.2 : Operation temperature with listed materials for each part of AMG jet engine **[7]**

Jet engine sections of AMG productions of operating temperature are listed above in Figure 1.2. As clearly seen, the highest temperature-operating components are nickel-based superalloys.

According to previous information the sections temperature are summarized below,

● Compressor: The compressor pressure ratio (PR) typically is 15–25 for most land based gas turbines (higher in the case of some aeroengines); the temperature increases to typically 750–850°F (400–465°C).

● Combustion: The combustion zone typically is 2500–2600° F (1370– 1427° C) for land based gas turbines. Flame temperatures may exceed 2000° C in some aircraft engines.

● Turbine: First-stage turbine inlet nozzles (1st stage NGVs) convert high-enthalpy gas to high-velocity gas. High-velocity gas turns the turbine rotor blades and buckets

● The turbine temperature is about 1650°C and turbine exhaust temperature is typically 900–1180°F (482–638°C). [8]

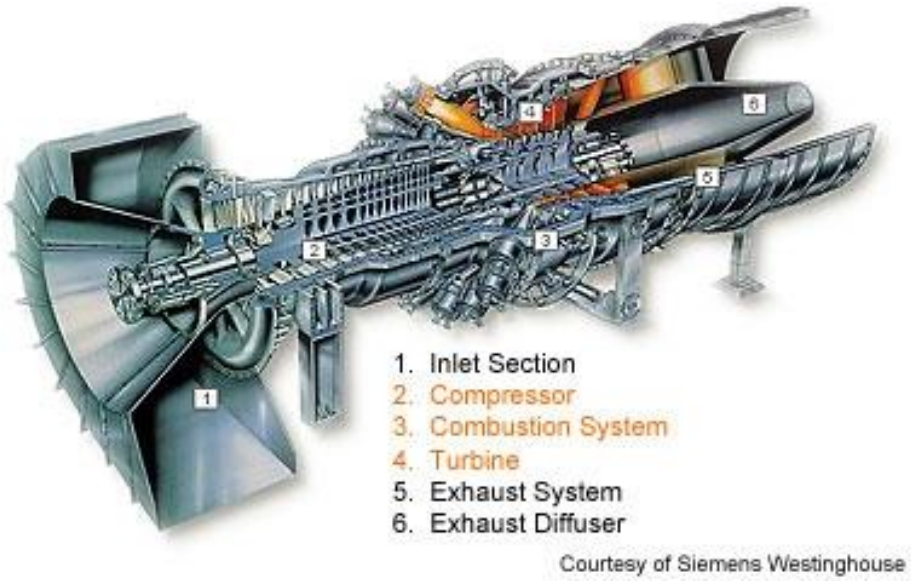

Figure 1.3 : Cross section view of gas turbine power plants of Siemens [9]

The sections temperatures show that the blades and vanes design have to meet the requirements of the operating temperature, on the other hand, they suffer from high temperature and pressure, and they became easily damaged. Therefore, the protection of the component is essential.

1.1.1 Turbine blades and materials

Airfoil parts, such as blades and vanes, are critical components in the gas turbine engines that are used to power jet aircraft or for the generation of electricity. The blades used in the high-pressure turbine rotor need to satisfy requirements including a balance of creep resistance, temperature capability, environmental resistance, and damage tolerance. Because they are often exposed to corrosion and oxidation-inducing combustion gas atmosphere containing sulfur, chlorine, vanadium, sodium and lead. [10]

The airfoil part may be either a rotating component or a non-rotating component of the gas turbine engine (Figure 1.4). If the part is a rotating component, during operation of the turbine engine the part is subjected to centrifugal forces that exert deforming stresses. These deforming stresses cause creep rupture and fatigue problems that can result in the failure of the part. Non-rotating components, such as vanes, are not subjected to centrifugal forces that exert deforming stresses. However, like the rotating parts, these parts are subjected to other deformation such as from hot gas erosion and/or foreign particle strikes. [11]

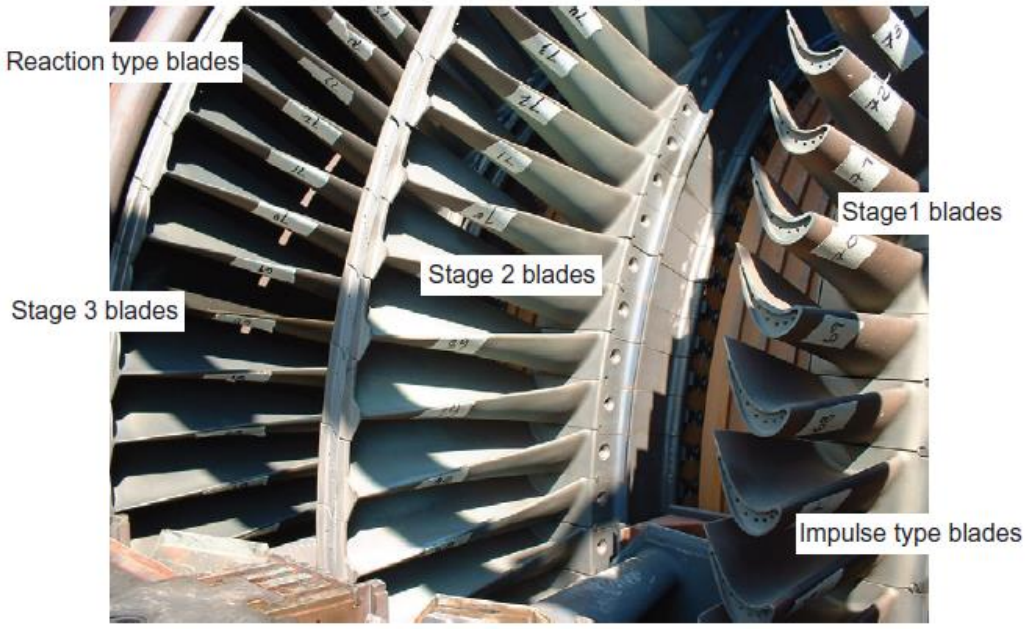

Figure 1.4 : Cooling blades in a turbine section of a frame-type gas turbine **[10]**

Both the compressor and turbine sections may include alternating series of rotating blades and stationary vanes that extend into the core flow path of the gas turbine engine. In the turbine section, turbine blades rotate and extract energy from the hot

combustion gases that are communicated along the core flow path of the gas turbine engine. [12]

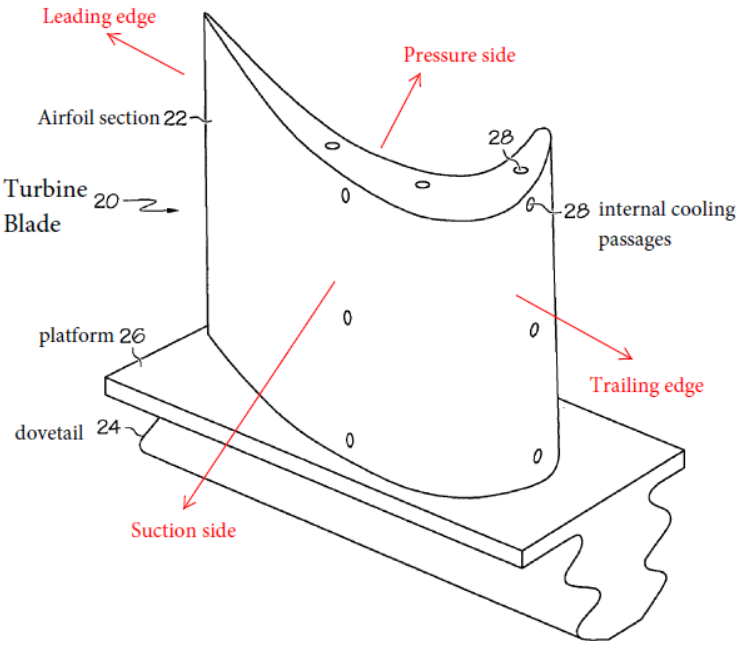

Figure 1.5 : Perspective view of turbine blade with descriptive numberings **[13]**

Individual blade structure is presented in Figure 1.5. The film cooling holes communicate cooling fluid from the cooling passages to areas on the exterior surface of the turbine blade. They work under high temperature, pressure and rotation numbers. Therefore suction and pressure surface and edges exposed to very erosive atmosphere under cycling load. By the way, leading edge region receives extremely hot mainstream flow when compare it with trailing edge. [13]

In Figure 1.5 the cooling passages also represented on suction and airfoil surface. The film cooling holes communicate cooling fluid from the cooling passages to areas on the exterior surface of the turbine blade to help the reduction of blade temperature. [14]

In modern engines, blade performance and durability is achieved through advanced superalloy single crystals combined with sophisticated internal cooling schemes (internal cooling passages are shown in Figure 1.5) and thermal barrier coatings. Low density alloys with improved strength at elevated temperatures is new direction for the research to provide further advances in new alloys. [13]

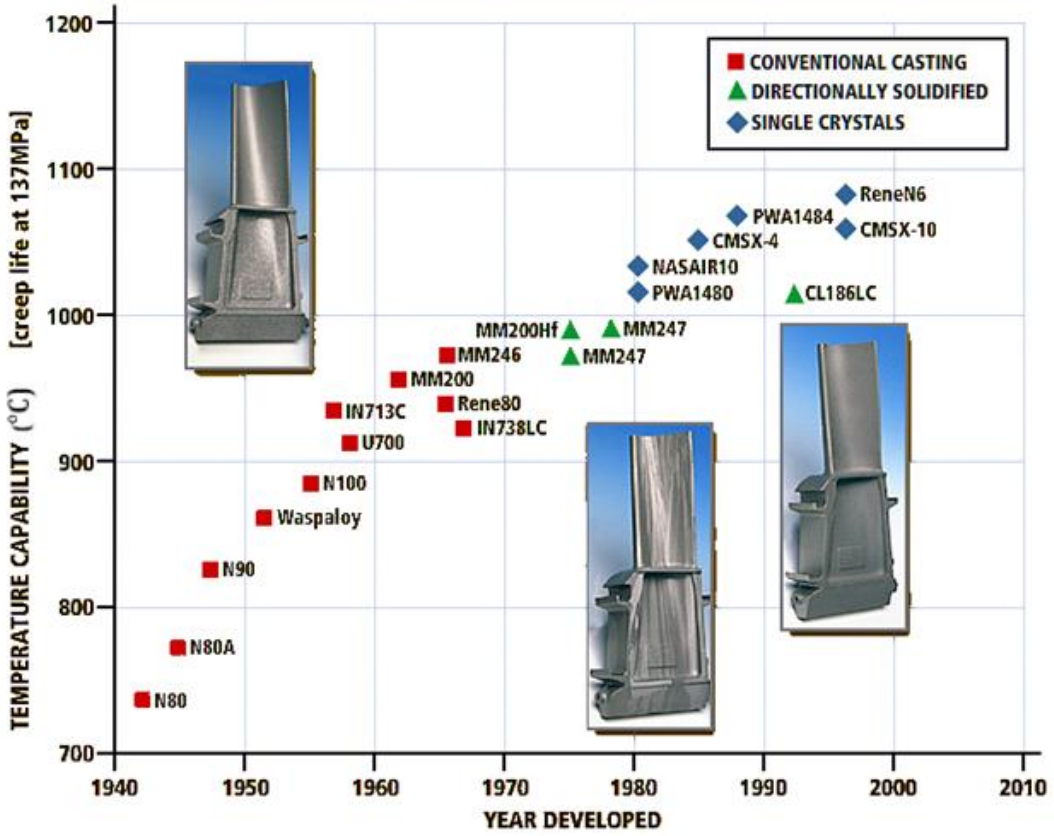

Figure 1.6 : Progress in turbine blade capability for over 50 years. **[15]**

According to Figure 1.6, the nozzle (vane) and blades (bucket) materials temperature resistance improvement is demonstrated. Over the last seven decades, the withstanding temperature has grown from 700°C to 1100°C. The improvements are generally achieved by advancement in substrate materials structural properties. Even though coating materials effect is not demonstrated, after 1990, application of thermal spray coating has provided further improvement at resistance of temperature. [15]

Modern industrial gas turbines (IGT) employ with blades and vanes that has

- advanced cooling schemes,
- thermal barrier ceramic coatings,
- directionally solidified and single crystal

The three properties are important to improve blades' temperature resistance.

Directionally solidified (DS) and single crystal (SX) structures are illustrated in Figure 1.7. The directionally solidified part is grown along the vertical axe so that single grains extend from the bottom to the top of the part. Consequently, a part has no grain boundaries in the direction normal to the main stresses. [16]

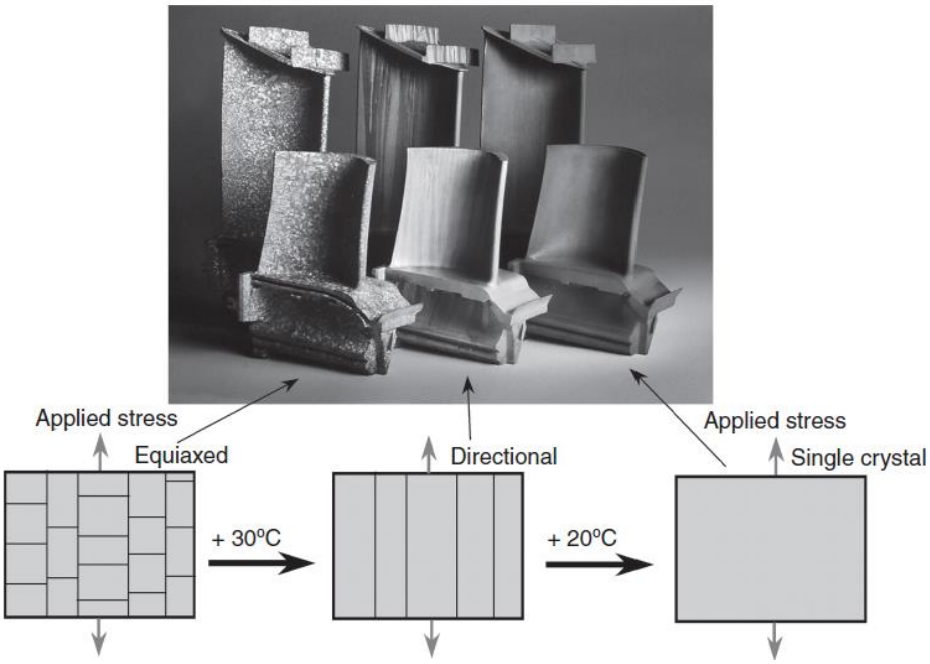

Figure 1.7 : Industrial gas turbine blades with conventional, directionally solidified and single crystal grain structure **[16]**

As mentioned before, advancement in substrate materials bring improvement of durability of buckets to the working temperature of gas turbine. The advancement is achieved basically by development of substrate microstructre from conventional casting to the single crystal. As seen in Figure 1.7. in the single crystal component, the entire part is one single grain, and grain boundaries are eliminated. The improvement also eliminates the some structural and mechanical problems that begin and grow at grain boundaries

2 SUPERALLOYS

Superalloys are classified according to the main alloying elements in the composition, with the three base metals being nickel, cobalt, and iron and they are generally used at temperatures above about 540 °C. [17]

The iron-nickel-base superalloys such as the popular alloy IN718 are an extension of stainless steel technology and generally are wrought. Cobalt-base and nickel-base superalloys may be wrought or cast, depending on the application/composition involved. The entire superalloy family shares a common basic microstructure, which is a face-centered cubic (fcc) matrix with a number of dispersed secondary strengthening phases. (One of them is represented at Figure 2.1) [18]

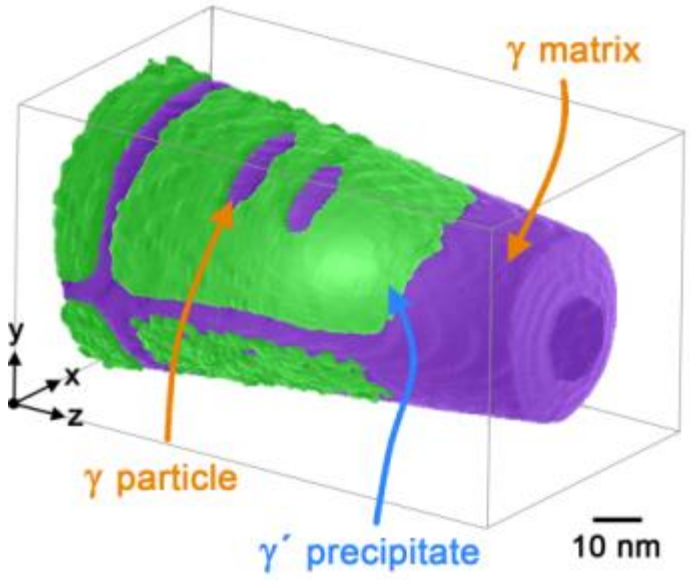

Figure 2.1: The γ matrix (purple) can be seen surrounding the cuboidal γ precipitates (green).[19]

Based on the matrix element(s), superalloys can be broadly be classified into three families:

- Nickel-iron base (Ni-Fe-base)

- Nickel-base (Ni-base)
- Cobalt-base (Co-base)

Ni-base superalloys are the most complex, the most widely used for the gas turbine engine parts experiencing the highest temperatures. They have the highest creep strength among the above families. [20]

Table 2.1 : Chemical composition of industrial gas turbine superalloys **[16]**

Type	Ni	Cr	Co	Mo	W	Re	Al	Ta	Nb	Ti	C	B
		Solid solution strengthening					γ′ forming				Grain boundaries strengthening	
IN 738 LC	BAL	16	8.3	1.75	2.6	0	3.4	1.75	0.9	3.4	0.1	0.001
GTD 111	BAL	14	9.5	1.5	3.8	0	3	2.8	0	4.9	0.1	0.01
IN 792	BAL	12.7	9	2	3.9	0	3.2	3.9	0	4.2	0.2	0.02
IN 939	BAL					0						
GTD 222	BAL	22.5	19	2.3	2	0	0.8	0	0	1.2	0.08	0.1
FSX 414	10	28	BAL	0	7	0	0	0	0	0	0.25	0.01
MarM 247LC	BAL	8.5		0.5	9.5	0	5.5	3.2	Hf 1.3	1	0.15	0.015
CM 247 LC	BAL	8		0.5	9.5	0	5.5	3.2	Hf 1.4	1	0.07	0.01
Rene N4	BAL	9	8	2	6	0	3.7	4	0.5	4.2		
Rene N5	BAL	7	8	2	5	3	6.2	7	0	0		
CMSX 4	BAL	6.5	9	0.6	6	3	5.6	6.5	0	1		
MK 4	BAL	6.5	9	0.6	6	3	5.6	6.5	0	1		
PWA 1483	BAL	12.8	9	1.9	3.8	0	3.6	4	0	4		
MD 2	BAL	8	5	2	8	0	5	6	0	1.5		
CMSX-8	BAL	5.4	10	0.6	8	1.5	5.7	8	Hf 0.3	0.7		

According to Table , superalloys typically contain ten or more alloying elements, grouped according to their function into three categories:

- Solid solution elements (Co, Cr, W, Mo, Re): The elements predominantly present in the austenitic γ matrix. W, Mo, Re are effective solid solution strengtheners due to their large atomic diameter; the main role of Cr is to provide corrosion and oxidation resistance through the formation of dense oxide scale; Co, being a minor matrix strengthener, stabilize γ' phase and increases γ' solvus temperature. These elements also replace Ni atoms in γ' phase lattice with a similar strengthening effect.
- Gamma prime formers (Al, Ti, Ta, Nb, Hf): They form an intermetallic γ' phase, replacing Al and, due to larger atomic diameter, strengthening this phase.
- Grain boundary strengtheners (C, B, and Zr, Hf, Ti, Ta, Nb): They form stable carbides and borides along grain boundaries. [21]

Second and third generation superalloys contain 3, 6 wt.% of the refractory (high-melting point) element rhenium, respectively. The aluminum concentration is

approximately 6 wt.%, which leads, together with elements such as Ti and Ta, to a high volume fraction of the hardening, L1 ordered, γ' phase. Higher Al concentration results in precipitation of the B2 ordered intermetallic phase NiAl, leading to an embrittlement at lower temperatures. [22]

Table 2.1 : Role of alloying elements in superalloys **[21]**

Effect(a)	**Iron-base**	**Cobalt-base**	**Nickel-base**
Solid-solution strengtheners	Cr, Mo	Nb, Cr, Mo, Ni, W, Ta	Co, Cr, Fe, Mo, W, Ta, Re
fcc matrix stabilizers	C, W, Ni	Ni	. . .
Carbide form:			
MC	Ti	Ti	W, Ta, Ti, Mo, Nb, Hf
M_7C_3	. . .	Cr	Cr
$M_{23}C_6$	Cr	Cr	Cr, Mo, W
M_6C	Mo	Mo, W	Mo, W, Nb
Carbonitrides: M(CN)	C, N	C, N	C, N
Promotes precipitation of carbides	P	. . .	. . .
Forms γ' $Ni_3(Al, Ti)$	Al, Ni, Ti	. . .	Al, Ti
Retards form. of hexagonal η (Ni_3Ti)	Al, Zr	. . .	. . .
Raises solvus temperature of γ'	. . .	. . .	Co
Hardening precipitates or intermet.	Al, Ti, Nb	Al, Mo, Ti(b), W, Ta	Al, Ti, Nb
Oxidation resistance	Cr	Al, Cr	Al, Cr, Y, La, Ce
Improve hot corrosion resistance	La, Y	La, Y, Th	La, Th
Sulfidation resistance	Cr	Cr	Cr, Co, Si
Improves creep properties	B	. . .	B, Ta
Increases rupture strength	B	B, Zr	B(c)

Table 2.2 (continued) : Role of alloying elements in superalloys **[21]**

Grain-boundary refiners	. . .	. . .	B, C, Zr, Hf
Facilitates working	. . .	Ni3Ti	. . .
Retard γ′coarsening	. . .	. . .	Re

(a) Not all these effects necessarily occur in a given alloy. (b) Hardening by precipitation of Ni3Ti also occurs if sufficient Ni is present. (c) If present in large amounts, borides are formed.

Table 2.1, general list of the role of some alloy elements in superalloys. Some elements go into solid solution to provide important improvements. According to table to summarize briefly the effect of element on the superalloys;

- strength (molybdenum, tantalum, tungsten, and rhenium);
- oxidation resistance (chromium and aluminum);
- hot corrosion resistance (titanium);
- phase stability (nickel); and
- increased volume fractions (*Vf*) of favorable secondary precipitates (cobalt).

The broad view of the alloying elements' effects are represented on the periodic table in Figure. As mentioned above, the related elements negative and positive effects can be clearly understood from the figure. [18]

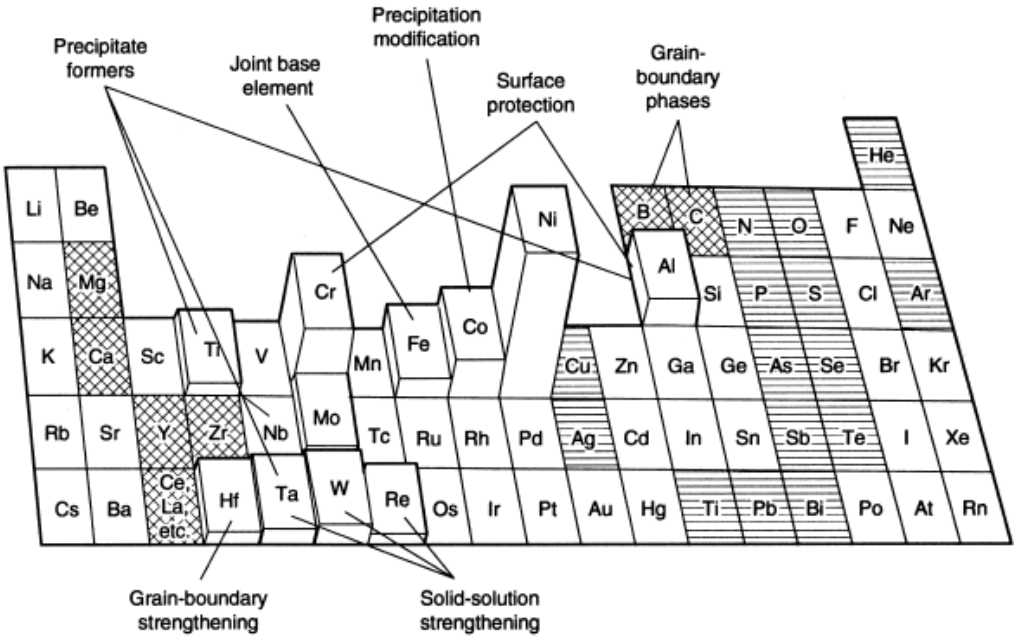

Figure 2.2 : Alloying elements used in nickel-base superalloys. Beneficial minor elements are marked with cross-hatch, while detrimental tramp elements are marked with horizontal line hatch. [21]

Figure2.2 and Table 2.1 make a summary of important phases. First important one is γ' and that is the principal precipitate phase in superalloys and the phase is an ordered ($L1_2$) intermetallic fcc phase having the basic composition Ni_3(Al, Ti). The other phase is η related with γ' and η, is an ordered ($D_0$24) hexagonal phase of composition Ni_3Ti that may exist in a metastable form as a titanium- rich γ' before transforming to η. The last critical phases are δ and γ'' are other types of intermetallic phases, such as δ orthorhombic Ni3Nb, or γ'' bct-ordered ($D_0$22) Ni3Nb strengthening precipitate, have been observed and contribute significantly to iron-nickel- and nickel-base superalloy strength. [21]

2.1 Iron-Nickel-Base Superalloys

Nickel-Iron (Ni-Fe) based superalloys are precipitation-strengthened alloys that contain substantial amounts of Ni and Fe (25-60% Ni 15-60% Fe), and they represent some of the most widely used superalloys and constitute their own class. [19] The alloys are characterized by their high toughness and ductility and are used mostly in applications where these properties are required, such as turbine discs or forged rotors. Consequently, nickel iron alloys are used only in the wrought condition, because this manufacturing method offers a wide variety of mechanisms for

controlling grain size and morphology. In addition to their high toughness, another advantage of nickel-iron-base superalloys is their lower cost due to the substantial amount of iron added. [2]

There are four general characteristics of the Fe-Ni alloys: Firstly, they are all FCC (γ) austenitic matrix based on both Fe and Ni. Secondly, solid solution strengthening is through alloy elements that partition to γ. Thirdly, the alloys are also precipitation hardened via intermetallics, borides, or carbides and finally, the alloys are also precipitation strengthened by modifying grain boundaries. [19]

The most common precipitate of the superalloys is γ'-Ni3(Al,Ti), an the some important examples are given below.

- A-286
- V- 57, or
- Incoloy 901
- Incoloy 800H

Some alloys, typified by which precipitate γ ″-Ni3Nb,

- Inconel (IN) 718, were formerly classed as iron-nickel-base but now are considered as nickel-base. [23]

The iron-nickel-base superalloys strengtheners are intermetallic compound precipitation and they are in an FCC matrix. [18]

2.2 Cobalt-Base Superalloys

Cobalt-based alloys have been in use for several decades in the manufacturing of various components such as vanes or combustion chambers in gas turbines (both the industrial type and aeroengines). They can be implemented as wrought or as precision-cast parts. [24]

Cobalt base superalloys strengthened by a combination of carbides and solid-solution hardeners. [25] Like all superalloys, the microstructures of cobalt-base superalloys consist of an FCC γ matrix with a number of strengthening phases. However, the precipitation hardening in cobalt-base superalloys is not as effective as γ′ or γ″, as observed in nickel-iron- or nickel-base superalloys. This has made the cobalt-base

superalloys heavily dependent on strengthening by carbide formation and solid-solution strengthening. [12]

The superalloys has better hot corrosion resistance in contaminated gas turbine atmospheres due to their higher Cr contents. In addition, it has better weldabilityand thermal fatigue resistance than Ni-base alloys. Some important Co-base superalloys are given at Table 2.4

Table 2.3: Some typical Co-based superalloys ans their elemental composition **[26]**

	Co	Ni	Cr	Al	Ti	Mo	W	Ta	B	Zr	C	Other
FSX-414	Bal.	10.5	29.5	–	–	–	7	–	0.012	–	0.25	2 Fe
Stellite 21	Bal.	2	28	–	–	5.5	–	–	–	–	0.3	–
Stellite 31	Bal.	10	20	–	–	–	15	–	–	–	0.1	–
MarM302	Bal.	–	21.5	–	–	–	10	9	0.005	0.015	0.85	–
MarM509	Bal.	10	23.4	–	0.25	–	7	3.5	–	0.35	0.6	–
Haynes-188	Bal.	22	22	–	–	–	14.5	–	–	–	0.1	3 Fe* 0.90La

The superalloys is very important for cutlery, machine tools, and wearresistant

hardfacing applications and common trade names of Co based superalloys are

- Stellite
- Hastelloy

both developed by the Haynes Corporation.

2.3 Nickel Base Super Alloys

In the 1950s, new casting methods appeared, including vacuum casting, which significantly reduced the occurrence of adverse events such as porosity in the castings. This allowed introduction of Ni alloys in the form of forgings, and also in the form of castings. The years between 1960 and 1970 were a period of particular development in the field of Ni alloys metallurgy. As a result, the largest increase in Ni applications in the structure of aircraft engines was noted in this period, and it continues to this day with great success. Currently, composite materials are being used, and intermetallic compounds such as Ti –Al are also being used increasingly. [27]

For nickel-titanium/aluminum alloys, the strengthening precipitate is γ'. Such alloys are typified by the wrought alloys

- Waspaloy and

- Udimet (U) 720,
- or by the cast alloys René 80 and
- IN 713
- René 95, Astroloy, IN 100 [23]

The other sample Nickel alloys and their chemical composition are displayed at Table 2.4

Table 2.4 : Chemical composition of selected Ni alloys (wt%) [27]

Ni alloy	C	Cr	Fe	Mn	Mo	Si	S	P	Al	Ti	Nb + Ta	Cu	W	Ni	Co
Inconel		17.0		0.35	2.80	0.35	0.015	0.015	0.20	0.65–	4.75–	0.30		50.0–	
718	0.08 max.	– 21.0	Balance	max.	– 3.30	max.	max.	max.	– 0.80	1.15	5.50	max.	–	55.0	
Inconel		20.0–		0.5		0.50	0.015	0.015	0.40	0.40	3.15–				
625	0.10 max.	23.0	5.0 max.	max.	8.0–10.0	max.	max.	max.	max.	max.	4.15	–	–	58 min.	1.0 max.
Hastelloy	0.05–0.15	20.5–	17.0–	1.0		1.0	0.03	0.04					0.20–		
X	max.	23.0	20.0	max.	8.0–10.0	max.	max.	max.	–	–	–	–	1.0	Balance	0.5–2.5
Udimet		18.0							1.40–						
R41	0.12 max.	– 20.0	5.0 max.	–	9.0–10.5	–	–	–	1.80	3.0–3.3	–	–	–	Balance	10–12.0
Nimonic		18.0		1.0		1.0	0.015					0.2			15.0–
90	0.13 max.	– 21.0	1.5 max.	max.	–	max.	max.	–	1.2–2.0	2.0–3.0	–	max.	–	Balance	21.0

Signifcant resistance to loading under static, fatigue and creep conditions requirement have emerged, the nickel-base superalloys as the materials of choice for high-temperature applications Nickel base superalloys are often used forming parts of gas turbines, that are exposed to heat of high temperature and erosive atmosphere. Thus, the alloys are required to have a both high mechanical strength at elevated temperature and corrosion, oxidation resistant properties against combustion gas. [28]

These superalloys are used in the most demanding portions of the turbine engine, where a wide balance of high strength, high toughness, oxidation and corrosion resistance, temperature capability, and processability are all needed.[21]

Most superalloys are Ni-based alloys, hardened with intermetallic γ' phase on a basis of Ni_3Al (40–70 vol-%), and carbides and borides along grain boundaries. [16]

The unique properties of the γ' phase is while most materials lose strength with increase of temperature above 600°C, the strength of γ' phase increases in temperature range from 600°C to about 800°C. [16] Above this temperature range, the strength lightly decreases, but up to solutioning temperature, it remains higher than that of the matrix. The γ' phase has a crystallographic lattice, coherent with that of the matrix. [29, 30]

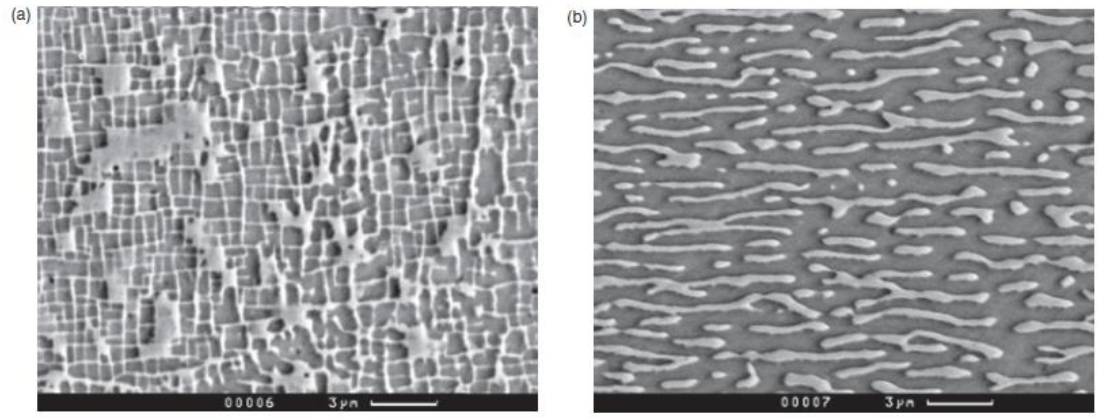

Figure 2.3: (a) The initial condition of cubical and (b) rafted morphology of continuous γ' phase after creep at 950°C, in highly alloyed superalloys. [16]

According to Figure2.3, microstructure of γ' phase is illustrated . Alloys with a very high fraction of γ' phase (usually >60 vol-%) tend to degrade, forming elongated, so-called 'rafted', structures perpendicular to stress axes and even to a reverse structure of γ in γ' matrix. A rafted structure is characterised by lower creep properties, and the inverse structure is prone to cracking. [28]

Precipitation hardened Nickel base Superalloys: A considerable increase in the creep strength of alloys for high temperature applications can be obtained by precipitation hardening (PH). In the case of nickel-base alloys, this can be achieved using elemental additions such as titanium, aluminum, and niobium. These elements have limited solubility in the alloy matrix, and the solubility is drastically reduced with a decrease in temperature; therefore, finely distributed precipitates can be generated in the matrix from a supersaturated solid solution during heat treatment. The precipitates, which are generally coherent intermetallic compounds such as γ'-$Ni_3(Ti,Al)$ or γ''-Ni_3Nb phase, can inhibit the movement of dislocations. [10,17]

The most important class of nickel base superalloys is that strengthened by intermetallic compound precipitation in an austenitic fcc matrix.

- For alloys with titanium and aluminum, the strengthening precipitate is γ'. Such alloys are typified by the wrought alloys Waspaloy, Astroloy, U700, and U720, or the cast alloys Rene 80, Mar-M-247, and IN713.
- For niobium-strengthened nickel-base superalloys, the strengthening precipitate is γ''. These γ''hardened alloys are typified by IN718.

- Some nickel-base alloys may contain niobium plus titanium and/ or aluminum and use both γ ′and γ ″ precipitates in strengthening. Alloys of this type are IN706 and IN909. These three alloys (IN- 718, IN-706, and IN-909) may sometimes be found listed as iron-nickel-base (or nickel iron- base) superalloys. [12]

Solid Solution Strengthened Nickel base Superalloys: Solid-solution hardening is the attainment of an increase in matrix strength by the addition of a different soluble element. The distortion of the atomic lattice caused by the misfit of atomic radius inhibits dislocation movement. [10,17]

The class of nickel-base superalloys that is essentially solid-solution strengthened is typified by such alloys as ,

- Hastelloy X and IN625.

The solid-solution-strengthened nickel base alloys may derive some additional strengthening from carbide and/or intermetallic compound precipitation. [21]

Oxide Dispersion Strengthened Nickel base Superalloys: Oxide dispersion strengthening (ODS) is a strengthening mechanism that the agent is added to the alloy. In ODS, oxide particles act in a similar way to γ′ intermetallics by blocking dislocation motion.[18]

A third class of nickel-base superalloys includes oxide-dispersion-strengthened (ODS) alloys such as,

- IN-MA-754 and IN-MA- 6000E, which are strengthened by dispersion of inert particles such as yttria, *coupled in some cases with γ ′ precipitation* (MA- 6000E). [21]

2.3.1 Inconel 718

Inconel 718 was first produced in 1960 in response to a demand from industry for high-strength nickel alloys. Inconel 718 is a precipitation-hardened nickel alloy with excellent corrosion resistance in many media. In addition, it is resistant to sulphur compounds because of a chromium addition. It's melting point is 1260–1336°C, and it has a density of 8.22 g/cm3 (Table 2.5). Currently, Inconel 718 is a commonly used nickel alloy for building the aircraft engines in all leading companies that design jet engines. [18]

Inconel 718 (IN718) has less nickel in it than other alloys and does not contain cobalt. Thus, it was cheaper to make and somewhat more readily available than other competitive alloys at that time. When a cobalt shortage and attendant high alloy prices occurred in the latter part of the 1970s, more designers switched to IN718. Cost and availability, accompanied by strength properties to about 649°C, have made it for use as gas turbine disks. [21]

The other application area of IN178 at gas turbine engines are

- Turbines
- Blisks (disks)
- Cases, rings
- Exhaust parts [32]

IN718 is a niobium-modified nickel-base superalloy that is usedin gas turbines, rocket motors, spacecraft, nuclear reactors, pumps and tooling. The alloy consist of several phases in the matrix including δ, γ', γ" and actually strengthened by order body centered tetragonal (BCT) precipitates, γ". (Exact composition is given at Table 2.3). [33]

Table 2.5 : Inconel 718 and AMS 5663 limiting chemical composition (wt%) [35]

Element	IN718	AMS:5663
Fe	18	16–20
Cr	19	17–21
Al	0.5	0.2–0.8
Ti	1	0.65–1.15
Mo	3	2.8–3.3
Nb	5	4.75–5.5
C	0.042	0.08 max
Ni	Balance	Balance

Inconel 718 superalloy is a face-centered cubic (FCC) austensite matrix strengthened precipitation of order intermetallic or carbide precipitates. Both of γ''and γ'phases are found in alloy, but γ''is the predominant strengthening agent.

IN718 γ" forms in the range of 705°C to 900°C and has solvus temperature of about 910°C. The δ phase, depending on exposure time, precipitates in the approximate temperature range 870°C to 1010°C and has solvus temperature about 1010°C. [34]

The superalloy is a solid solution strengthened, age hardenable, Ni based alloy. The matrix phase is a FCC austenitic phase. It can be age-hardened by the precipitation of γ' (ordered Ni_3(AI, Ti)), γ'' (ordered BCT Ni_3Nb), η (HCP Ni_3Ti), δ (orthorhombic Ni_3Nb), or any combination of the preceding. In addition, various carbides can form at the prior austenitic phase boundaries. The melting range is typically 1260-1335°C. [36]

Inconel 718's recommended operating temperature is up to 650°C. It's properties largely depend on phase γ" precipitation strengthening (Ni_3Nb) during hardening. The standard heat treatment involves solutioning at 930–1010°C with rapid cooling, followed by hardening at 720°C for 8 h, slow cooling at a rate of 508C/h to a temperature of 620°C, and standing for the next 8 h. The total hardening time is approximately 18 h. Hardness obtained after curing is at least 36 HRC. [27]

After heat treatment the solution and ageing treatment on Inconel 718 superalloy casting are needed. Because the Inconel 718 superalloy has a composite structure of austensite matrix and precipitated γ'and γ''phases produced by the heat treatment. The strengthening phase in the alloy is the metastable body centered tetragonal Ni3Nb, γ''. The creep phenomenon can't be ignored in the condition of heat treatment. The mechanical properties depend on the morphology, size and contents of δ, γ', and γ''phases in Inconel 718 superalloy. [33]

Table 2.6 : Physical properties of inconel 718 [31]

	Solution Treated	Solution Treated and Aged
Density	0.296 lb/in^3 (8.192 g/cm^3)	0.297 lb/in^3 (8.22 g/cm^3)
Specific Gravity	8.19	8.22
Melting Range	2500-2600°F	1370-1430°C

The superalloys high-strength, corrosion-resistant nickel chromium material used at 217° to 704°C. Typical composition limits are shown in Table 2.5. The age-

hardenable alloy can be readily fabricated, even into complex parts. Its welding characteristics, especially its resistance to postweld cracking, are outstanding. [37]

Some important mechanical, physical and thermal properties of IN718 are show following tables.

Table 2.7 : Mechanical Properties of Inconel 718 [31]

	Yield Strength Min (0.2% offset)	Ultimate Tensile Strength Min	Elongation (% in 2")
Sheet and strip	80,000 psi (550 MPa)	14,000 psi (965 MPa)	30 (min)
Plate	105,000 psi (725 MPa)	150,000 psi (1,035 MPa)	30 (min)

IN718 is generally used in the solid solution and aged condition; the exact condition of the temperatures, times, and cooling rates depends on the application and mechanical property need. Many aerospace application requiring high tensile and fatigue strength as well as good stress rupture properties. Use a solution treatment below solvus and a two-step aging treatment as follows:

- Solution heat treatment at 925 to 1000°C for 1-2 h (air cooling or faster)
- Age at 720 °C for 8 h followed by furnace cooling to 620°C
- Hold at 620°C for total aging time of 18 h (air cooled). [34]

Inconel 718 superalloy is a niobium-modified nickel-base superalloy that is used widely in gas turbine and related high temperature of aerospace applications.5,6) Inconel 718 superalloy is a precipitation hardenable, nickelbased superalloy that has high strength at room temperature and excellent creep as well as fatigue strengths at high temperatures. It used in gas turbines, rocket motors, spacecraft, nuclear reactors, pumps and tooling. The alloy consist of several phases in the matrix including δ, γ’ , γ’’and NbC. [33]

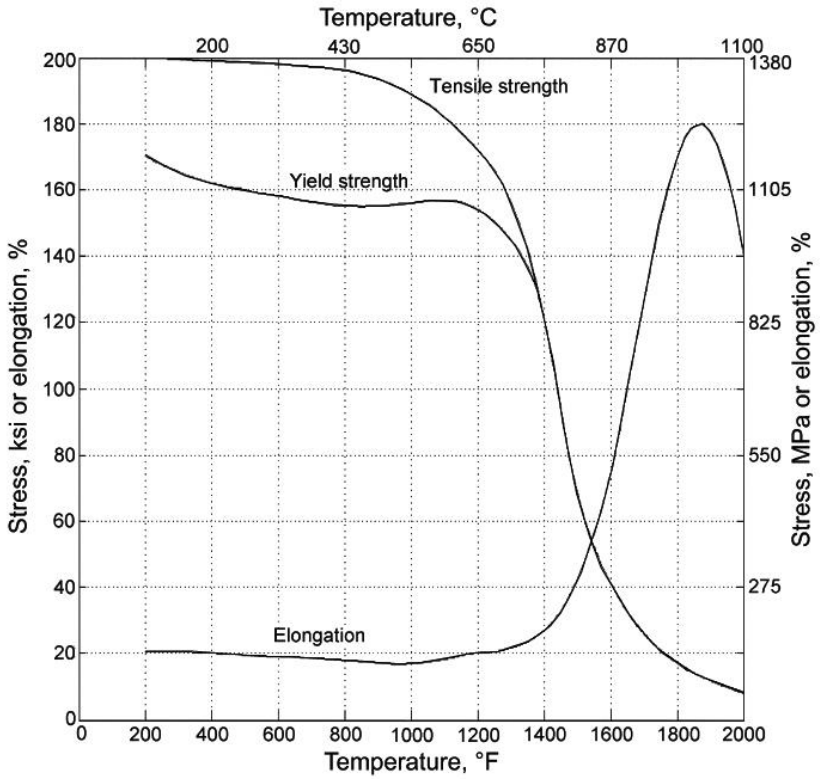

Figure 2.4 : Mechanical properties of solid-solution-hardened and aged IN718. [10]

Precipitation-hardened alloys exhibit mechanical property changes in the vicinity of the solvus temperature of the strengthening precipitate. As can be seen in Figure2.4, the mechanical properties for Inconel 718 experience changes at approximately 700 °C, which is the solvus temperature for this alloy. Creep rates and stress rupture are likewise affected by precipitate dissolution.[10]

Inconel 718 application area in engine is clearly seen in Figure2.5. Its usage ratio is 22% at PW4000 and 34% at CF6 engine and when compare the ratio with the other alloys it has almost highest level in both engine and its clearly show the importance of IN178 in jet engines.

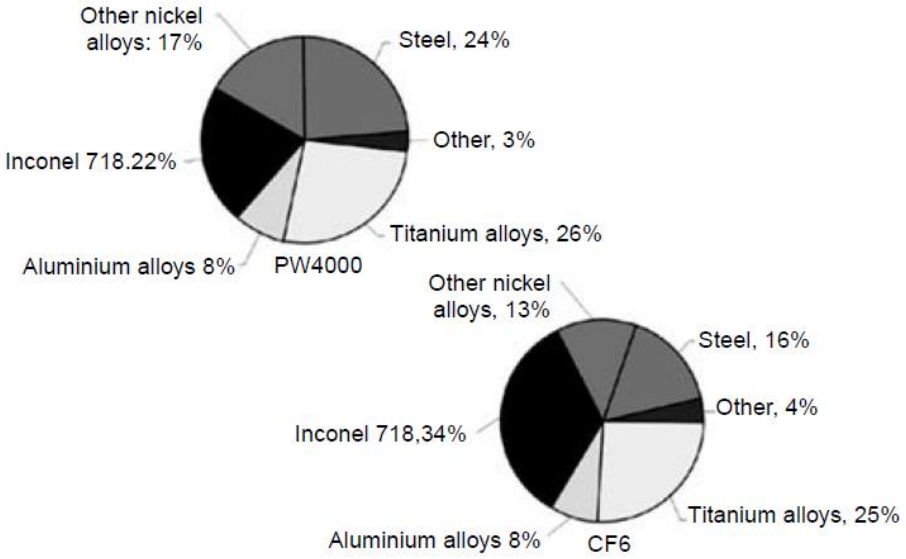

Figure 2.5 : Comparison of proportional parts of individual material groups in thestructure of a Pratt & Whitney PW4000 aircraft engine, and a CF6 engine produced by GE Aircraft, including Inconel 718 [27]

An additional factor in the selection of an alloy for this disk application becomes the cost and availability of material. An example is the prevalence of IN718 as the standard low intermediate-temperature turbine disk in aircraft gas turbine engines [38]. Until about 1975, IN718 had wide acceptance but not necessarily better properties overall than some competitive materials. However, the alloy has less nickel in it than other alloys and does not contain cobalt. Thus, it was cheaper to make and somewhat more readily available than other competitive alloys at that time. When a cobalt shortage and attendant high alloy prices occurred in the latter part of the 1970s, more designers switched to IN718 [39].

The price availability and its other significant mechanical properties of IN718 makes it desirable by more manufacturers and so IN718 became the premier wrought iron-nickel-base superalloy, in fact, the premier wrought superalloy in the world. Cost and availability, accompanied by excellent strength properties to about 649 °C, have made IN718 the world standard for use as gas turbine disks. [12]

3 COATINGS FOR HOT GAS PATH PARTS

The gas turbine efficiency, whether for industrial power generation, marine applications, or aircraft propulsion, has steadily improved for years. These advances have come about, in large part, because the means have been found to operate the gas-generator portion of the engine at increasingly higher temperatures. The need for greater performance from advanced turbine engines will continue, requiring even higher operating efficiencies, longer operating lifetimes, and reduced emissions. [40]

Nickel and cobalt base superalloy blades and vanes are widely used in the hot section of gas turbines. To protect the superalloy, they are often coated to prevent environmental degradation and more recently, to provide thermal barriers, which allow higher operating temperatures. [41].

Protective coatings have been used to enhance superalloy resistance to hot erosion/corrosion. The most widely used coatings are those based on the NiA1 (on nickel base superalloys) and CoAl (on cobalt base superalloys) formed by interaction of superalloy surfaces with aluminum. To improve the resistance to hot erosion/corrosion, aluminide coatings are modified to contain elements such as chromium, platinum, rhodium and silicon. [42]

Thermal barrier coating (TBC) systems are widely used to provide thermal and oxidation protection to nickel base superalloy components used in gas turbine engines. In these systems, a metallic bond coat is used to provide a strong, oxidation protection layer for the superalloy substrate. The bond coat’s oxidation resistance is achieved by the use of sufficient aluminum to result in the formation of alumina upon high temperature oxygen exposure [44].

Turbine engine, blade, and Thermal barrier coating are displayed in Figure1.3. According to image, high pressure turbine blades consist of a three part system:

- The superalloy substrate,
- The bond coat/environmental barrier,
- The thermal barrier coating. [15]

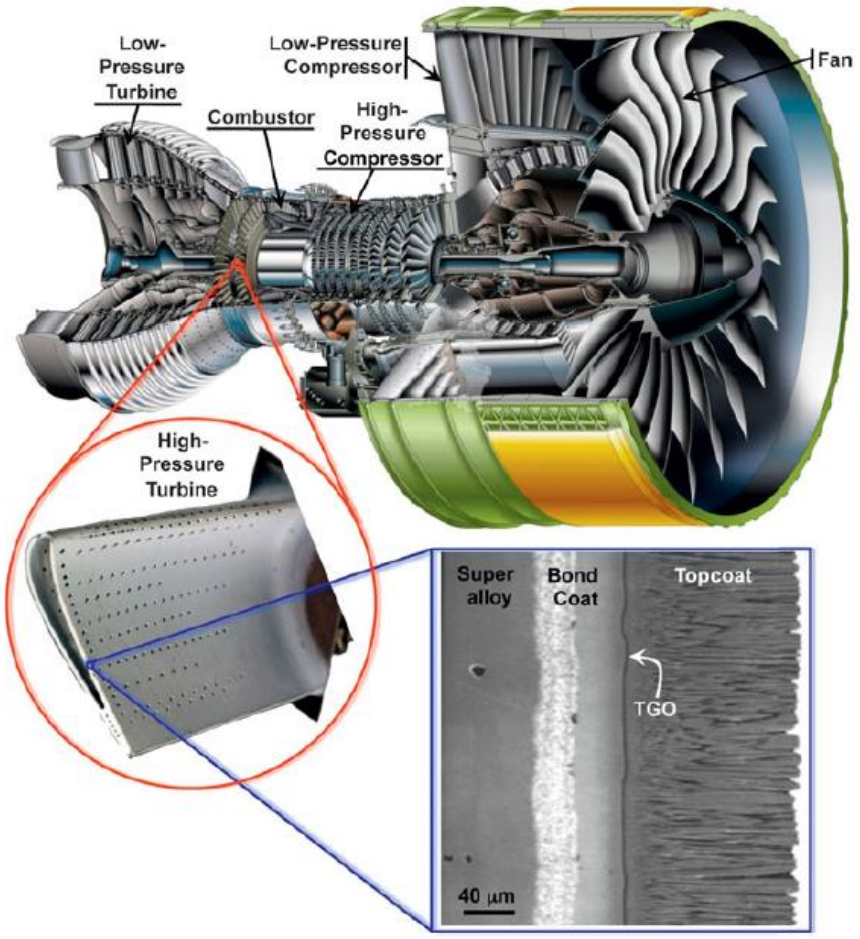

Figure 3.1 : Cutaway view of engine Alliance GP7200 aircraft engine, photograph of a turbine blade (~ 10 cm long) with thermal-barrier coating (TBC) from the high-pressure hot section of an engine, and a scanning electron microscope (SEM) image of a cross-section of an electron beam physical vapor deposited 7 wt% yttria-stabilized zirconia TBC,TGO, thermally grown oxide. [43]

While the bond coat protect the substrate from environmental, top coat (TBC) also provide good isolation between substrate and operating atmosphere. TBCs are ceramic coatings (e.g., partially stabilized zirconia) that are applied to an oxidation-resistant bondcoat, typically a MCrAlY or aluminide [45].

The sample SEM image of thermal barrier coating is shown at Figure 3.1 and the definitive sketch of the coating is given at Figure3.2.

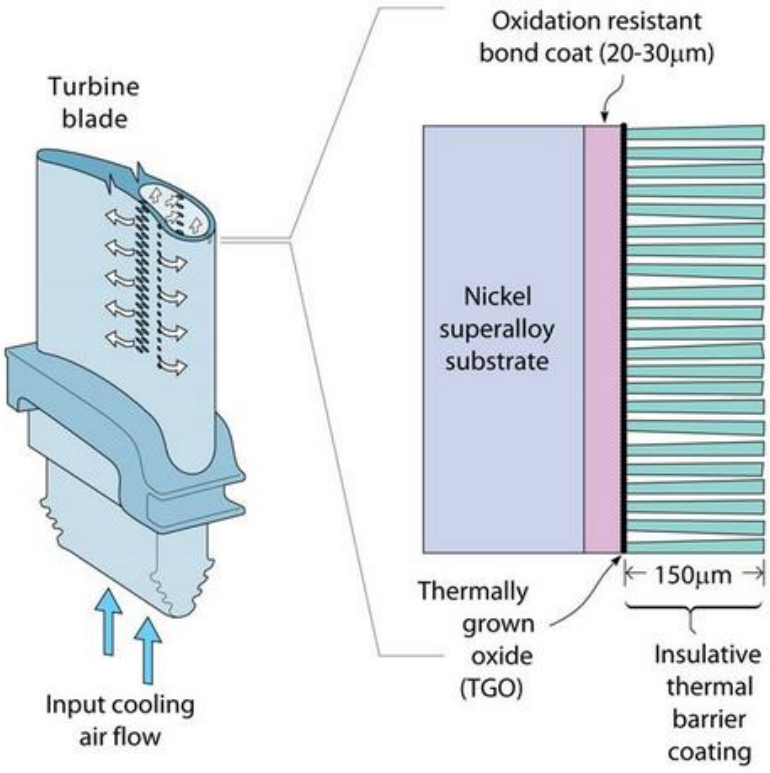

Figure 3.2 : A schematic illustration of hollow air cooled turbine blade (left) and bond coat, thermally grown oxide and thermal barrier coating layers [46]

The temperature at the bond coat surface then governs the rate of oxidation. For internally cooled components, this temperature can be reduced by applying a low thermal conductivity ceramic layer to the bond coat. The durability of the resulting TBC system depends on the ability of a candidate bond coat alloy to form an alumina layer with minimal intermediate phase formation during oxidation, the adherence of the resulting alumina layer to the bond coat and the high temperature strength/creep resistance of the bond coat. All these features are significantly affected by the bond coats composition. [47]

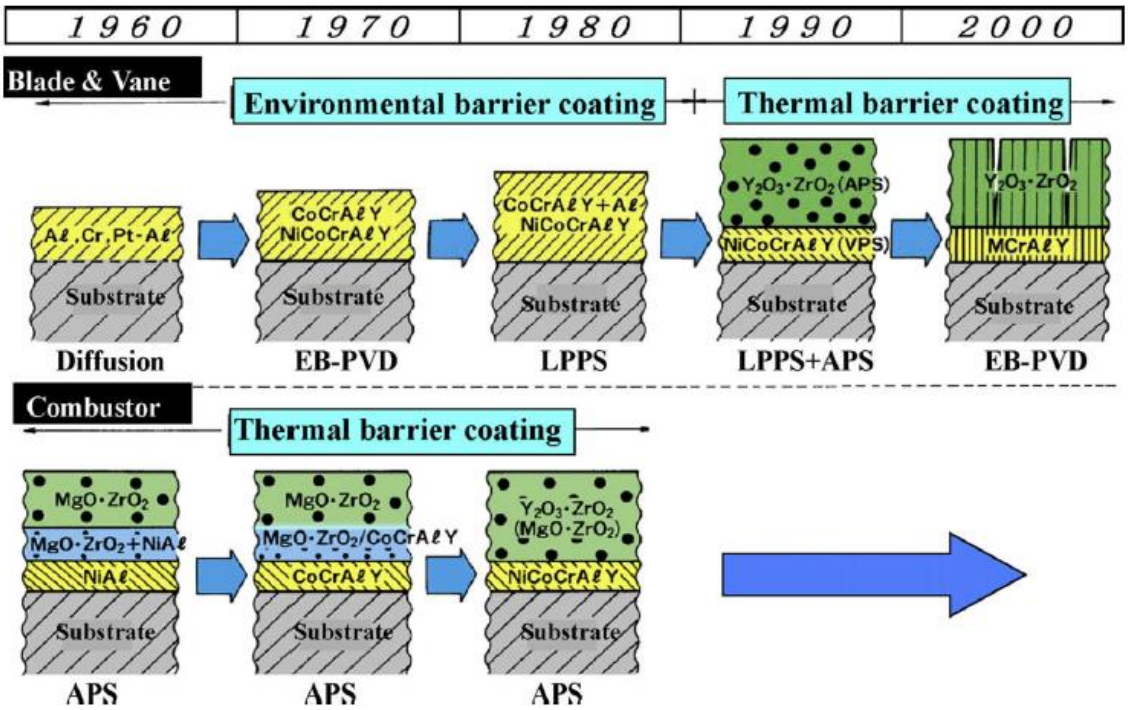

Figure 3.3. Progress of coating technologies for gas turbine hot parts at high temperature. [8]

Figure3.3 shows the progress in development of corrosion resistant and oxidation-resistant coatings (environmental barrier coatings) and thermal barrier coatings for gas turbine hot parts. The severity of the operating conditions of gas turbines differs greatly among the combustor, rotor blades, and stator vanes where thermal barrier coatings have been applied greatly differ accordingly [8].

Superalloy coatings are divided into two main categories: (1) diffusion coatings are coatings that diffuse into the surface and react with alloying elements to form the protective coating, and (2) overlay coatings that are deposited on the surface but only react with the substrate to the extent that an adherent bond is formed [41].

3.1 Diffusional Coatings

Diffusion coating processes have been applied for more than half a century as a cost-effective method of improving the environmental resistance of a base alloy by enriching the surface in Al, Cr, Si, B, Ti, Zn, etc. The coating is also called surface modification process wherein the coating species is diffused into the substrate surface to form a protective layer. Diffusion coatings are the most used method for

providing improved hot-corrosion and oxidation resistance for nickel-or cobalt-base superalloys. Diffusion coatings have been produced with aluminum, chromium, silicon, hafnium, zirconium, and yttrium alloys. The aluminum, chromium, aluminum-chromium duplex, aluminum-silicon duplex, and platinum-modified aluminide coatings are the most commercially significant. [49]

The choice of surfacing material to be used depends on the base alloy and the final application of the component once surface-treated. For example, bolt stock are widely available zinc-coated using the sheradizing process to resist atmospheric and aqueous corrosion, while for high temperature applications, similar bolt materials could be chromized, that is, surfaceenriched in chromium to produce a stainless steel surface layer. [50]

Diffusion of these elements into the material leads to the formation of a surface zone enriched in the elements, thus providing an alloy reservoir for the formation of protective oxide scales under subsequent high temperature exposure. Aluminizing is a widely used method to apply protective coatings on intermetallic titanium aluminides.[51]

In diffusional coating (Figure 3.4) γ' is important phase and behave like a diffusion barrier to decreases the diffusion rates of elements like chromium and aluminum from the protective layer to substrate at the high operating temperatures used in modern aeroengines [52]

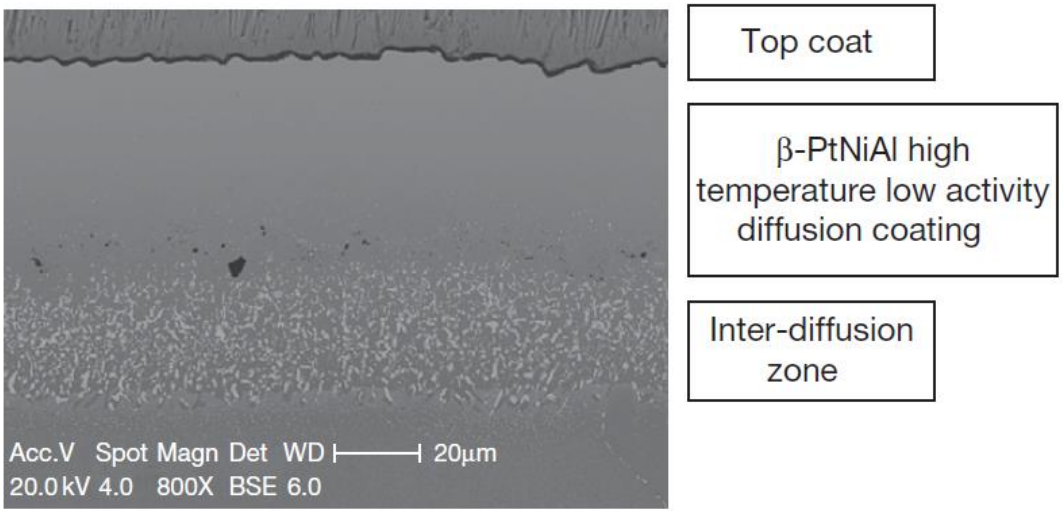

Figure 3.4 : Micrograph of a nickel aluminide coating produced by the Cranfield vapor aluminizing process at a deposition temperature of 1050°C. [50]

The application of aluminium as an alloying element in diffusion coatings is an effective way to increase the oxidation corrosion resistance of treated parts. The coating growth takes place primarily by inward diffusion initially, followed by an intermediate stage where the growth involves both inward Al and outward Ni diffusion. In the final stages, the outward diffusion of Ni dominantes the coating formation. [53]

Two types of processes have been considered. In the first type, the high activity process, the coatings are formed by inward aluminium diffusion and the major phases are Ni_2Al_3 and NiAl. In this case, further annealing of the specimen is necessary for the formation of the desired NiAl phase over the entire coating. The second type of process is the low activity process. In this case, the coating comprises mainly of the NiAl phase and is formed by simultaneous outward nickel and inward aluminium diffusion. [53]

Aluminizing the surface of a nickel-based alloy has been proven to be an effective method to form and maintain a protective Al_2O_3 scale, where the coating behave as a reservoir of Al. [54]

3.2 Overlay Coating

Overlay coatings are different from diffusion coatings in that interdiffusion with the substrate is not required to generate the desired microstructure. Pre-alloyed materials are applied over the substrate. Thus coating composition and microstructure are pre-determined.[22]

As depicted in Figure 3.5, unlike diffusion coatings, overlay coatings admit the control of their composition, thickness, and combination of physical-chemical and mechanical properties within wide ranges. [3]

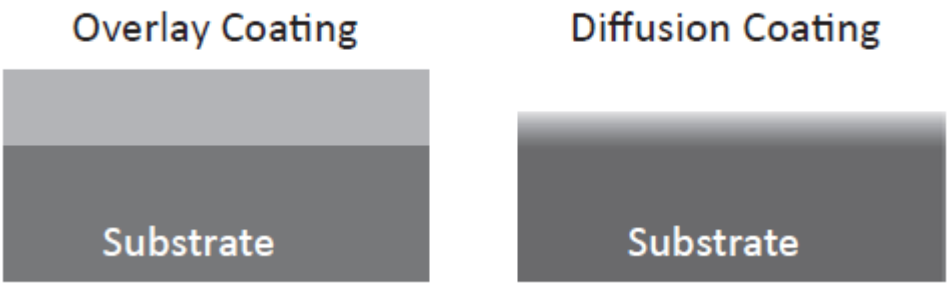

Figure 3.5 : Schematic representation of overlay and diffusion coatings MCrAlYalloys, mainly consisting of an Al-rich β-NiAl phase and an Al-poor γ Ni solid solution, are widely used as stand-alone overlay coatings orbond coats in thermal barrier coatings (TBC) to protect the components in gas turbine engines against oxidation and corrosion. [56]

The behavior of diffusion coatings is strongly dependent on the composition of the substrate alloy because the alloy participates in the formation of the coating. These coatings are based on the βNiAl phase of the Ni–Al alloy system. NiAl has poor solubility of other elements. As a result, these coatings do not offer wide flexibility for the incorporation of minor elements. [57]

In order to address this limitation, a new class called ‘‘overlay’’ coatings has been developed with minimal direct contribution of the substrate alloy. The overlay coatings have a typical composition represented by MCrAlX, where M stands for Ni, Co, and occasionally Fe, and X represents oxygen-reactive elements such as Zr, Hf, Si, and Y. The composition is so selectedthat the microstructure consists of varying amounts of β/γ phase in a matrix. [58]

3.3 Thermal Barrier Coatings

Thermal-barrier coatings (TBCs) are refractory-oxide ceramic coatings applied to the surfaces of metallic parts in the hottest part of gas-turbine engines, enabling modern engines to operate at signifi cantly higher gas temperatures than their predecessors [58].

Gas-turbine engines, used to propel aircraft and to generate electricity, are Carnot engines where their efficiency and core power are directly related to the gas temperature entering the turbine section. Further increases in the energy efficiency of gasturbine engines, both to increase the electricity output and, for jet engines, the

thrust-to-weight ratio and durability, will rely on further improvements in TBCs. At the same time, as gas temperatures are increased in the pursuit of higher engine efficiency, there are new challenges to existing TBCs. [43]

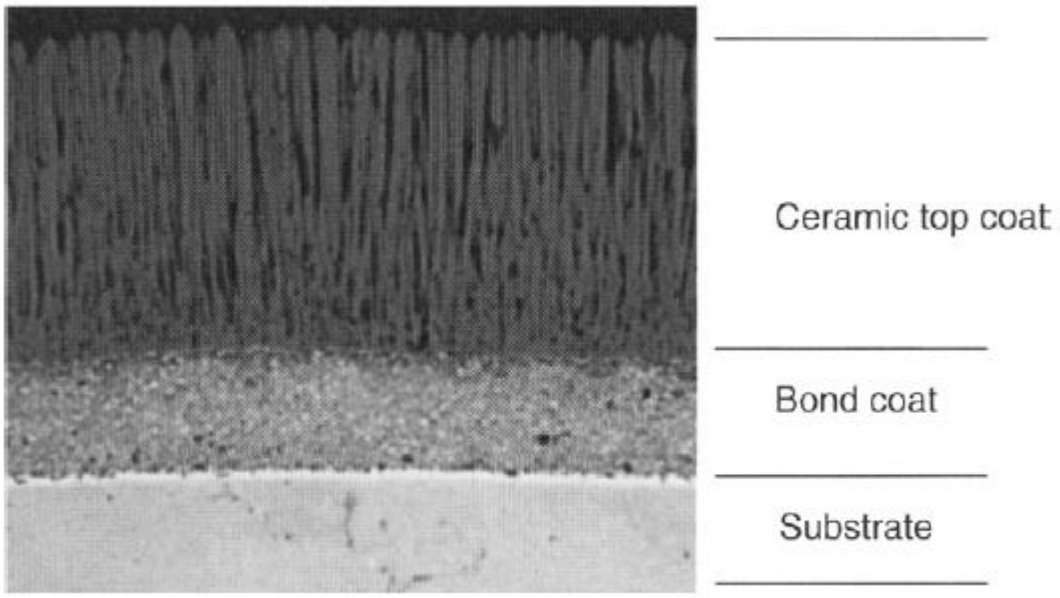

Figure 3.6. Thermal Barrier Coating consisting of metallic bond coat on the substrate and ceramic top [59]

Research has been initiated the understaing of thermal barrier systems to aid in the development of more durable coatings (Figure 3.6-7). Early improvements based on durability of bond coat (MCrAlY) were based on better oxidation and hot corrosion resistance, and oxide adherence of these coatings. The large benefical effect effects of thermal barries lowering blade matel temperature up to 170°C. [60]

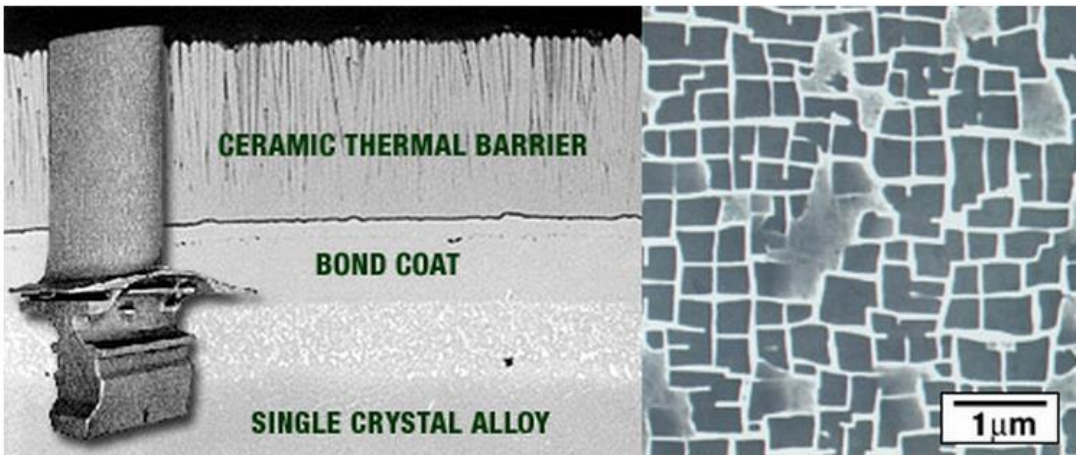

Figure 3.7 : High pressure turbine blade (left), structure of the blade (center) and a magnified view of a single crystal alloy (right). **[15]**

Modern TBCs consist of four primary layers: (i) the superalloy substrate, (ii) an aluminum-rich bond coat that is formed or deposited on the surface of the superalloy, (iii) a thermally grown oxide (TGO) that grows on the top of the bond coat and (iv) a ceramic top coat. [61]

The outer ceramic layer is typically zirconium oxide (ZrO_2) with 6–8% yttrium oxide added to partially stabilize the zirconia tetragonal phase. A dense interfacial ZrO_2 film provides chemical bonding between the columnar zirconia top coat and the inner oxidation resistant bond coat. [41]

3.4 Degradation Mechanisms of Coatings

The working condition of hot gas path component is very challenging therefore demand protective coating on surface of the component. The coating must have capability to number of defect such as high temperature oxidation, corrosion, creep, fatigue etc. as seen at Figure 3.8. The capability is achieved by alloying element to make coating as a physical barrier between aggressive environments and the substrate. Due to the 42 percent of the failures in gas turbines caused by blading problems, the failures and protection ways are essential. [62]

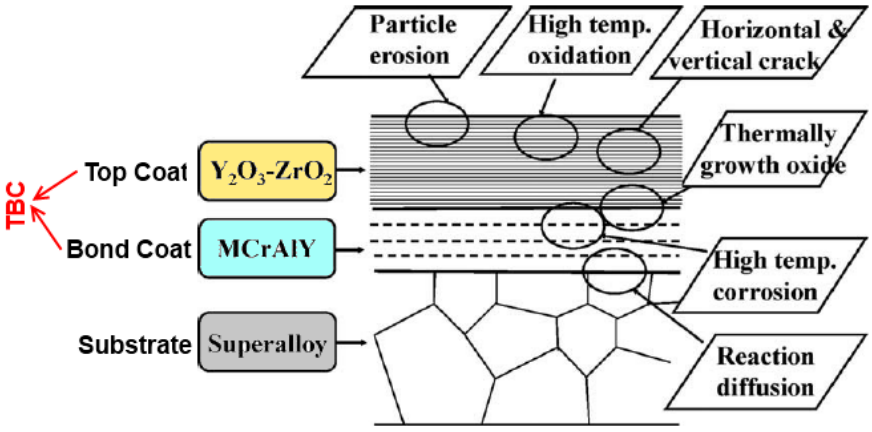

Figure 3.8 : Various damage modes observed in thermal barrier coatings during operation **[48]**

Oxidation or corrosion of the alloy in the hot gas path is environmental degradation of component. Reaction between oxygen and the metal alloy to form various oxides. These chemical reactions remove material or deplete the material of strength. At high temperatures, these reactions can occur rapidly and create the potential for failure if an excessive amount of the alloy is consumed. [63]

The alloys chemistry determines the oxidation behavior. At high temperatures, rapid oxidation attack can occur unless there is a barrier to oxygen diffusion and reaction on the exposed alloy surfaces. Ni-base superalloys containing a sufficient amount of Al will form a protective, adherent, and slow growing alumina (Al_2O_3) scale to prevent extensive oxidation damage. Alloy chemistries can be furthered modified to improve oxidation behavior by adding Y or reducing S. [3]

Hot corrosion is a rapid form of attack that is generally associated with alkali metal contaminants, such as sodium and potassium, which react with sulfur in the fuel to form molten sulfates. In general, uncoated, cooler areas of a hot gas path component are susceptible when fuel is contaminated, synthetic fuel is used, or there is a lot of debris taken into the turbine from the environment. Basicall, molten deposits on the component break down the protective oxide scale, and rapid, unpredictable degradation proceeds [2].

Without the introduction of protective coatings, safety of Ni-base superalloy from oxidation and corrosion is difficult. Many high strength Ni-base superalloys are not capable of forming a sufficiently protective oxide scale because the chemistry of the alloy. However it cannot be optimized for oxidation or corrosion resistance because it must meet other requirements such as high strength, creep resistance, and microstructural stability[64]. In today's advanced industrial gas turbines, coatings are required to provide protection from;

- oxidation,
- corrosion, and
- mechanical property degradation with service.

The function of these coatings is to provide a surface reservoir of elements such as Al and Cr that will form stable, adherent oxide layers that will protect the substrate alloy from environmental attack. [65]

4 MICROSTRUCTURE AND MECHANISM OF COATING

While the formation of the coating, diffusion of the elements and their respond to anneling time and temperature under required specified conditions are play important role. The diffusion and temperature could give the coating good condition or have ability to make it worsen. Therefore examination of the microstructure is important to understand the effect of environemntal condition (annealing time, temperature, gas) and elements responds. To make it understandable it begins with the phase diagram of the Ni-Al. [66]

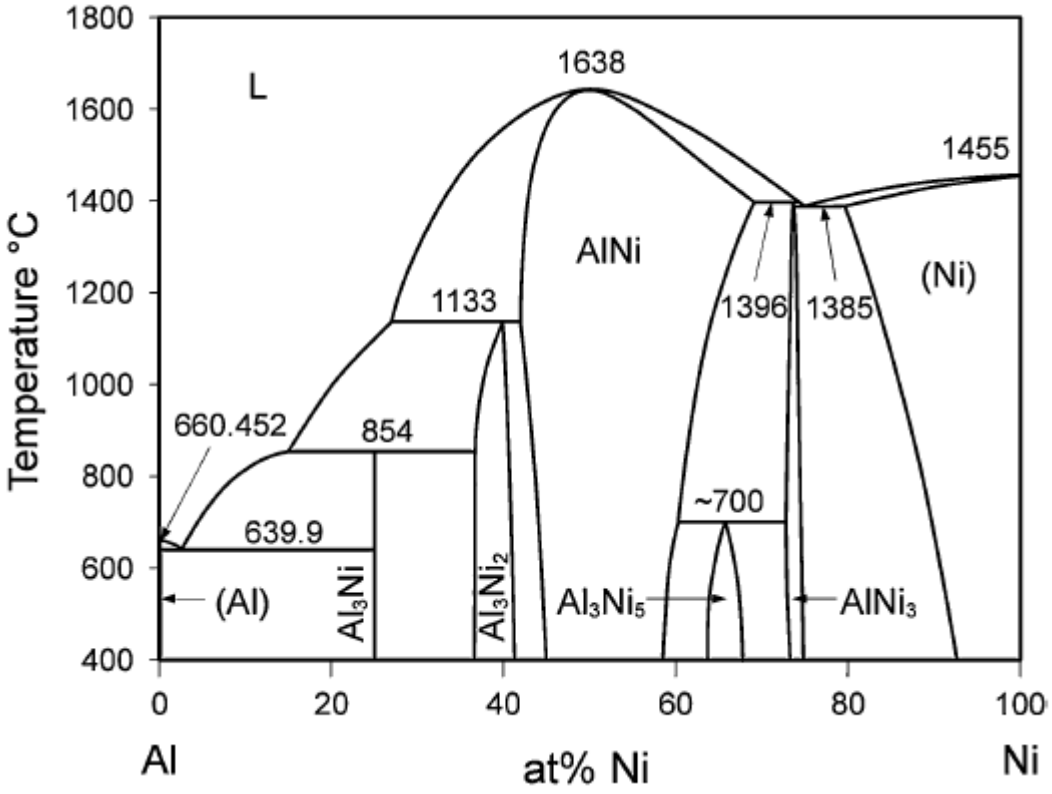

Figure 4.1 : The Al-Ni phase diagram **[67]**

The phase diagram (Figure 4.1) for this system exhibits two solid solutions (0.1 at. % solubility of Ni in Al, and approximately 7 at. % solubility of AI in Ni at 400 ºC), and five stable compounds, $NiAl_3$, Ni_2Al_3, NiAl, Ni_5Al_3, and Ni_3Al [68].

The $NiAl_3$ phase forms with only 3:l stoichiometry. This phase was the initial phase formed in earlier investigations of Al/Ni bilayers. The equilibrium phase is AlNi, when Ni concentrations between 45 and 59 at. % at temperatures of 400°C. In addition, there is at least one metastable compound, usually formed by rapid quenching of aluminum alloys containing 2-12 at. % Ni, which has been identified as the η phase[69, 64].

Ni_3Al (Figure 4.2-a) is L_{12}-type ordered crystal structure based on FCC lattice. The other important phase is near equiatomic,β-phase (Figure 4.2-b), nickel aluminide alloys have a B2 crystal structure and a high melting point (approximately 1995 K) and a low density (approximately 5.9 g/cm3) [71].

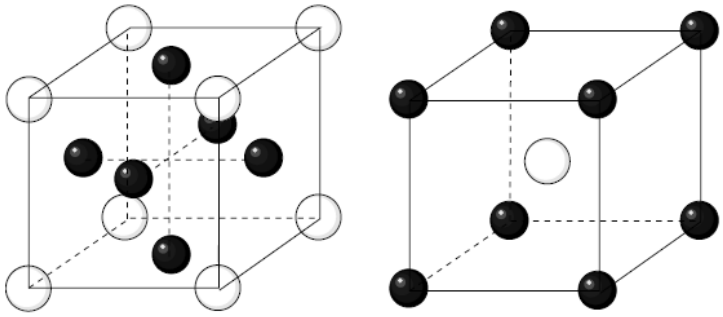

Figure 4.2 : Lattice structures of the aluminides: Ni_3Al, NiAl, and Al atoms are represented by black spheres, respectively. [71]

They have been shown to be highly resistant to oxidation and corrosion, while maintaining structural integrity during thermal cycling. These characteristics have resulted in the widespread use of NiAl-based bond coats in TBC systems.[47]

The three important aluminides and their crystal structure are given at Figure 4.3

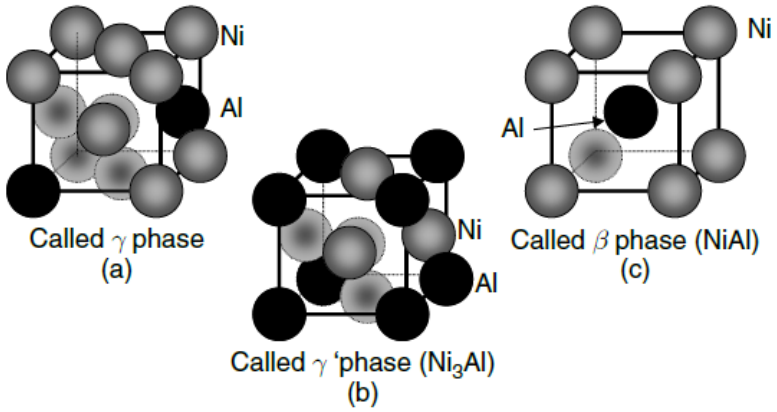

Figure 4.3 : Gamma (γ), Gamma prime (γ') and gamma double prime (γ") phaseslattice structure

The formation of aluminides in the coating is critical in respect to mechanism that takes place.Thus, the diffusion aluminide coatings on superalloys are classified by microstructure as being of the "inward diffusion"(high activity process) or "outward diffusion"(low activity process) type (Figure 4.4). An inward coating is formed when the aluminum activity is higher than the nickel activity. Aluminium diffuses inward faster than nickel diffuses outward through the nickel – aluminide intermetallics that is formed on the surface. A brittle Ni_2Al_3 outer layer with adjacent NiAl intermetallic phase is formed due to high aluminium activity. As such a coating is brittle and has a low melting point, the additional heat treatment is required to convert the brittle Ni_2Al_3 phase into less brittle NiAl – Al rich>50%at [72].

Outward diffusion coatings are formed when aluminium activity is lower than the nickel activity and processing is carried out at a higher temperature (between 980 and 1090°C). Under these conditions, coatings are formed by the selective diffusion of nickel outward through the monoaluminide layer. [73]

The γ phase dissolves up to 4 wt % Al below 400°C. The solubility increases as the temperature is raised. The melting point of the resulting alloy decreases as Al content is increased in this phase. The γ' phase, on the other hand, has a narrower phase field, which means that the composition does not depart significantly from Ni_3Al. The β fields very broad, indicating that in this phase the concentration of Al can depart widely from the stoichiometric composition NiAl. Also, the melting point of the β phase is much higher than that of pure Ni [2]. The high Al concentration of β phase helps in providing a large reservoir of Al for oxidation protection through the

formation and replenishment of Al_2O_3 scale. The change in microstructure of a β-phase-containing coating on thermal exposure can also be analyzed by the use of the phase diagram. [53]

Diffusivities of Ni (D_{Ni}) and Al (D_{Al}) are strong functions of the stoichiometry of NiAl For example

- Low-activity: $D_{Ni}/D_{Al} \approx 3.0$ for Ni-rich NiAl with Al content <50 at %, but
- High-activity: $D_{Ni}/D_{Al} \geq 3$ for Al-rich NiAl at about 51.5 at % Al,

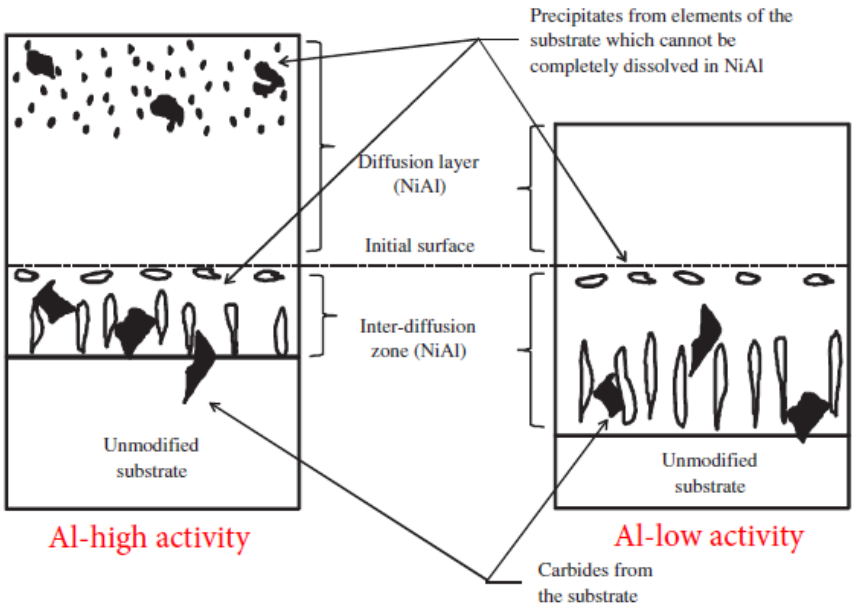

Figure 4.4 : Schematic illustration of NiAl coating structure on nickel-base superalloy produced by high (left) and low activity (right) process [74]

The aluminum activity, therefore, plays a critical role in determining the predominant diffusing species. Depending on the content of aluminum in the pack and the processing temperature, the coating process istermed a ‘‘low-activity’’ or ‘‘high-activity’’ process. When the

- Low-activity: Aluminum activity is low, and the temperature is in the high end of the temperature window (>1000°C), the predominant diffusing species is Ni, which diffuses out of the alloy, producing an ‘‘outward diffusion’’ coating. [74]
- High-activity: If the aluminum activity is high, as happens in the low end of the temperature range (<950°C),Al diffuses inward, resulting in an ‘‘inward

diffusion'' coating. Aluminum is also the predominant diffusing species in Ni2Al3. [5] [74]

- ε(Al_3Ni) and δ(Al_3Ni_2) phases involves virtually singular aluminum diffusion while the opposite, virtually singular nickel diffusion occurs during the formation of the β(AINi) and γ'($AlNi_3$) phases. [72]
- Al_3Ni and Al_3Ni_2 which is very brittle at room temperature. Post-heat treatment is required to convert from these phases to NiAl having better strength at high temperature. [2]

4.1 Low Activity, Outward Diffusion

The high-activity pack process, the coating growth takes place primarily by inward diffusion initially, followed by an intermediate stage where the growth involves both inward Al and outward Ni diffusion (Fifure 4.5). In the final stages, the outward diffusion of Ni dominantes the coating formation. [53]

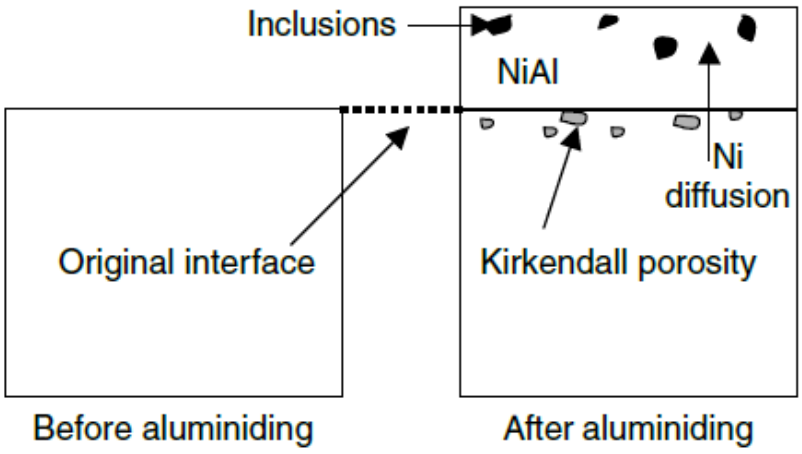

Figure 4.5 : Diffusion aluminide formation on pure Ni. **[2]**

In the low-activity process Ni is the predominant diffusing species, which diffuses outward and combines with aluminum to form the external NiAl zone (Ni+Al = NiAl). Near the interface, the internal zone, which is also called the interdiffusion zone (IDZ), loses Ni. The loss of Ni from the alloy results in the formation of NiAl. The NiAl so formed in the inner zone has very low solubility for many of the alloying constituents of the alloy. These constituents, therefore, precipitate out as

shown later . The low-activity coating appears to have two zones, both of which are NiAl phase. The total coating thickness includes both external and interdiffusion zones. [2]

4.2 High Activity, Inward Diffusion

The high-activity coating process is characterized by Al as the predominant diffusing species. The consequences of higher inward diffusion of Al relative to outward Ni diffusion are the absence of Kirkendall porosity, elimination of embedded pack particles, and the original surface becoming the external surface of the coating. (Figure 4.6)The microstructural detail and the coating composition depend on the Al activity. [72]

The process' major phases are Ni_2Al_3 and NiAl. In this case, further annealing of the specimen is necessary for the formation of the desired NiAl phase over the entire coating. The second type of process is the low activity process. In this case, the coating comprises mainly of the NiAl phase and is formed by simultaneous outward nickel and inward aluminium diffusion. [53]

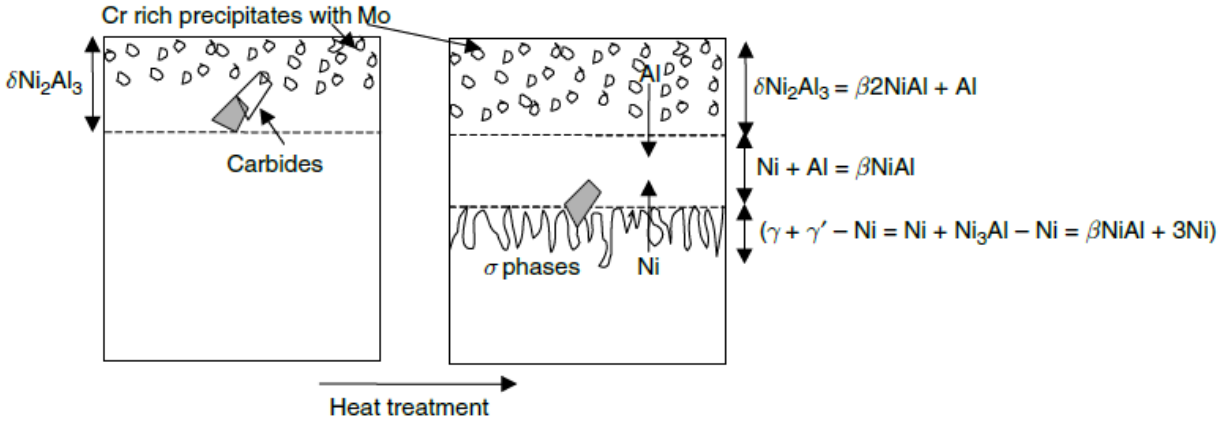

Figure4.6 : Microstructure formation in high-activity process. **[2]**

Qualitatively, three possibilities exist:

(a) Very high Al activity results in the formation of a δNi_2Al_3 phase.

(b) High Al activity results in a δNi_2Al_3 outer layer with adjacent NiAl of high Al content.

(c) Moderate Al activity results in βNiAl of high Al content. [73]

To form acceptable coatings, cases (a) and (b) require additional heat treatment to convert the brittle δNi_2Al_3 phase into less brittle, Al-rich ‘‘hyper-stoichiometric’’ (>50 at %) βNiAl. Whereas Al is the predominant diffusing species in hyperstoichiometric βNiAl and δNi_2Al_3, Ni diffusion dominantes in ‘‘hypostoichiometric’’ (<50 at % Al) composition. Therefore, Al diffuses inward in the top third of the coating while Ni diffuses outward in the bottom third, the interdiffusion zone. The NiAl in the middle zone forms because of the combination of the Ni moving out of the inner zone and the Al moving in from the outer zone. [53]

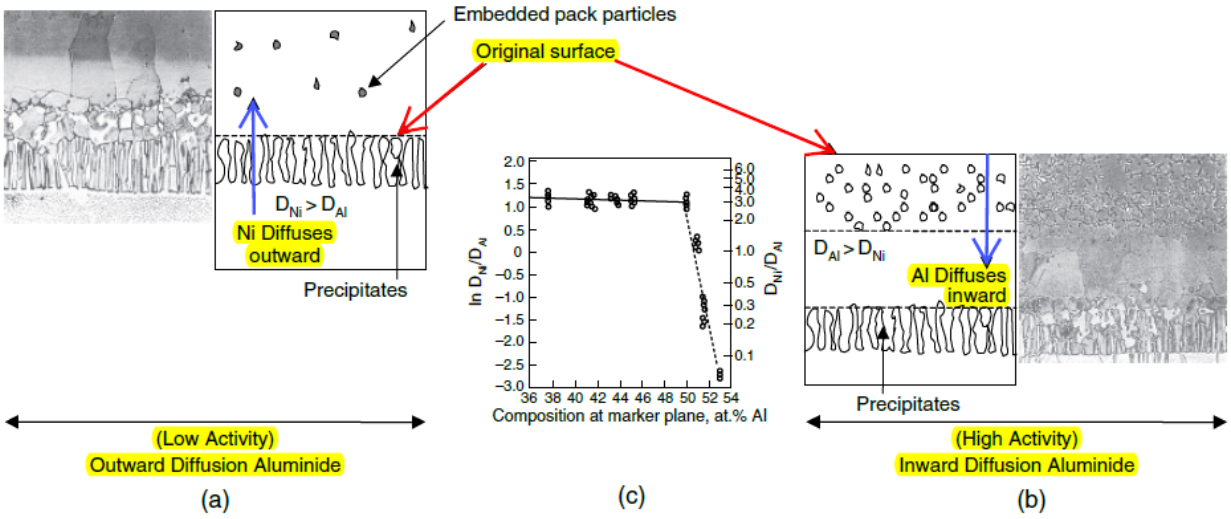

Figure 4.7 : Microstructure of (a) low- and (b) high-activity aluminide coatings (c) Dependence of Ni and Al diffusivities as a function of NiAl composition [2]

The growth mechanism and the formation of coating microstructure of the low- and highactivity aluminides are compared in Figure 4.7

The growth of the coating is diffusion controlled. The thickness, therefore, increases roughly as the square root of exposure time at the processing temperature. The coating thickness can be increased to some extent by raising the process temperature. However, the possibility of interface melting and depletion of the strength of the pack material become matters of concern.[2]

5 PROCESSES FOR APPLYING COATINGS

High temperature operating components require coating process and thermal barrier coating (TBC) find a increasing application in the most demanding high temperature environment of aircraft. Therefore the most important method is applied during years is thermal spray coating to resurfacing engineering components. It provides functional surface to protect or modify the behavior of substrate material by spraying powder onto surface and bonded them with mechanical and kinetic enegy [75]

Performing under increasing firing temperatures and excessive contamination in the operating environment, it has become difficult to design superalloys, which have the necessary creep strength on one side and the required resistance to corrosion / oxidation on the other side. Bring coating on to surface of the blades is unevitable to provide the necessary protection to the blades. [49]

The function of the coating is to act as reservoir of elements, which will form very protective and adherent oxide layers, thus protecting the underlying base material from oxidation, corrosion attack and degradation. To provide that kind of protection, many types of coating are applied to blade surface therefore there are many branch on application technique. [76]

Figure5.1 depict the thermal spray injecting process onto materials surface by high gas velocities through gun. The spraying creates a protective and adherent layer on to surface.

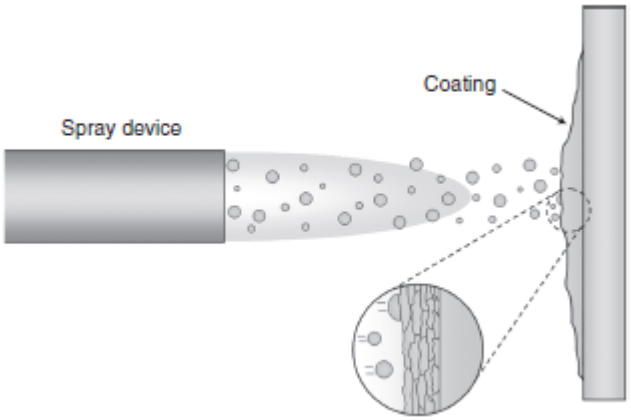

Figure 5.1 : Generic thermal spray process. Molten or semi-molten droplets are sprayed onto a target surface where they 'splat' cool and form a layeredmicrostructure. [77]

Five basic thermal spray processes are available commercially (Figure 5.2). Flame spray powder/wire, detonation, and High Velocity Oxygen Fuel (HVOF) are three of the basic processes associated with combustion. Plasma and wire arc are two other processes that utilize electric energy to help melt consumable materials. The five processes, HVOF and detonation spraying are two that result in high bond strength with extremely dense microstructures. Plasma coatings are also known to have high bond strength with relatively dense oxide-free microstructures when sprayed in either Low-Pressure Plasma Spray (LPPS) or Vacuum Plasma Spray (VPS) Systems [75]

Table 5.1: Relative Particle Velocity/Process Temperatures to Thermal Spray Process **[75]**

Process	ParticleVelocity (m/s)	Process Temperature (°C)
Cold Spray	800-900	500-900
Combustion Powder	30-200	2,500-3,000
Combustion Wire	30-100	2,500-3,000
HVOF Powder	700-800	2,500-3,000
Plasma APS	200-300	15,000
Plasma LPPS/VPS	200-300	15,000
Arc Wire	50-150	3,000

The other and important kind of coating is cold gas dynamic spray and it is the main coating application technique of the thesis. The following passages are survey the basic principle and general technique of before mentioned coatings.

HVOF processes are suitable not only for applying Tungsten Carbide-Cobalt and Nickel Chromium-Chromium Carbide, but also for depositing wear and corrosion alloys such as Inconel (NiCrFe), Triballoy (CoMoCr) and Hastelloy (NiCrMo) materials. HVOF MCrAlY (M5Ni,Co or Fe) coatings are also replacing some LPPS coatings for high temperature oxidation, hot corrosion and thermal barrier bond coat applications for repair and restoration of existing components. [75]

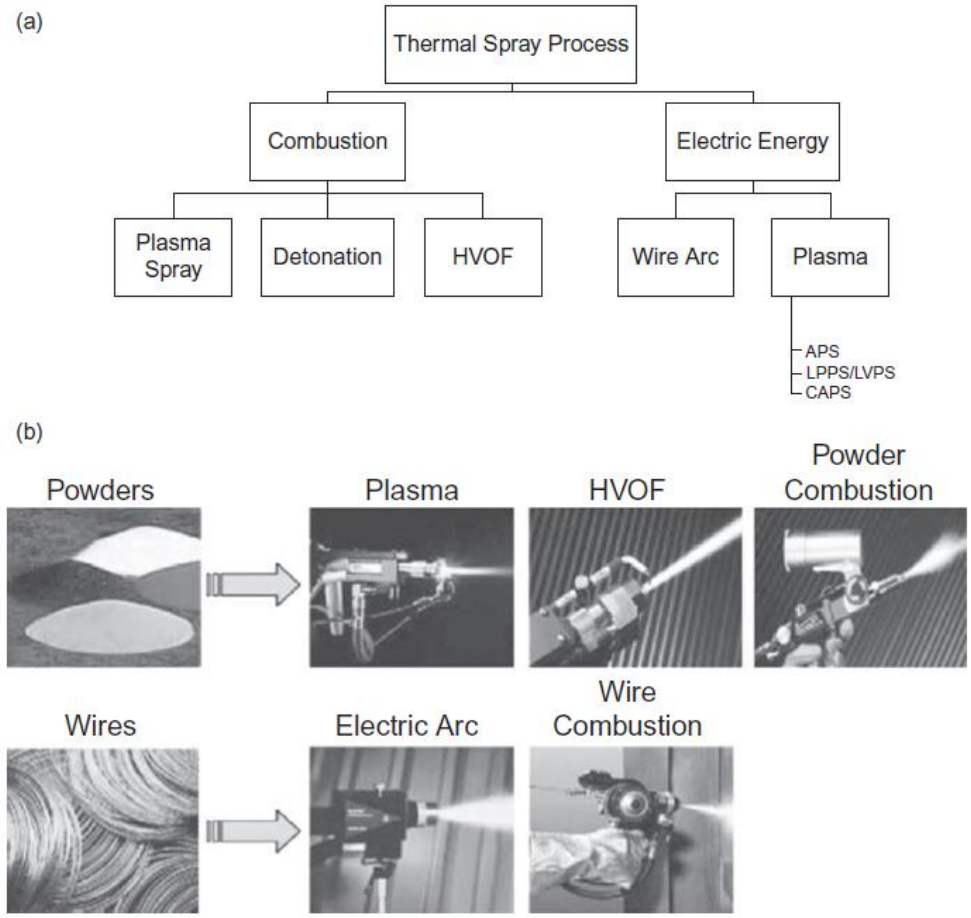

Figure 5.2 : (a) Types of thermal spray processes. (b) Thermal spray materials and processes. [75]

Plasma LPPS and VPS coatings typically have high bond strengths with very low levels of porosity and oxides. High quality coatings are achieved by placing a plasma gun in a reduced pressure between 50_200 mbar. Major applications for LPPS spraying are MCrAlY bond coats for thermal barriers, MCrAlY coatings for blades/vanes and buckets for oxidation and hot corrosion, and repair of superalloy components. [75]

5.1 Cold Gas Dynamic Spray (CGDS)

Cold spray was originally developed in the mid-1980s at the Institute of Theoretical and Applied Mechanics of the Russian Academy of Sciences in Novosibirsk by Dr. Anatolii Papyrin and his co-workers. They successfully deposited a wide range of pure metals, metallic alloys, polymers and composites onto a variety of substrate materials, and they demonstrated that high density coating and deposition rates can be obtained using the cold spray process.[78]

Various terms—including "kinetic energy metallization," "kinetic spraying," "high-velocity powder deposition," and "cold gas-dynamic spray method"—have been applied to the general form of this technique. In most instances, deformable powder particles are brought to high velocities through introduction into a nozzle, employing gas-dynamics principles of converging/diverging flows to develop high-velocity gas streams.[79]

5.1.1 Overview of cold spray

Cold spray (or fully cold gas-dynamic spray) is an evolving technology for the production of coatings and bulk forms (Figure 5.3). In the cold spray process, powder particles are accelerated to very high speeds (500-1200 m/s) by high-pressure compressed gas at a temperature that is always lower than the melting point of the deposited material, forming coatings from particles in the solid state [1-6]. Due to the low-temperature deposition process, cold sprayed coatings are essentially free of thermally induced deleterious defects commonly observed in traditional thermal spray coatings, such as oxidation, evaporation, gas release, shrinkage porosity and thermal residual stresses. [80]

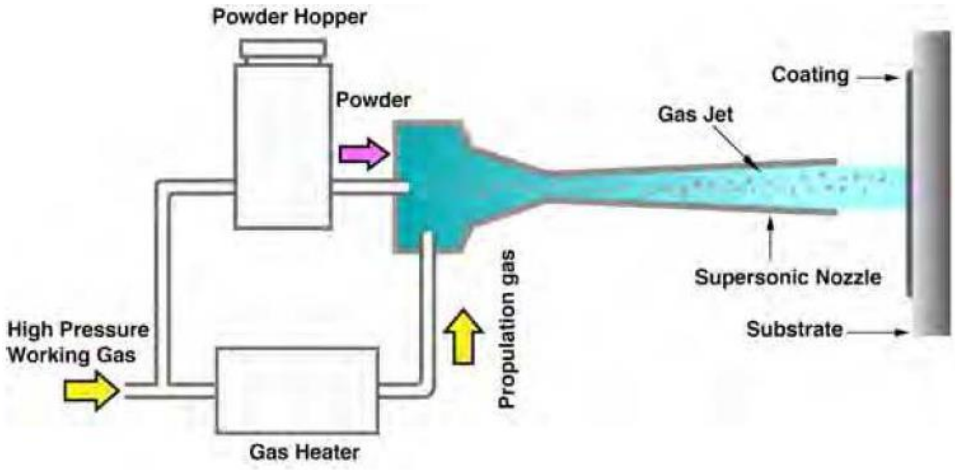

Figure 5.3 : Schematic illustration of cold spray apparatus [81]

The cold spray system accelerates powder particles, making them impact, deform and bond to create a dense layer of material on the substrate. A critical velocity needs to be attained before bonding takes place.[82]

Table 5.2. Typical range of gas-jet parameters for cold spray coating [79]

Parameters	**Range**
Stagnation jet pressure, MPa (psi)	1–3 (145–435)
Stagnation jet temperature, °C (°F)	0–700 (32–1290)
Gas flow rate, m^3/min (ft^3/min)	1–2 (35–70)
Powder feed rate, kg/h (lb/h)	2–8 (4–18)
Spray distance, mm (in.)	10–50 (0.4–2)
Power consumption, kW (for heating gas)	5–25
Particle size, µm	1–50

Operating gases: air, nitrogen, helium, and their mixtures.

The metallic particles range in size from 5 to 50 µm and are accelerated by injection into a high velocity stream of gases. (Table 5.2)The high velocity gas stream is generated through the expansion of a pressurized, preheated gas through a nozzle (converging-diverging). The pressurized gas is expanded to supersonic velocity, with an accompanying decrease in pressure and temperature. The powder particles, initially carried by a separate gas stream, are injected into the nozzle either prior to the throat or downstream of the throat. [83]

The temperature of the gas stream is always below the melting point of the particulate material during cold spray, and the resultant coating and/or freestanding structure is formed in the solid state. Since adhesion of the metal powder to the substrate, as well as the cohesion of the deposited material, is accomplished in the

solid state, the characteristics of the cold spray deposit are quite unique. Because particle oxidation is avoided, cold spray produces coatings that are more durable with better bonding. [84]

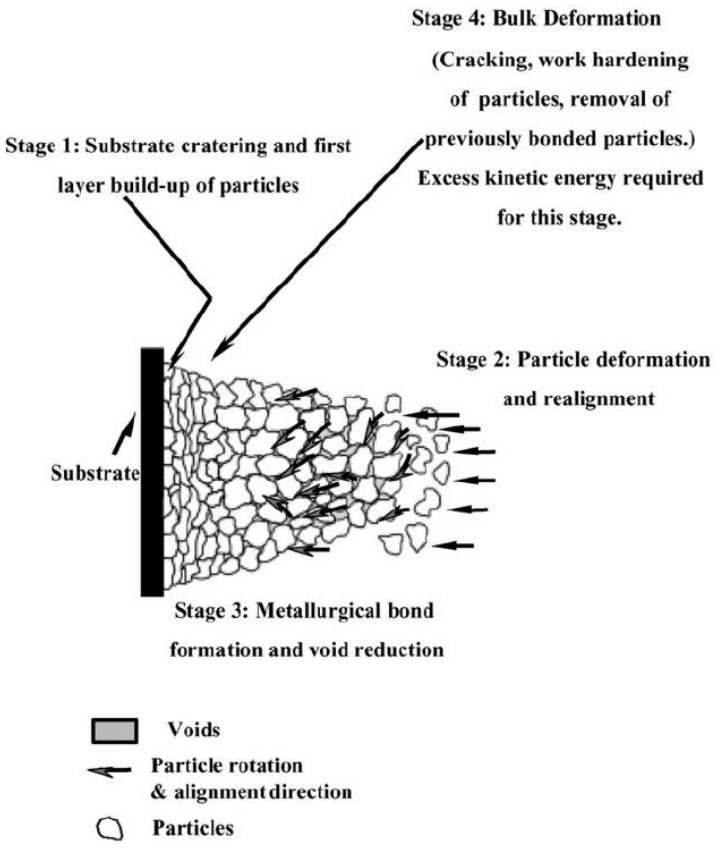

Figure 5.4 : Stages of coating formation in the cold spray process [85]

The process, involving highvelocity impact of solid powder particles. Coating is formed through plastic deformation upon impact of spray particles, temperatures of which are much lower than the melting point of spray material. (Figure)Therefore, oxidation and composition and phase changes during cold spraying can be minimized or avoided [86]

The particles are accelerated by main nozzle gas flow and are impacted onto a substrate after exiting the nozzle. Upon impact, the solid particles deform and create a bond with the substrate. As the process continues, particles continue to impact the substrate and form bonds with the deposited particles, resulting in a uniform coating with very less pores and high bond strength. The term “cold spray” has been used to describe this process due to the relatively low temperatures of the expanded gas stream that exits the nozzle. [85, 87]

A key concept in cold spray operation is that of critical velocity. The critical velocity for a given powder is the velocity that an individual particle must attain in order to deposit after impact with the substrate. Small particles achieve higher velocities than do larger particles, and since powders contain a mixture of particles of various diameters, some fraction of the powder is deposited while the remainder bounces off. The quality of the cold sprayed coating is affected by not only particle velocity, but also the particle size and size distribution. [81]

5.2 Comparing Cold spray with Thermal Spray Coating Technologies

On eof the main difference of cold spray form traditional spraing technique is, the heating the cold spray process gas (300–800 °C) is not to melt the spray material. The gas is heated primarily to increase the sonic velocity of the gas in the 'throat' (point of smallest diameter) of the converging–diverging nozzle, which creates a higher spray jet velocity, while also reducing process gas consumption. Because expansion of the gas in the diverging portion of the nozzle rapidly cools the gas, it exits the spray gun nozzle at a much lower temperature, in some cases even below room temperature. Hence, the name 'cold' spray. [77]

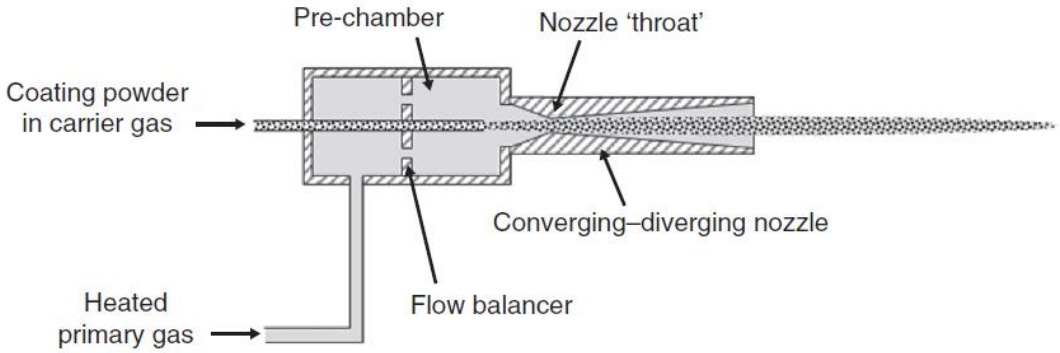

Figure 5.5 : Schematic diagram of a cold spray gun. [77]

The most deleterious effects of depositing coatings at high temperatures is the residual stress that develops, especially at the substrate-coating interface. These stresses often cause debonding and this is compounded when the substrate material is different from the coating material. This problem is minimized when cold spray is used and it overcome important limitations of traditional thermal spray technologies, such as high levels of porosity and oxide in the sprayed material. Nevertheless, it

represents an important new process capability that may replace more traditional spray processes in selected applications. [77]

6 SIMILAR PRIOR ARTS

Untill the section, the diffusional coatings and their creation ways are examined. However, some part of the literature fit better the thesis filed. Terefore the studies of the important prior art documents are enlighten the working way therefore there is a section about the papers.

The study of Zielinska et al. (2011) examine the aluminide layer behavior that is deposited by CVD method on Inconel substrate. [73]

The begining of the paper outward and inward diffusion of aluminum is described according to followings;

- Inward diffusion"(high activity process): Al diffuses faster inward than Ni diffuses otward through nickel-aluminide intermetallic layer that is formed on surface. The production phases of the diffusion are δNi2Al3 (brittle- outer layer) and βNiAl. The coating is brittle and has low melting temperature. Additional heta treatment is required to conversion of brittle δNi2Al3 to βNiAl (Al rich>50%at)
- Outward diffusion"(low activity process): Ni diffuses faster than Al about between 980 and 1090°**.** Under the condisiton Ni outward through the monoaluminide layer. Overall aluminum content is hypostoichiometric, providing somewhat better ductility in the coating.

The paper is interested with five types of inconel however only IN718 result is shared. The applied process aluminum activity is low and conducted at 1050°C for 8 hours by CVD method.

The SEM image of the sample that is aluminide coating on IN718 obtained in a low activity CVD process at the temperature 1050°C for 8h, presented at Figure. According to figure, the interdiffusion zone (point 2-3) and aluminide layer (point 1) are clearly seen.

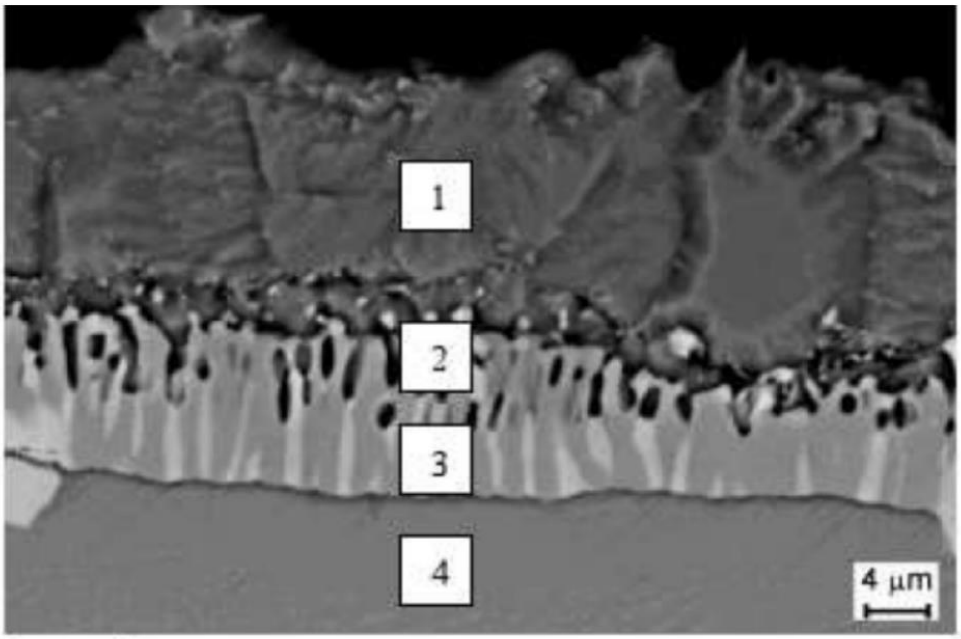

Area (Fig. 5)	Element content, % mas						
	Al	Ti	Cr	Fe	Ni	Nb	Mo
1	24.71	-	5.31	8.69	61.3	-	-
2	18.87	1.51	6.82	9.50	59.69	3.61	-
3	1.43	0.37	37.83	22.84	17.64	19.9	-
4	4.11	1.13	20.35	18.94	49.08	3.67	2.7

Superalloy	Elements content, %mas.														
	Ni	Cr	Co	Mo	W	Ta	Al	Ti	C	B	Zr	Fe	Nb	Si	Mn
Inconel 718	52.5	19.0	–	3.0		–	0.5	0.9	0.03	–	–	18.5	5.1	0.2	0.2

Figure 6.1 : Microstructure of aluminide coating on IN718 obtained in a lowactivity CVD process at the temperature 1050°C for 8handcorresponding chemical compositions in the areas marked in the figure, below is corresponding chemical composition of IN718. [73]

The elemental contents table of the Figure 6.1 is graphed at Figure6.2 clearly understand the percentage change of the constituent elements. The nickel mass raction decrease at point 3 due to outward diffusion of nickel.

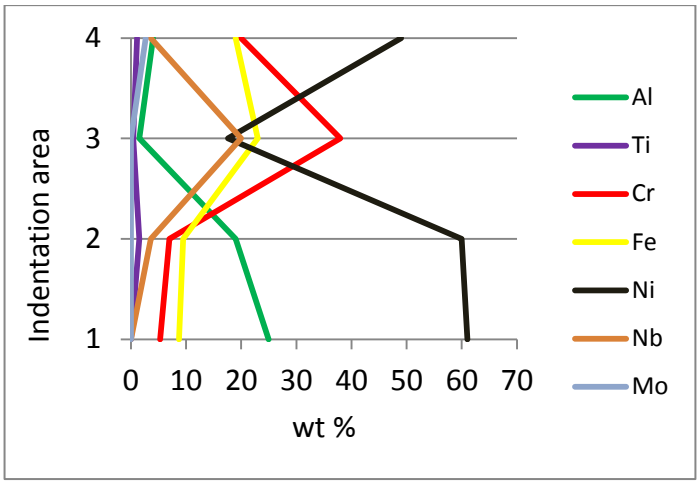

Figure 6.2 : Elemental mapping of Zielinska paper

According to Figure6.1 and Figure6.2, the following results obtained,

- Chromium, molybdenum and tungsten segregate to the coating and form precipitates such as carbides MC and $M_{23}C_6$, or sigma phases which make the nickel diffusion difficult (point 2-3)
- The aluminide phase is formed by transformation of γ+ γ' to β-NiAl because of nickel withdrawal to the outer coating zones, not by aluminium diffusion into the substrate.
- The internal zone – so-called interdiffusion zone which consist of refractory metal (tungsten molybdenum, tantalum etc) carbides, and/or complex intermetallic phases in NiAl and/or Ni_3Al formed by the removal of nickel from underlying alloy. (point 2-3) [73]

The study Das et al. (1998) provide extensive research about inward and outward diffusion mechanism and the substrate material is heat-treated CM-247 rods were aluminized using a high-activity pack.

The pack mixture used a

- Ni-Al alloy powder (5-15 wt %) as the aluminum source,
- NH4Cl (2 wt %) as the activator, and
- Alumina powder (balance 93- 83 wt %) as the inert filler.

According to composition, percentage there is two different coating composition and their code names are 5-2-93 and 15-2-83

The aluminizing treatment was carried out at 1034 ºC using 50 g of the pack mixture in a horizontal tube furnace having a constant temperature zone of about 200 mm in length. Samples were aluminized for varying lengths of time ranging from zero hour to 10 hours.

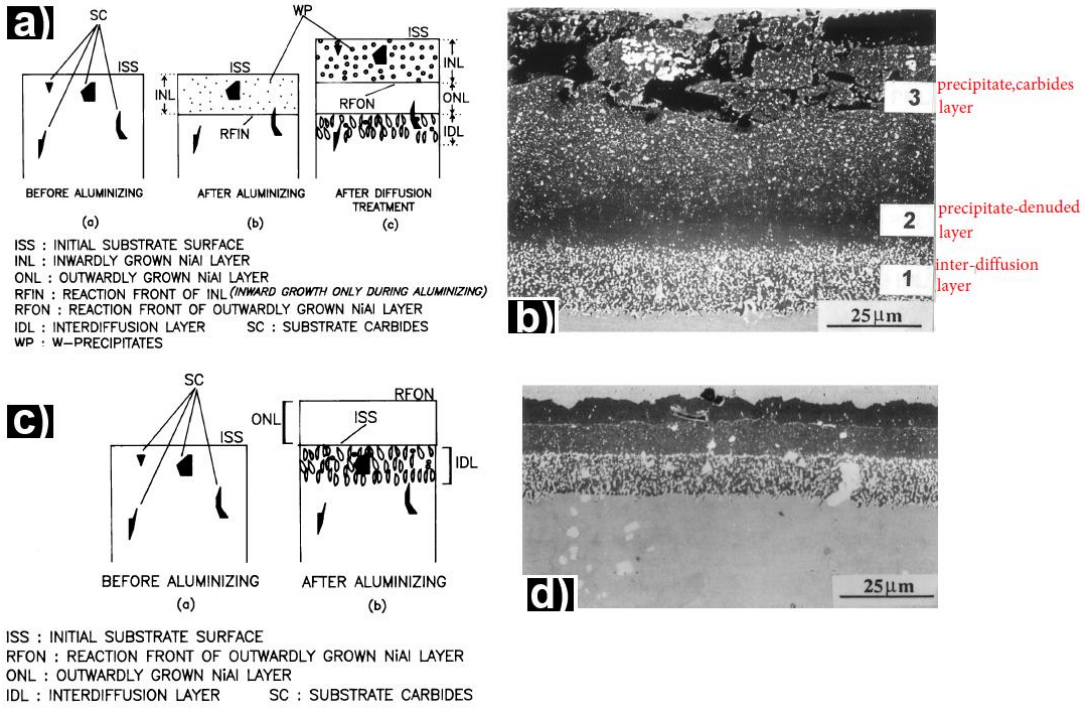

Figure 6.3 : Diffuison mechanism (inward) (a) and microstructure of 15-2-83 pack (b) and diffusion mechanism (outward) (c) and microstructure of 5-2-93 pack (d). The coatings are aluminized at 1034 ºC for 4 h [88].

The selected specimens annealing duration is 4 h and their diffusion mechanisms are sketched next to SEM image of the samples. The important point of the paper, it used structural carbides as a marker to determine the diffusion of nickel, aluminum and other constituent elements.

Figure 6.3 (a), show the high activity aluminizing process in two step and temperature in the range 700ºC to 850ºC a layer of an aluminum-rich phase, which is usually Ni_2Al_3 or a mixture of Ni_2Al_3 and hyperstoichiometric NiAl, forms on the substrate. This is a result of predominant inward diffusion of aluminum from the pack, which causes the coating layer to grow into the substrate starting from its surface. The carbide in this layer is indicative sign of inward coating growt during aluminizing.The lack of sufficient solubility of substrate elements Cr, W, Mo, *etc.* in Ni_2Al_3 and NiAl phases also frequently causes these elements to precipitate out in the above layer.

The high-activity pack process, the coating growth takes place primarily by inward diffusion initially, followed by an intermediate stage where the growth involves both inward Al and outward Ni diffusion. In the final stages, the outward diffusion of Ni dominantes the coating formation.

Figure6.3 (c) is show the mechanism of outward diffusion which is usually carried out above 1000ºC Ni amount become reduce and it causes the precipitation varirous elements originally present in the solid solution of superalloys. The low activity coating includes two layers, outer layer is NiAl layer which does not include carbide and precipitates. The second layer is inner layer, includes carbides, and precipitates due to Ni reduction.

To conclude the two mechanism; low activity diffusion consist of only nickel outward while at high activity diffusion outward and ainward diffusions are takes place together and they creates diffusion layers [88].

7 DIFFUSION MECHANISM

Transport in materials via random individual atomic migration steps (jumps) is called ‘diffusion’. While in liquids and gases, diffusion rate ranges up to millimeters or even centimeters per second, transport in solid materials is rather slow. In densely packed metals near to the melting point,

one can expect about a micrometer per second and this rate drops down to about a nanometer per second at half the melting temperature. At room temperature atomic migration is practically frozen,

except for few exceptional cases of small interstitial impurities [89]

7.1 Fick’s First Law

Fick’s first law defines the diffusion coefficient ($D1$) of the component 1

and flux in an inhomogeneous single-phase binary alloy due to concentration

gradient as:

$$J = -D\frac{dC}{dx} \qquad \textbf{(7.1)}$$

The constant of proportionality D is called the diffusion coefficient, which is expressed in square meters per second. The negative sign in this expression indicates

that the direction of diffusion is down the concentration gradient, from a high to a

low concentration If the concentration of the diffusant can be defined at the entrance and exit surfaces of the sample separated by distance x in steady-state condition, the diffusivity can be measured easily by monitoring the flux in the absence of a driving

force. [70]

7.2 Fick's Second Law

Most practical diffusion situations are nonsteady-state ones. That is, the diffusion flux and the concentration gradient at some particular point in a solid vary with time, with a net accumulation or depletion of the diffusing species resulting. Fick's second law describes diffusion in a non-steady-state condition when the concentration changes with time but particles are neither created nor destroyed. [90]

For variable *D*, Fick's second law is written as:

$$\frac{\partial C}{\partial t} = \frac{\partial}{\partial x}\left(D\frac{\partial C}{\partial x}\right) \qquad \textbf{(7.2)}$$

Fick's second law is the basis of most diffusion measurements in solids in general. It has been widely used in samples in rod, plate, and thin-layer geometry. It has been used for measurements of diffusion in single-crystal specimens, and along grain boundaries and dislocations. [50]

8 EXPERIMENTAL STUDIES

The experimental procedure substrate is the Inconel 718 and chemical composition is represented at Table 7. The precipitation strengthened AMS-5663 type substrate is used during the experiment. Samples were gently cut from a bar rod that's radius 2.55mm then grounded using 120, 240, 400, 800 and 1200 grit SiC paper. Final polishing was made with 1 μm Al_2O_3 slurry abrasive to achieve a mirror-like surface finish. After the metallographic step is completed, samples washed in distilled water and methanol before treatment.

Table 7 : Chemical composition of IN718 (wt%)**[91]**

Ni	Fe	Cr	Nb	Co	Mo	W	Ti	Al	C
52,5	18,5	19	5,1	-	3	-	0,91	0,5	0,08

The coating powders are elemental aluminum (Al) powders (Alfa Aesar™, 99.5% purity, 7-15 μm average particle size) and elemental Nickel (Ni) powders (Alfa Aesar™, 99.8% purity, 5-15 μm average particle size),

The first part of the samples are coated with only aluminum powder and remaining part is coated with both aluminum and nickel in separate steps; first aluminum is sprayed onto IN718 substrate then nickel is deposited on the aluminum coated surface powders or mixture.

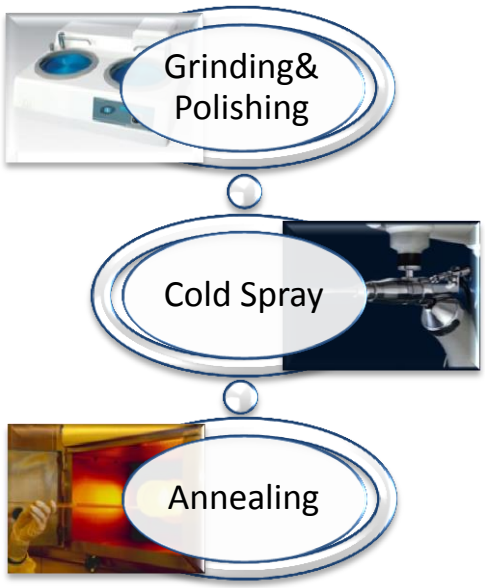

Figure 8.2 : Flow schema of experimental procedure

After coating, each samples is subjected to annealing steps at different temperature and time that will be explained at flowing sections.

8.1 Equipment

In this section, utilised equipments and their functions are described. As mentioned above, first step is metallographic process, second step is cold spray coating, and then all the samples are heated at the related temperatures in air circulated electric furnace.

To make it sensible, Figure is given as an example of coating and annealing. The sample is coated with aluminum and (a) annealed at 900°C for 24 hours (b). At b) annealing effect on the coated specimen is clearly seen.

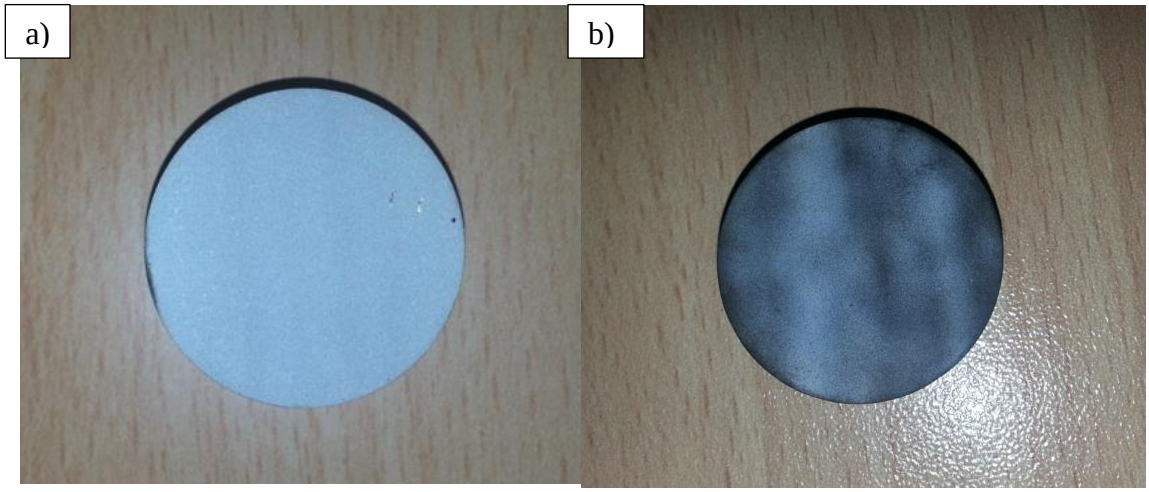

Figure 8.3 :. a) Cold spray coated and after coating b) annealed samples

8.1.1 Cold gas dynamic spray deposition on a sample

The metallographic procedure applied samples are coated by RUSONIC Model K-201 (Rus Sonic Technology, USA) cold spray equipment (Table 8.2) with converging diverging type tubular nozzle having an expansion ratio of 2.3. Powder was fed to the flowing gas downstream from a nozzle. Compressed air at a nozzle inlet pressure of 6 bar (600 kPa) was used as a process gas. The substrate was manipulated on a sample stage controlled by two servo-motors which enable two-axis motion of the stage.

Table 8.2 : Colds Gas Dynamic spray parameters

Cold spray parameters	
Travel speed	10mm/s
Stand of distance	10 mm
Beam distance	2mm
Powder feed rate	2/8 unit
Gas pressure	6 bar
Gas temperature	Air
Substrate	IN718
Powder	Al&Ni

8.1.2 Annealing treatment and codes

Heat treatment procedures of coated specimens were carried out in a laboratory type air circulated electric furnace (Nabertherm, Germany) for different temperature and time.

There are a number of heat treatment parameters and different coating powders, thus an indicative code is given to samples to recognize easily, related annealing temperature, time and sprayed powder. Two examples of codes are demonstrated at below.

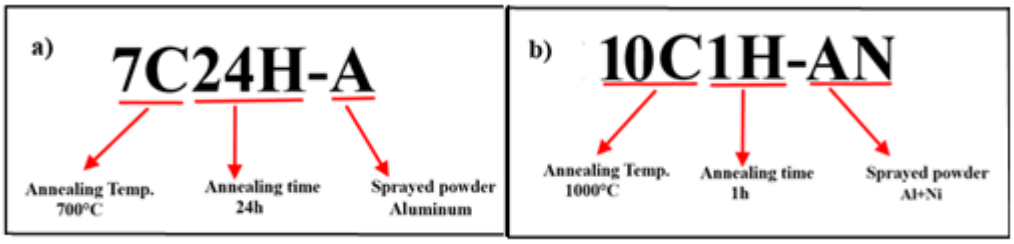

Figure 8.3 : Codes and meaning of the letters a) 7C24H-A is aluminum coated sample and annealed at 700°C for 24h b) 10C24H-AN is aluminum and nickel coated sample and annealed at 1000°C for 1h

According to Figure, the example codes and meaning of the letters are given. The logic of the coding is, the annealing time presented by first digit groups, and "C" stands for the celsius temperature. The numbers coming before "C" infer the anneling temperature. The second letter groups are designated the annealing hour (H) and the numbers refer the exact annealing time. The final groups represent the sprayed powders on IN718 and capital letter of the powders are used as an indicator. For example Aluminum is displayed by "A" and Nickel is shown by "N.

The annealing temperature of 850°C and 1050°C are shown as 85C24H-A and 105C1H-A to prevent the temperature confusion.

The following tables display the whole samples according to annealing temperature, hour and sprayed powders. Table represent the only aluminum coated samples and their annealing condition. Table displays aluminum and nickel coated samples.

Table 8.4 : The codes, annealing time and temperature of the Al coated samples

No	Codes	An. T. (°C)[1]	An. t (h)[2]	Powder
1	000-A	…	…	Aluminum
2	5C24H-A	500	24	Aluminum
3	6C24H-A	600	24	Aluminum
4	7C24H-A	700	24	Aluminum
5	85C24H-A	850	24	Aluminum
6	9C24H-A	900	24	Aluminum
7	95C1H-A	950	1	Aluminum
8	10C1H-A	1000	1	Aluminum
9	105C1H-A	1050	1	Aluminum

The coated but not annealed samples are represented by 3 digits of "000" and sprayed powders the indicating letters are "A" or "AN". For instance, aluminum coated but not annealed samples' code are "000-A", nickel and aluminum applied and not annealed samples code are "000-AN"

Table 8.5 : The codes, annealing time and temperature of the Al+Nickel coated samples

No	Codes	An. T. (°C)	An. t. (h)	Powder
1	000-AN	…	…	Aluminum+Nickel
2	85C24H-AN	850	24	Aluminum+Nickel
3	9C24H-AN	900	24	Aluminum+Nickel
4	95C1H-AN	950	1	Aluminum+Nickel
5	1C1H-AN	1000	1	Aluminum+Nickel
6	105C1H-AN	1050	1	Aluminum+Nickel

8.2 Characterisation

After a series of metallographic treatments, microstructural examinations of the annealed samples were conducted by X-ray diffraction (XRD, Phillips PW 1700) with Cu Ka (1.54060 Å) radiation in the 2θ range of 10–100° with a step size of

[1] Annealing temperaure-Celsius
[2] Annealing time-Hour

0.02° at a rate of 2°/min. The International Center for Diffraction Data® (ICDD) powder diffraction files were utilized in the identification of crystalline phases. X'pert high score plus software is used determining the phases.

The cross-section morphologies of samples were directly observed by SEM (Philips-XL30 SFEG) in high vacuum mode after coating with gold operated at 15 kV and equipped with an energy dispersive spectroscopy (EDS) detector.

The results of XRD, SEM and EDS analysis are examined in detail, at the following section.

9 RESULTS AND DISCUSSION

The section displays the characterization results and interpretations. In order to simplify the results, the section is divided to subsections as regards to coating powders and annealing temperature.

9.1 SEM and XRD Results of IN178, 000A, 5C24H-A, 6C24H-A, 7C24H-A

During the section, XRD and SEM results of IN718 and Al cold sprayed samples; 000-A, 5C24H-A, 6C24H-A, 7C24H-A are examined.

Figure is X-ray diffraction of the related samples. The IN718 diffraction shows the two main phases of γ and γ". The additional aluminum peaks are produced, and they are represented by peak position of the aluminum in the diffraction peak of 000-A,

5C24H-A and 6C24H-A samples provide the expected phase peaks, Al_3Ni and Al_3Ni_2. By the way, Al_3Ni_2 peaks are dominant in 6C24H-A due to the annealing temperature increment.

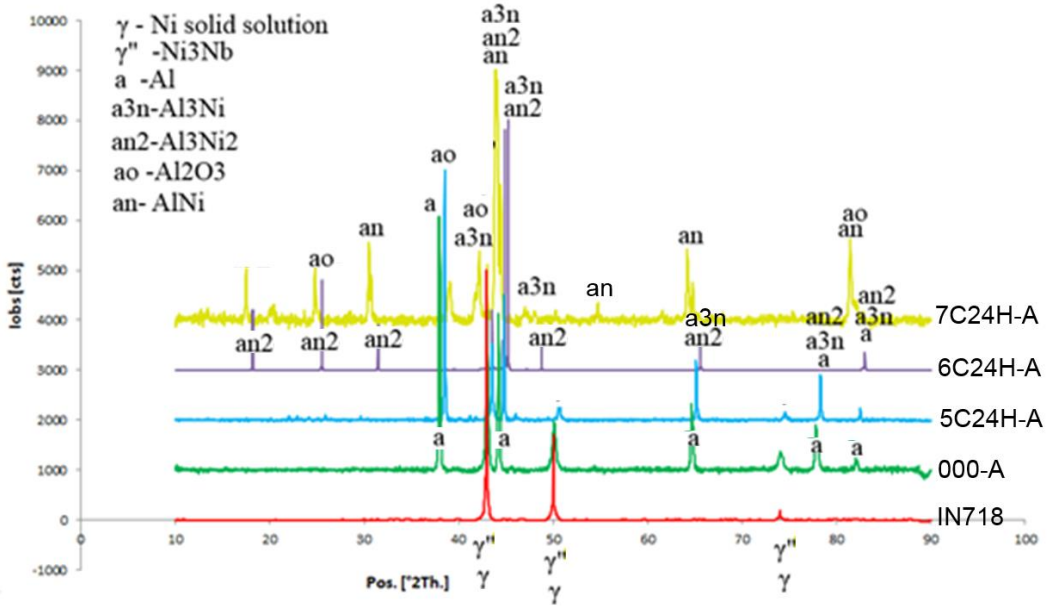

Figure 9.1 : XRD Results of IN178, 000A, 5C24H-A, 6C24H-A, 7C24H-A

The AlNi peaks are only detected on the surface of peaks 7C24H-A . It can be seen that the relative intensities, which express volume fractions, of $NiAl_3$ decreases with decreasing amount of Al in the slurries but volume fraction of Ni_2Al_3 increases.

IN718 SEM image is shown in Figure 9.2. The substrate is age hardened AMS 5663 and the white plate like phases are **γ”** (Ni3-Nb,Ti) and the matrix is Ni solid solution of the γ phase.

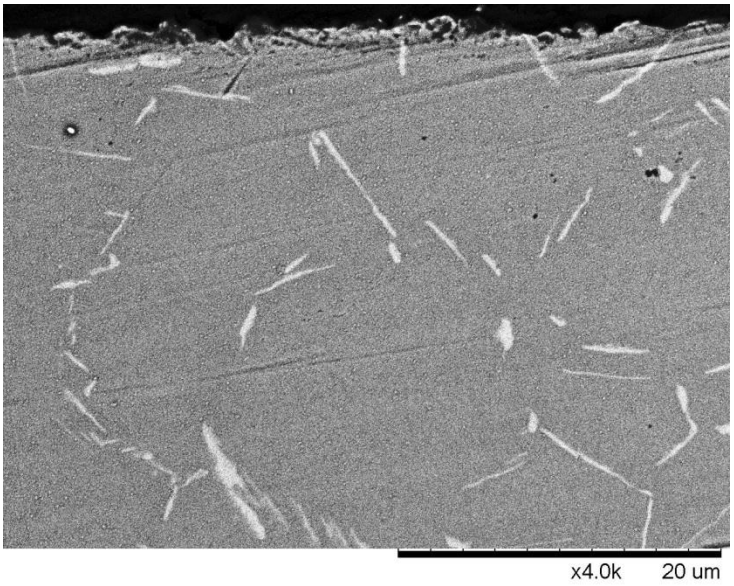

Figure 9.2 : SEM Results of IN718

Figure 9.3 (a) is displayed the SEM image of aluminum cold spray applied sample (000-A). The sprayed coating is approximately 13 μm and it is successfully deposited on the surface. According to the image, aluminum and substrate are easily distinguished from each other.

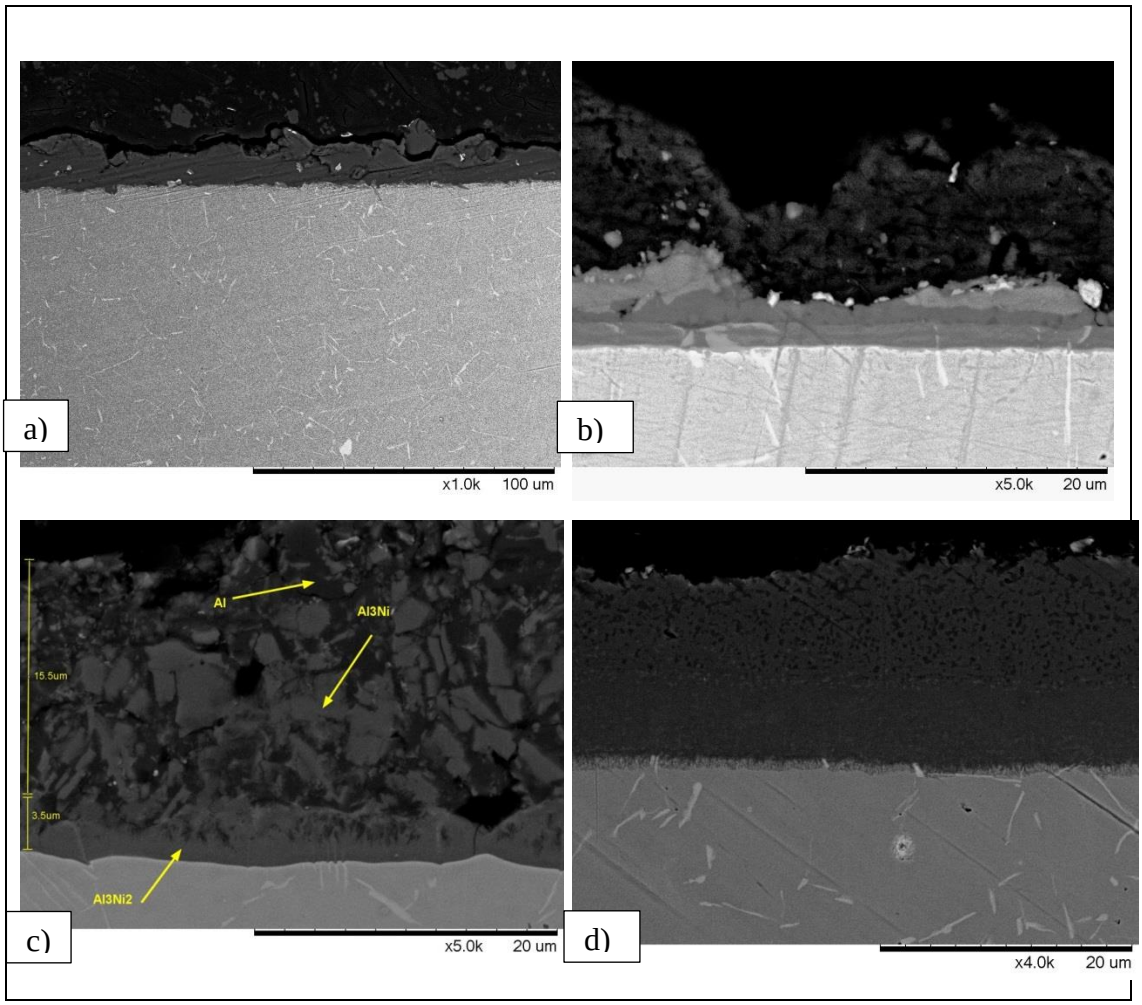

Figure 9.3 : SEM Results of 000A, 5C24H-A, 6C24H-A, and 7C24H-A

The 5C24H-A SEM image shows the first phase formation of almonds. Between aluminum and substrate, there are two different phases; darker phase (next to the substrate) is Al_3Ni_2 and the lighter phase in is Al_3Ni. Their formation reactions are given below

- First of all, Al_3Ni form by reaction of Ni + 3Al
- Then the Al_3Ni phase becomes transform to Al_3Ni_2 by second reaction : $Al_3Ni + Ni \rightarrow Al_3Ni_2$

The 6C24H-A SEM image also supports the reactions of Al_3Ni and Al_3Ni_2. In addition, temperature increase also raises the volume fraction of Al_3Ni_2 while aluminum amount is decreased. Moreover, Al_3Ni are seen like fragmented in the aluminum phase and it tries to consume Al and the Al volume fraction become less at the Figure 9.3 (c)

The AlNi phase become remarkable in the SEM image of 7C24H-A and it shows the first presence of three-layered structure, high activity coating and the multiple layers are formed by inward diffusion aluminum throughout to the substrate.

9.2 SEM and XRD Results of 85C24H-A, 9C24H-A, 95C1H-A, 10C1H-A, 105C1H-A

The following XRD results belongs to the samples are 85C24H-A , 9C24H-A, 95C1H-A, 10C1H-A, 105C1H-A. The figure proves that dominant phase at the related temperature and time is AlNi phase.

The XRD results of 85C24H-A and 9C24H-A samples are clearly shown the AlNi peaks because of their longer annealing time (24h). However, the 95C1H-A, 10C1H-A, 105C1H-A AlNi peaks become smaller from 950°C to the 1050°C. It also shows that the volume fraction of the phases becomes decrease by increase of temperature.In addition the peaks of Al_2O_3 has also become disappear by the means of temperature.

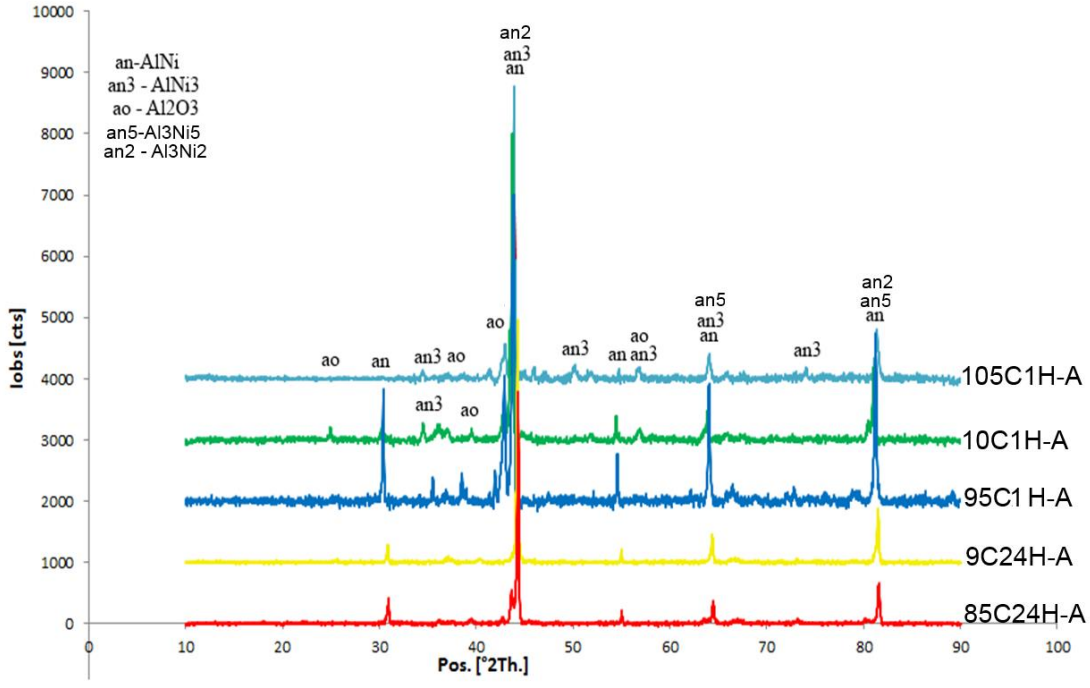

Figure 9.4 : XRD Results of 85C24H-A, 9C24H-A, 95C1H-A, 10C1H-A, 105C1H-A

The following figure is SEM images of 85C24H-A, 9C24H-A, 95C1H-A, 10C1H-A, 105C1H-A and the common feature of the images is all of them depict the same three-layered structure as seen previously in 7C24H-A.

The three-layered structure is formed by predominant inward diffusion of aluminum through the substrate which causes the coating layer to grow into the substrate starting from its surface. The lack of sufficient solubility of substrate elements' Cr, Fe, Ti, *etc.* in Ni_2Al_3 and NiAl phases also frequently cause these elements to precipitate out in the above layer.

The NiAl phase, in the middle layer, was formed owing to the outward diffusion of Ni from the matrix and inward diffusion of aluminum, thus providing a reservoir of Al shows that the thickness of the aluminide coating is uniform. In addition, NiAl phase is a solid solution with Cr and Fe dissolved. However, the solubility limit of most elements in superalloys, such as Cr, Mo, Nb and Si in NiAl phase, is very low therefore; the aluminide layer contains fine precipitates in a matrix of NiAl.

In the final stages, the outward diffusion of Ni dominants the coating formation and reduction of Ni cause the precipitation of carbides (MC, $M_{23}C_6$) and sigma phases (σ-Cr,Fe)

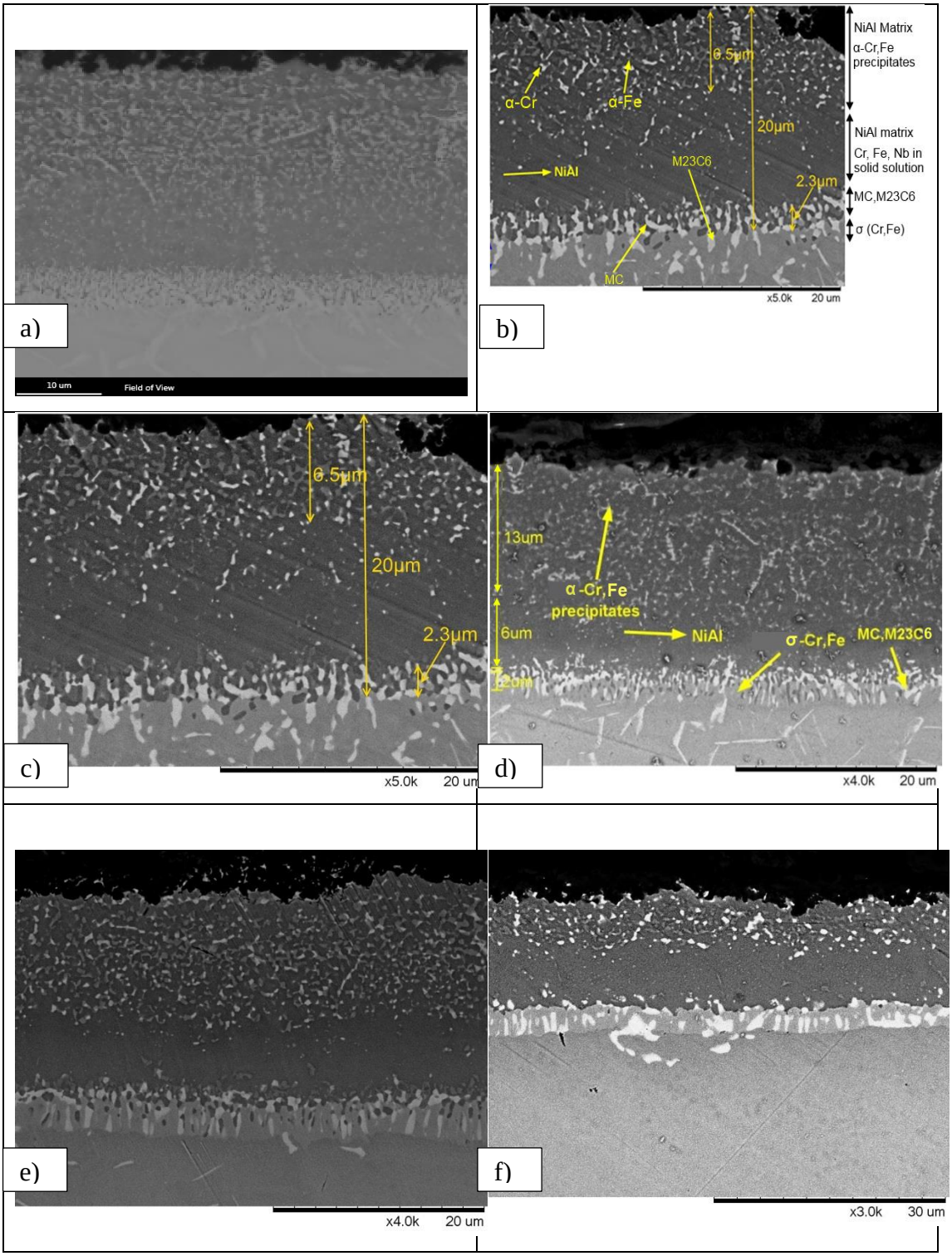

Figure 9.5 : SEM Results of a) 85C24H-A b) 9C24H-A indexed c) 9C24H-A d) 95C1H-A e) 10C1H-A f) 105C1H-A

Formation of σ phase in the vicinity of MC carbides is further assisted by the fact that the carbides and σ phase have similar crystal structures and is highly coherent, but the growth of these σ plates is restricted by the MC carbide and dependent on the

availability of σ-forming elements in the region surrounding the carbide in the third (lowest) layer.

The conditions that favor σ-phase precipitation (chromium, and iron enrichment) can also favor the precipitation of $M_{23}C_6$ carbides. Because the carbide has a lower free energy than σ phase, the presence of carbon in the dendritic region can promote the formation of $M_{23}C_6$, retarding σ-phase formation by depleting chromium, and iron.

The consumption of niobium, and titanium by MC carbide formation has also been observed to reduce σ-phase formation. Consumption of these γ ′-forming elements through carbide formation reduce γ ′volume fraction, improving microstructural stability but reducing the strength.

The first and third zones are mechanically weak, brittle due to the formation of refractory precipitates, and carbides.

9.3 SEM and XRD Results of 000AN, 85C24H-AN, 95C1H-AN, 10C1H-AN, 105C1H-AN

The section, aluminum and nickel coated samples SEM and XRD results are examined. The codes of the related samples are 000AN, 85C24H-AN, 95C1H-AN, 10C1H-AN, 105C1H-AN and the cold sprayed but not annealed sample is 000A.

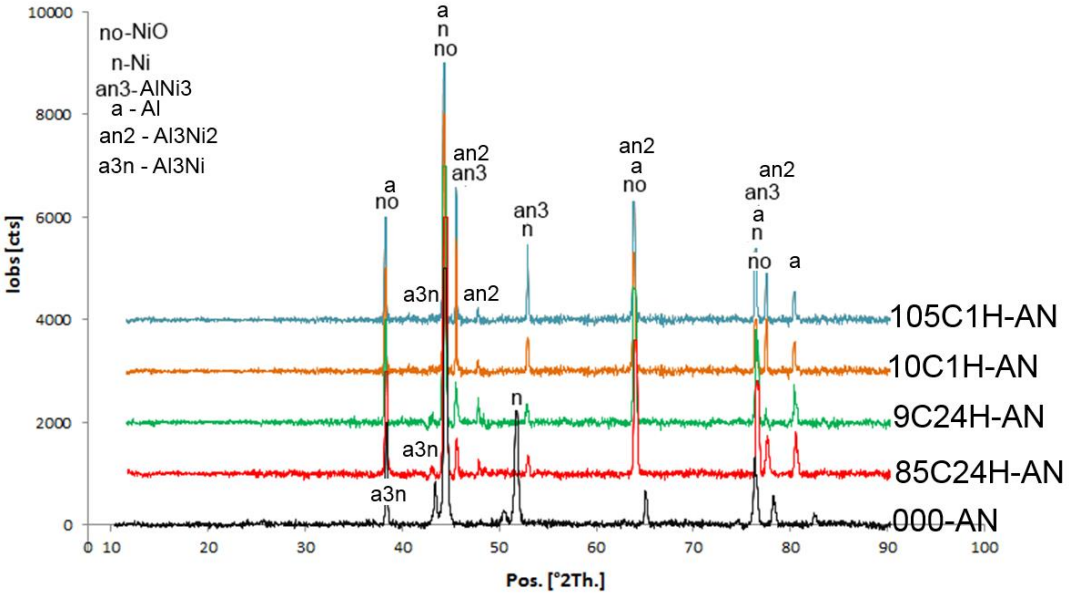

Figure 9.6 : XRD Results of 000-AN, 85C24H-AN, 95C1H-AN, 10C1H-AN, 105C1H-AN

Figure provides the XRD study of 000AN, 85C24H-AN, 95C1H-AN, 10C1H-AN, 105C1H-AN. The 000-AN peaks show the aluminum nickel and other substrate constituent phase peaks clearly. From 85C24H-AN to 105C1H-AN the Al_3Ni peaks transform to Al_3Ni_2 peaks because the volume fraction of the phase is increased in respect to temperature rise.

According to Figure (a), Ni and Al phases are easily distinguished from each other. Light phase is Ni and dark phase is Al.

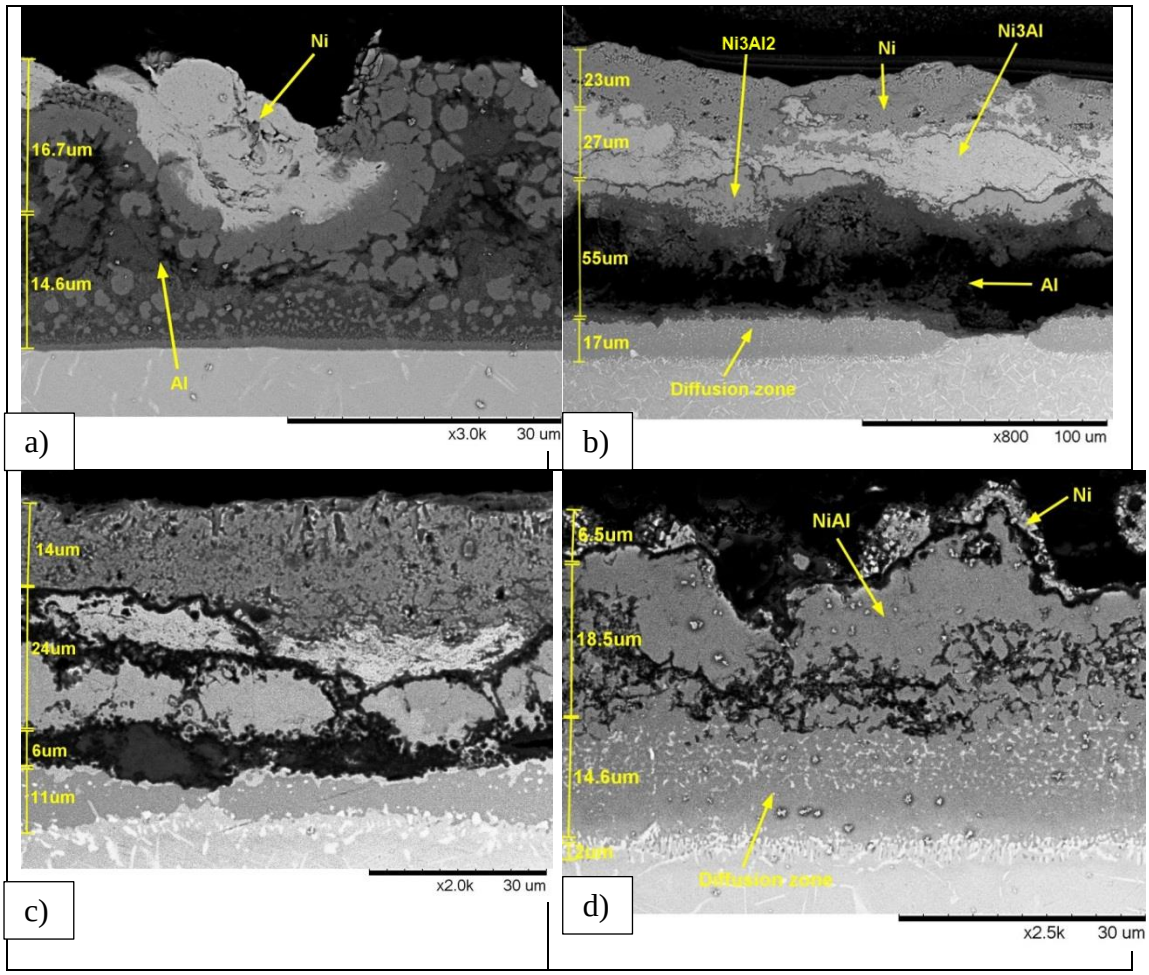

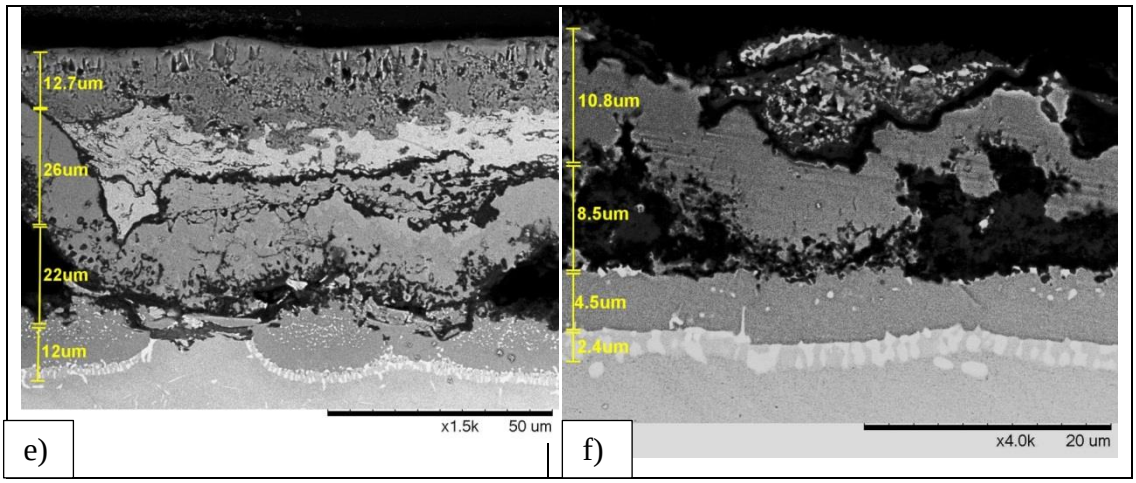

Figure 9.7 : SEM results of a) 000AN b) 85C24H-AN c) 9C24H-AN d) 95C24HAN e) 10C24H-AN f) 105C24H-AN

The 85C24H-AN samples' microstructure looks like cracked and porous due to the aluminum consumption. The high activity diffusion is taking place in the coating, and aluminum is consumed before create a bond between nickel and substrate. Moreover, the two sides produce their own diffusion zones. The separately placed $NiAl_3$, Ni_2Al_3 phases (in the nickel side) and the three-layered structure (in the substrate side) are proof of the independent reaction and phase formation.

When comparing, the 9C24H-AN and 95C24H-AN, the cracked type structure becomes vanished, and at 10C24H-AN nickel and substrate side try to create bond between each others. The 105C24H-AN does not offer so many difference, and it just produces more homogeneous middle layer phase (AlNi) when compare with earlier samples.

Among the aluminum and nickel coated specimen, the most successful sample is 95C1H-AN, because of the gap between nickel and substrate is disappearing by time and the three-layered diffusion zone is clearly seen. However, it still does not a best candidate for high temperature coating because of the cracked type structure is still present and temperature increment does not eliminate the detrimental formation.

The temperature increment boosts the volume fraction of the AlNi phase between the coating. However there is still nickel or nickel aluminide which does not transform to the NiAl phase. Because, aluminum cannot wet nickel surface due to the formation of nickel aluminide layer which separates the liquid aluminum and the nickel matrix. Nickel aluminide layer prevents liquid aluminum from spreading, therefore cannot

cover the entire surface of nickel. That is also explanation of nickel presence although the annealing temperature rises.

9.4 EDS Analysis Elemental Mapping of 9C24H-A

The following Figure 9.8, shows the elemental analysis point on the 9C24H-A. According to the point analysis in Figure 9.8, Energy Dispersive X-ray spectroscopy (EDS) results and chemical distribution of elements are generated.

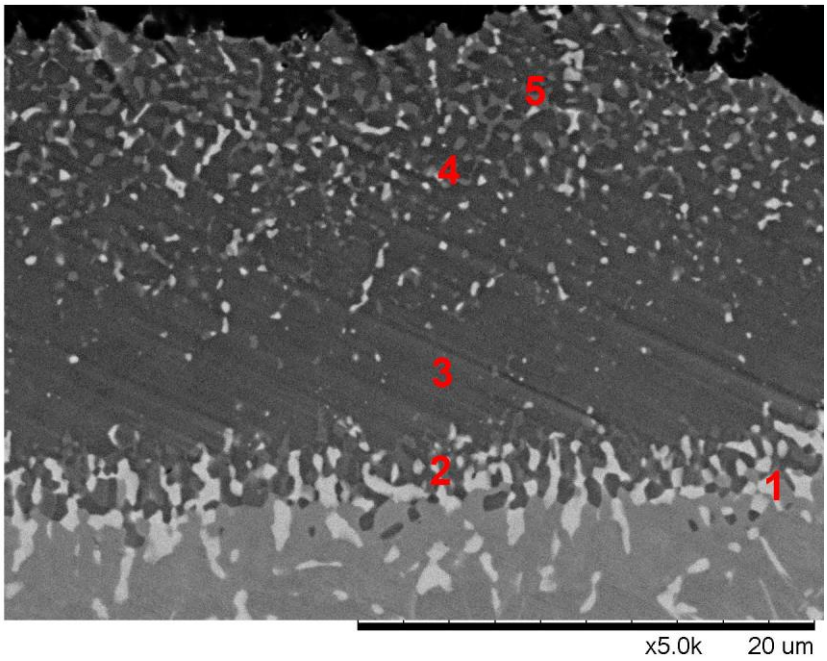

Figure 9.8 : EDS analysis point of 9C24H-A

Point 1 is placed at the carbide phase, and dominant element is nickel. The area is close to inner diffusion zone. Therefore the Cr and Fe contents are high. Point 2 is indented on the σ-(Cr,Fe) phase because Cr, and Fe content are at highest fraction. Point 3 located in the middle diffusion zone; therefore, nickel and aluminum content are very high and their amount close to each other. Further, the other constituent elements distribution is very low at the point because the nickel withdrawal from the substrate (outward diffusion) is lower the amount of elements (etc. Fe, Cr, Nb) in the layer.

Nickel and aluminum content are still dominant and close to each other at the point 4 and 5. Moreover, Fe, Cr and other refractor element contents are high when compare the values with point 3. It indicates that inward diffusion of aluminum let the

refractory elements precipitate. Figure, elemental distribution of the elements also supports the previous assumptions.

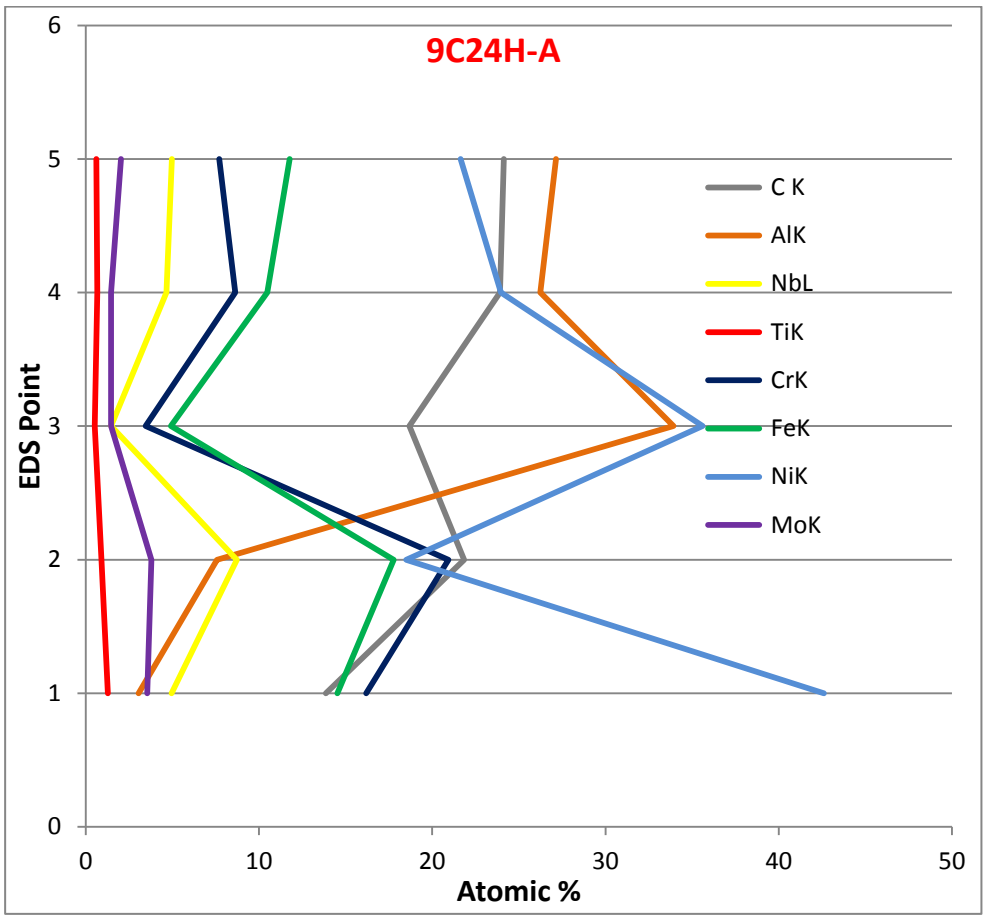

Figure 9.9 : The elemental mapping of 9C24H-A according to related points

The white particles that are seen from SEM image of 9C24H-A, dispersed in the aluminide layer (NiAl) were confirmed to be $M_{23}C_6$ by EDS studies. Due to the elements from the substrate alloy having a low solubility in the aluminide coating, the formation of σ phase also tended to segregate at the coating/substrate interface An EDS analysis of the cross-section of the coating is shown in Figure. This shows that σ phase precipitated in the interdiffusion zone is composed mainly of chromium, and iron. The nickel diffusion causes the formation of σ phase, because nickel cannot solve the element anymore due to reduction in content.

Table 9.1 : 9C24H-A EDS analysis

EDX	NO	Chemical%		
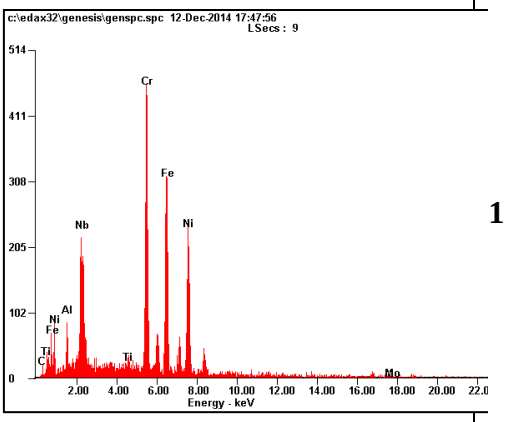	1	***Element***	***Wt %***	***At %***
		C K	03.16	13.86
		AlK	01.56	03.05
		NbL	08.72	04.94
		TiK	01.16	01.28
		CrK	16.00	16.19
		FeK	15.42	14.53
		NiK	47.53	42.61
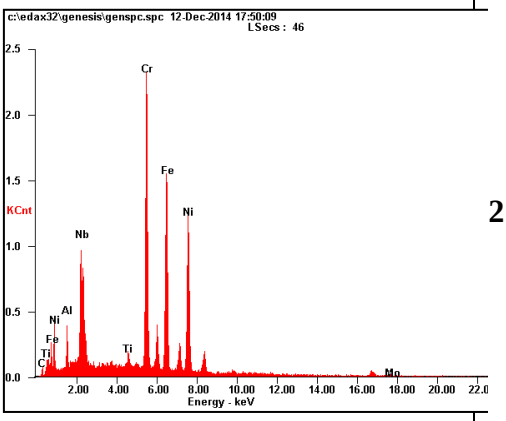	2	***Element***	***Wt %***	***At %***
		C K	00.00	21.84
		AlK	00.00	07.57
		NbL	00.00	08.71
		TiK	00.00	00.90
		CrK	00.00	20.93
		FeK	00.00	17.77
		NiK	00.00	18.50
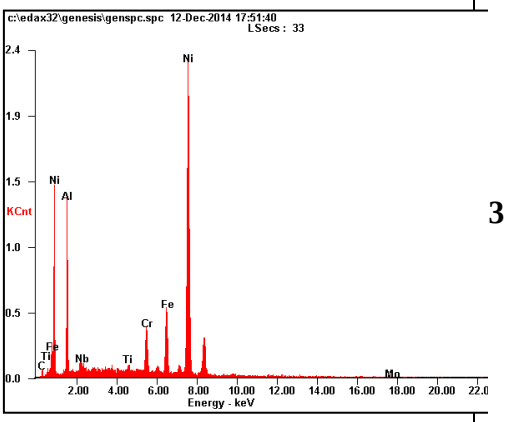	3	***Element***	***Wt %***	***At %***
		C K	00.00	18.68
		AlK	00.00	33.93
		NbL	00.00	01.45
		TiK	00.00	00.51
		CrK	00.00	03.45
		FeK	00.00	04.91
		NiK	00.00	35.61

Table 9.1(continued) : 9C24H-A EDS analysis

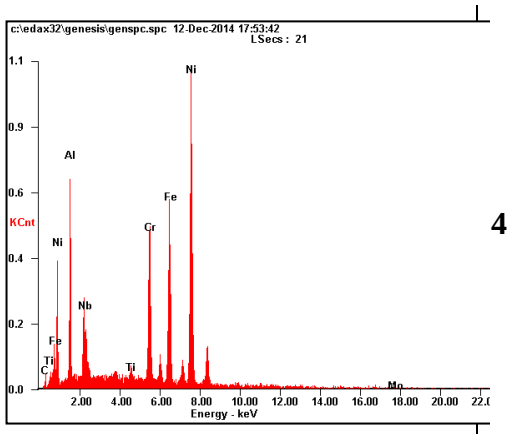

4

Element	*Wt %*	*At %*
C K	00.00	23.91
AlK	00.00	26.24
NbL	00.00	04.66
TiK	00.00	00.67
CrK	00.00	08.62
FeK	00.00	10.48
NiK	00.00	23.96

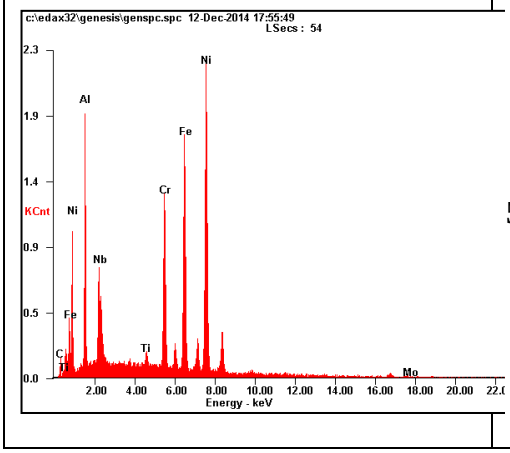

5

Element	*Wt %*	*At %*
C K	00.00	24.14
AlK	00.00	27.15
NbL	00.00	04.96
TiK	00.00	00.60
CrK	00.00	07.71
FeK	00.00	11.77
NiK	00.00	21.63

The point 1 (lower layer) elemental value is close to IN178 composition while the point 2, nickel has lowest atomic fraction, by the way chromium, carbon and iron contents are highest. The composition indicates the outward diffusion of nickel through to coating. The nickel reduction creates carbides and σ phase in the layer.

EDS line analysis of point 5 shows a large amount of aluminum at the top surface, which becomes less at increasing depth from the surface. Until point 3, aluminum and nickel contents dramatically increase. NiAl phase formation on point 3, lower the other elements' amounts because of the inward and outward diffusion of Al and Ni.

Distribution and concentration gradient of nickel and aluminum suggests that nickel atoms diffuse through solid NiAl layer and then dissolve into liquid aluminum at the aluminizing temperature.

It is found that at point 4 and 5; Fe, Cr, Nb, Mo amount increases in the volume fraction of the composition. The presence of the elements indicates that, they have been already there before aluminum diffusion, and they do not change their location.

Therefore, point 5 is the surface of the substrate and it becomes visible by inward diffusion of aluminum. In addition the precipitated islands of first layer (point 5-4) are identified as refractory precipitates (etc., α-Cr, Fe)

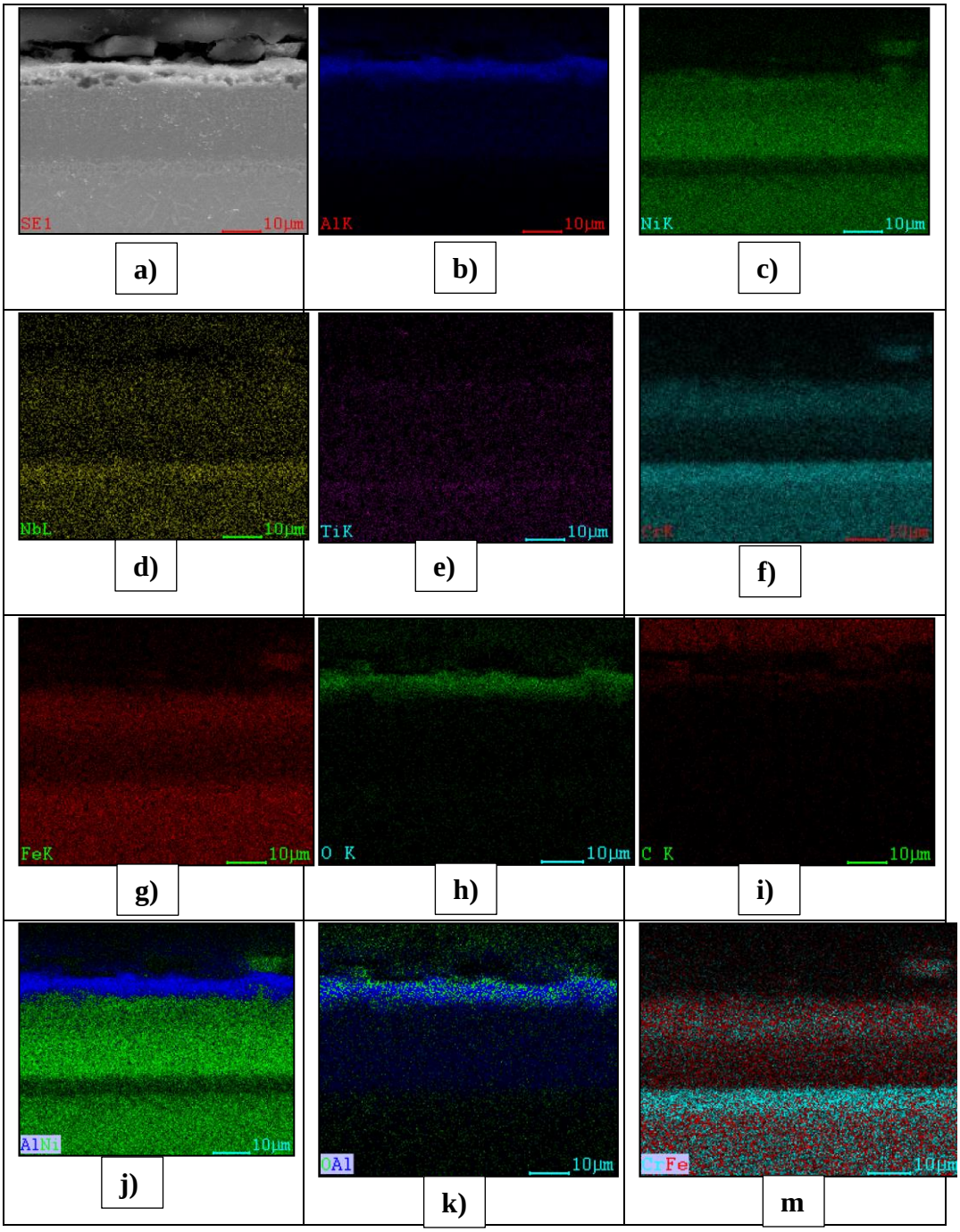

Figure 9.10 : Sample 9C24H-A SEM image and elemental mappings a) SEM image, b) Al distribution c) Ni distribution d) Nb distribution e)Ti distribution f) Cr distribution g) Fe distribution h) O distribution i) C distribution j) Al-Ni distribution k)O-Al distribution m) Fe-Cr distribution on the diffusion zone

Figure 9.10 shows the elemental mapping of the 9C24H-A sample that is annealed at 900°C for 24h. According to SEM image (a) the structure basically include the inward diffusion type of coating. The Coating includes three main zone and according to mapping the zone phases are examined. Image (b) is elemental mapping of aluminum through the coating area and Al elements are accumulated on the surface of the coating. If inner zones are inspected closely, Al distribution can be seen easily, and the distribution shows that the NiAl phase formation when combined with image (c) nickel elemental mapping. Both Ni and Al distribution prove that the NiAl phase is formed in the middle of the zone. The assumption also would be corrected by point analysis of point 3 (Table).

The nickel distribution is low on the inner zone of the coating. This also provides that, Ni diffuse outward of the substrate in order to form NiAl phase. Niobium (d), titanium (e), chrome (f), and iron (g) indicates that, the elements are accumulated in the inner zone. The accumulation proves the formation of σ-(Cr,Fe,Nb,Ti) and MC, M23C6 carbides in the related zone. The formations also confirmed by point 2 analysis.

When look at the upper zone of the coating, Cr (f), Fe (g), Niobium (d), aggregation is observed easily and they create α-(Cr,Fe) phase on the upper layer.

9.5 EDS Analysis Elemental Mapping of 9C24H-AN

The following Figure show the elemental analysis point on the 9C24H-AN. According to the point analysis of Figure, Energy Dispersive X-ray spectroscopy (EDS) and chemical distribution of elements are generated.

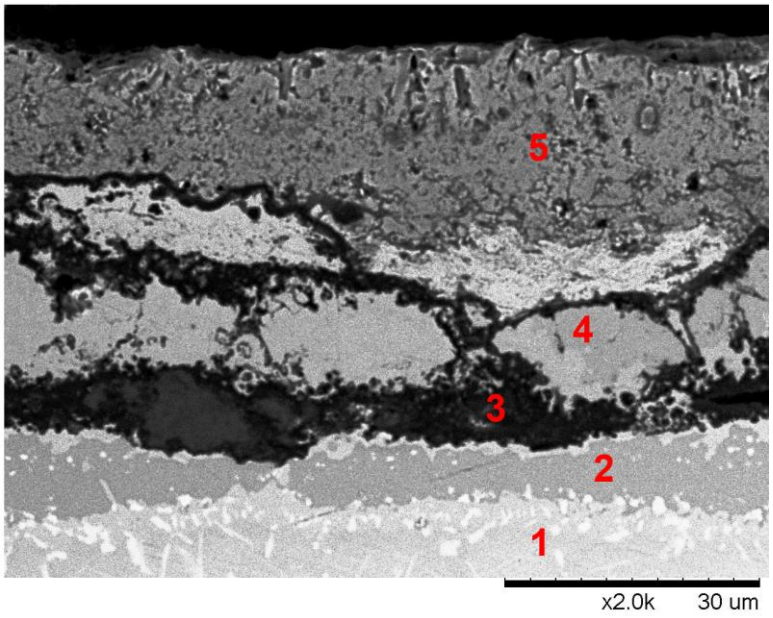

Figure 9.11: EDS analysis point of 9C24H-AN

Point 1 is placed at the IN718 substrate the elemental distribution show the IN718 composition. Point 2 is indented at middle layer of the three-layered structure, therefore Ni, Al contents are close to each other, and they create NiAl phase

The point 3 is located at the detrimental layer which has highest Al level as expected. The point reveal that, aluminum does not consumed completely yet by the nickel and IN718 and the presence is create detrimental, problematic structure as seen from SEM image of 9C24H-AN.

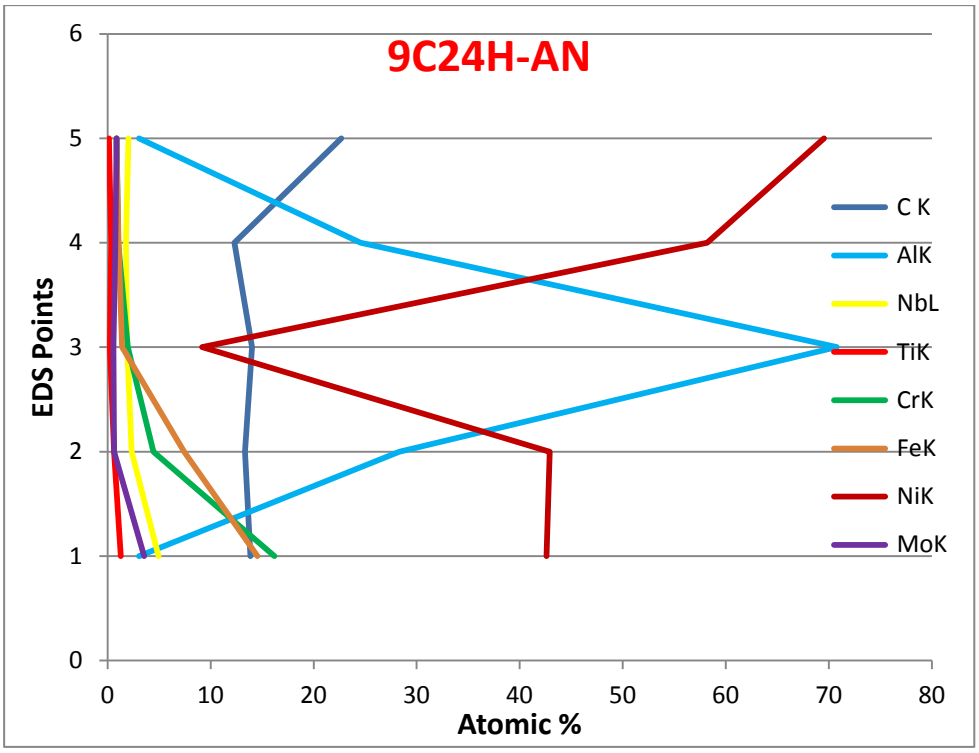

Figure 9.12 : The elemental mapping of 9C24H-AN according to related points

The point 2 is important, in terms of the creation of three-layered structure. In careful looking, the first layer is a refractory precipitation phase; middle layer is AlNi phase; and lower layer is carbide phases. The atomic fraction of the Ni and Al are almost same, and they create AlNi phase.

The three-layered structure proves that i some part of the aluminum is consumed by the coating. The remaining Al is consumed by nickel in order to produce aluminide phases (etc. Ni_3Al). However, Al cannot consume all nickel because of the created aluminide retards the Al diffusion in the Nickel.

The separate consumption of aluminum is led the formation of two different layers, Ni_3Al and three-layered structure, on the substrate surface.

Table 9.2 : EDX analysis of 9C24H-AN

EDX	No	Chemical%

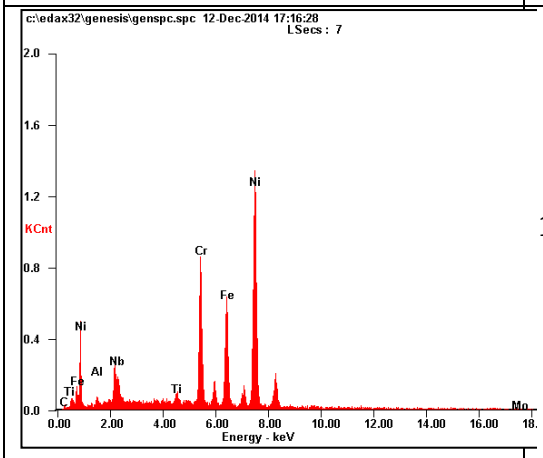

1

Element	Wt %	At %
C K	03.16	13.86
AlK	01.56	03.05
NbL	08.72	04.94
TiK	01.16	01.28
CrK	16.00	16.19
FeK	15.42	14.53
NiK	47.53	42.61

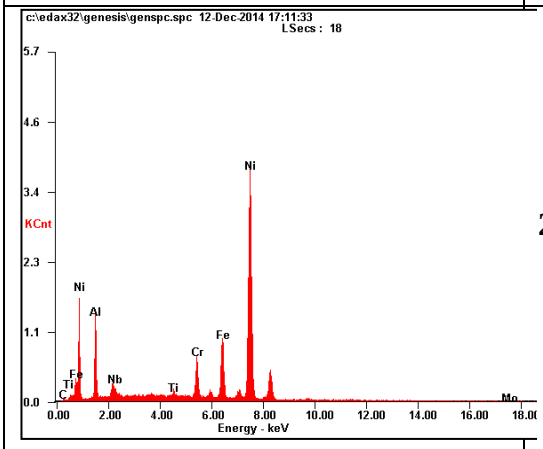

2

Element	Wt %	At %
C K	03.64	13.33
AlK	17.38	28.31
NbL	04.93	02.33
TiK	00.68	00.63
CrK	05.25	04.44
FeK	09.44	07.43
NiK	57.33	42.92

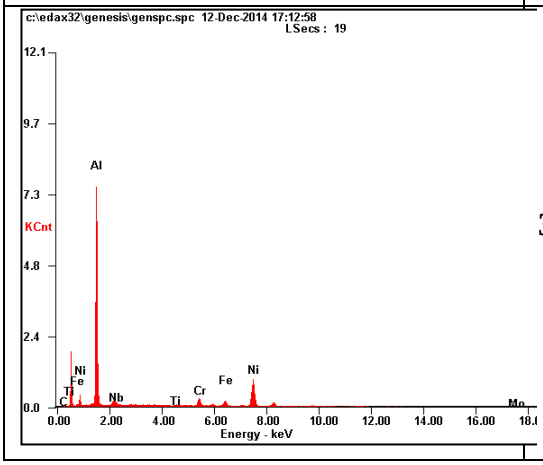

3

Element	Wt %	At %
C K	05.54	14.00
AlK	62.87	70.78
NbL	05.81	01.90
TiK	00.35	00.22
CrK	03.35	01.96
FeK	02.58	01.40
NiK	17.69	09.16

Table 9.2 (continued) : EDX analysis of 9C24H-AN

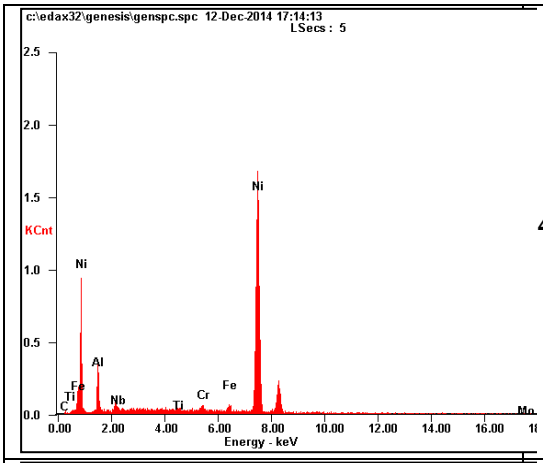

4

Element	*Wt %*	*At %*
C K	03.22	12.32
AlK	14.43	24.56
NbL	03.57	01.76
TiK	00.35	00.33
CrK	01.16	01.02
FeK	01.29	01.06
NiK	74.43	58.20

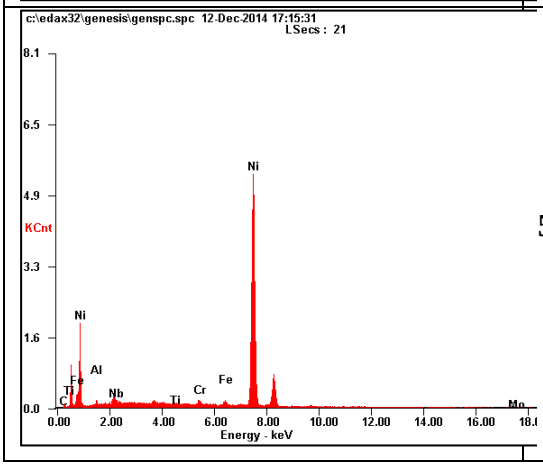

5

Element	*Wt %*	*At %*
C K	05.67	22.67
AlK	01.71	03.05
NbL	03.93	02.03
TiK	00.14	00.14
CrK	00.94	00.87
FeK	00.96	00.83
NiK	84.91	69.53

According to the elemental analysis (Table 9.2), the previous suggestion of nickel presence is supported that can not be fully consumed even though the specimen is annealed at 900°C for 24h. The aluminum presence is explicit on the IN718 and nickel surfaces (Figure, (b)-(c)), and the detrimental structure (void-cracked layer) is almost free of any of elements which is a gap between substrate and Ni.

The three-layered structure shows the similar elemental distribution with 9C24H-A EDS results. The layer contains a high amount of Al and Ni and Cr, Fe, Nb and Ti distributions are support the formation of the coating type. Because there is an accumulation of refractory elements in lower layer of the structure.

The upper structure, created by only Ni and Al, proves the production of aluminide phases. In addition, the Ni distribution is very significant and the absence of other elements at the aluminide layer (next to nickel) expresses diffusion performance of elements they are unable to diffuse throughout the substrate to Nickel layer. Because the aluminide layer and gap, prevent the dispersion of the elements.

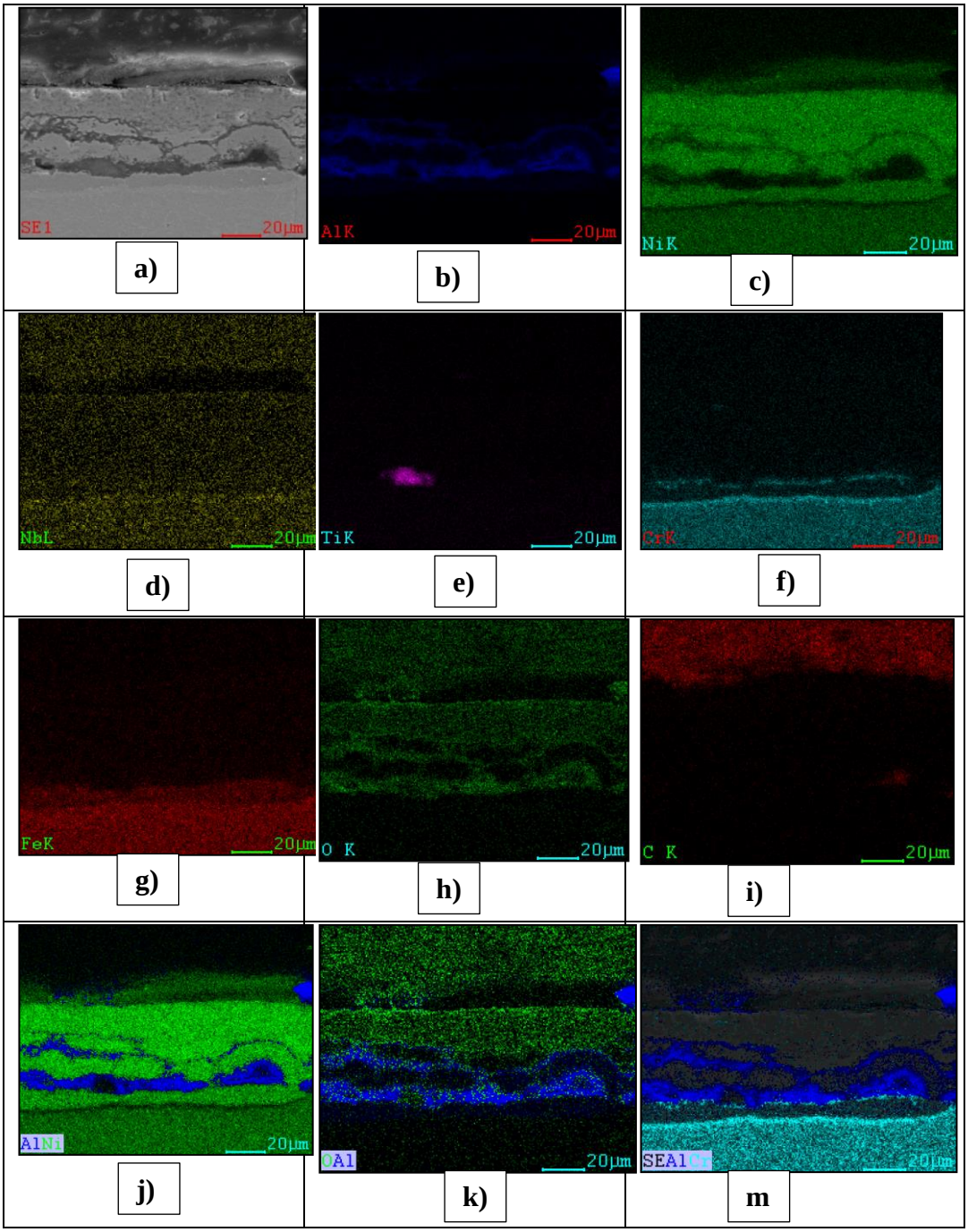

Figure 9.13 : Sample 9C24H-AN SEM image and elemental mappings a) SEM image, b) Al distribution c) Ni distribution d) Nb distribution e)Ti distribution f) Cr distribution g) Fe distribution h) O distribution i) C distribution j) Al-Ni distribution k) O-Al distribution m) Al-Cr distribution on the diffusion zone.

According to Figure9.13, oxygen (h) penetration is obvious throughout the aluminide zone and diffusion zone while carbon (i) generally localized at the upper side of the

nickel and there is sub localization of carbon at the lower the layer of three-layered structure to create carbides.

The most important result of the SEM and EDS analysis is an eagerness of IN718 and nickel to elemental aluminum produce a gap between the structures, because aluminum shows high activity and inward diffusion throughout the substrate and nickel. The gap also proves that there is no outward diffusion either substrate or Ni. Therefore, the void type structure is produced by consumption of aluminum.

9.6 Hardness Test

The 9C24H-A (aluminum coated and annealed at 800C for 24h) sample is subjected to hardness test. The test measurements were conducted on the cross-section of the samples with a Vickers pyramid indenter by utilizing a depth-sensing CSM micro-hardness testers. Test load was 10 g for the hardness measurements and for each layer at least 3 successive measurements were made.

Table 9.3 : The hardness value of 9C24H-A and applied load is 10 g (Vickers)

Layer name	No	Avarage-Hv	1.Hv	2.Hv	3.Hv
A-Cr	1	**817**	850	803	799
B- NiAl	2	**554**	570	531	562
Carbides, σ	3	**860**	824	872	886
IN718	4	**394**	352	408	423

To make a better hardness assumption of the layers (Figure9.14) at least three indentations are run. The generated values (**Table.**) averages are calculated in terms of the arithmetic average. The related sample is 9C24H-A, aluminum coated, and annealed at 900ºC for 24 hour.

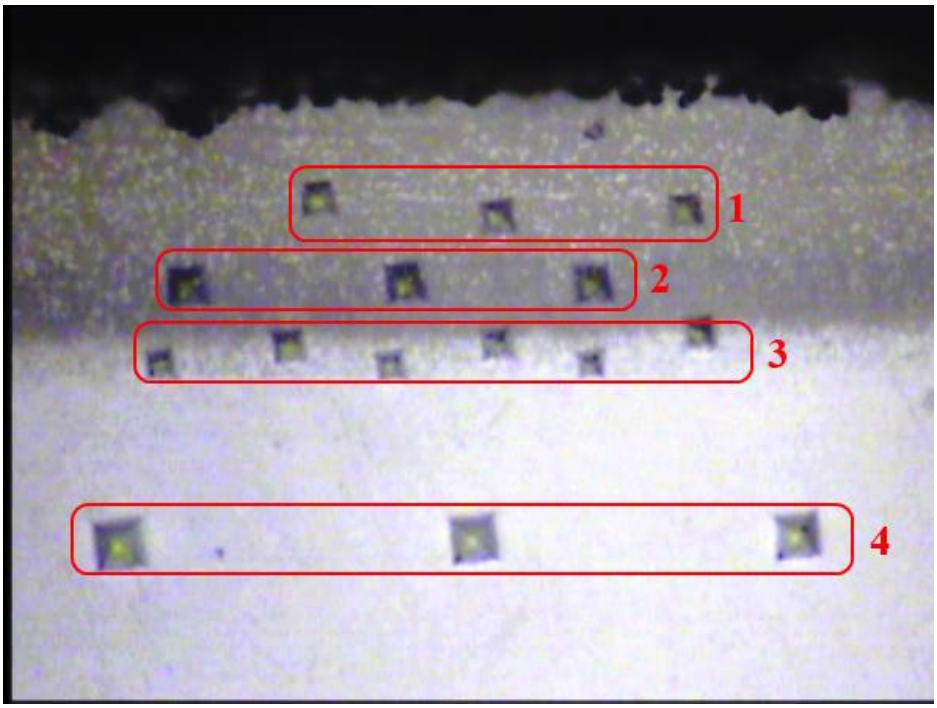

Figure 9.14 : The hardness image of 9C24H-A. The red squares show each coating layers and they are indicated by numbers.

The hardness value of the refractory precipitated layer (upper layer) is 817 Hv as expected, and it is indicated by a "red box 1". The aluminide layer (middle layer-NiAl) has 554 Hv (red box 2) and the lowest. Carbide layer (red box 3) has 860 Hv. The substrate (red box 4) has 397 Hv as espected.

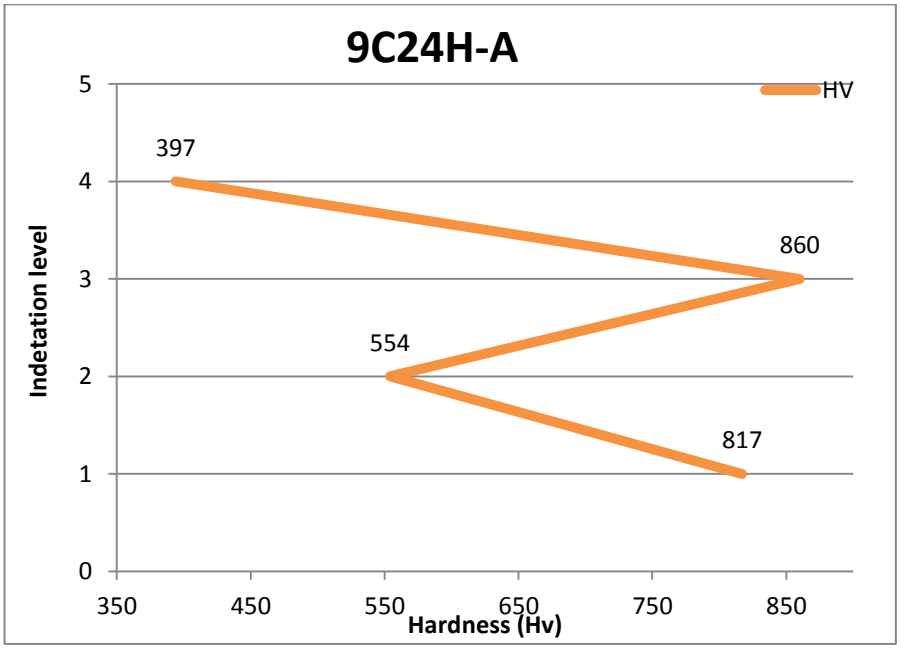

Figure 9.15 : The Vickers hardness of 9C24H-A according to indentation levels in red square

The hardness results reveal the hardest and brittle layers are precipitated layer (upper layer), and carbide layer (red box 3). The aluminide layer (middle layer-NiAl) hardness is lower and than the layers. However it indicates the ductile structure.

10 CONCULUSION

The study is related with the aluminum and the aluminum+nickel coating of the IN718 and the diffusion mechanism of aluminum and nickel. In terms of the completed study, the following results are revealed.

- The samples, annealed below the aluminum melting temperature (640°C) at 500°C 600°C for 24 hours, show the formation of Al_3Ni and Al_3Ni_2 phases on the substrate surface. Although, aluminum does not totally consumed at 500°C, the Al volume fraction become reduced by the fragmented distribution of Al_3Ni phases in the 6C24H-A, while Al_3Ni_2 phase is spread along the substrate as monolithic formation.
- The samples annealed at 700°C -850°C -900°C-950°C -1000°C and 1050°C at different time, let the formation of a coating, which includes three distinct zones (three-layered structure). The first, upper zone of the coating, aluminum has a extremely high activity and the zone matrix of the AlNi aluminum content is very high, therefore, β phase cannot solve the refractory elements, and they become precipitate. The middle zone is formed by both aluminum and nickel diffusion because of, there is a uniform AlNi area. Nickel diffusion (outward diffusion) at the lowest zone is resulted in the formation of carbides and σ-phases because there is no enough nickel in order to solve Cr or other elements, and they become transformed to the carbide and σ-phases.
- There are no cracks or voids in the coating, and the bonding between the coating and substrates is strong at the aluminum-coated samples.
- ε(Al_3Ni), and δ(Al_3Ni_2) phases involve almost singular aluminum diffusion while the opposite, virtually singular nickel diffusion occurs during the formation of the β(AINi), and γ'($AlNi_3$) phases.

- NiAl phase is a solid solution with Cr and Fe dissolved. However, the solubility limit of most elements in superalloys, such as Cr, Mo, Nb in NiAl phase, is very low therefore; the aluminide layer contains fine precipitates in a matrix of NiAl.
- The formation of σ phase also tended to segregate at the coating/substrate interface, due to the elements from the substrate alloy having a low solubility in the aluminide coating,
- In the high-activity process, the coating growth takes place primarily by inward diffusion initially at the upper layer, followed by an intermediate stage where the growth involves both inward Al and outward Ni diffusion (middle layer-aluminide). In the final stages, the outward diffusion of Ni dominates the coating formation (lowest layer-Carbides).
- The aluminum and nickel coated samples are annealed at 850°C -900°C-950°C -1000°C and 1050°C for different annealing time. According to the SEM image, XRD and EDS results, a gap is produced between substrate and nickel, by the absence of aluminum, which shows high activity. By the way, inward diffusion takes place at substrate and nickel. The gap also proves that there is no outward diffusion from either substrate or Ni and the gap is produced by consumption of aluminum.
- A produced nickel aluminide layer prevents liquid aluminum from spreading, therefore, cannot cover the entire surface of nickel. That is an explanation of nickel presence on the top of the coating, although the annealing temperature rises.
- The Al and Ni coated samples have cracked type void structure. Therefore, bonding between substrate and coating is very weak.
- The refractory precipitates (upper layer) and carbide zone (lowest layer) have a high hardness value and brittle feature due to refractory precipitates, and carbides. Due to the detrimental effect of the layers, they must be eliminated to prevent the spallation of coating from the layers.
- The diffusion of aluminum in IN718 shows the non steady state diffusion, however, aluminum flux is not abundant (not infinite) on the substrate surface.

REFERENCES

[1] **A. J. A. Mom,** (2013), 1 - Introduction to gas turbines, in *Modern Gas Turbine Systems*, P. Jansohn, Ed. Woodhead Publishing, pp. 3–20.

[2] **S. Bose,** (2007), *High temperature coatings*. Amsterdam; Boston: Elsevier Butterworth-Heinemann.

[3] **Y. Tamarin and ASM International**, (2002). *Protective coatings for turbine blades*. Materials Park, Ohio: ASM International.

[4] **M. P. Boyce,** (2012). 1 - An Overview of Gas Turbines, in *Gas Turbine Engineering Handbook (Fourth Edition)*, M. P. Boyce, Ed. Oxford: Butterworth-Heinemann, pp. 3–88.

[5] **J. H. Horlock,** (2003). Chapter 1 - A brief review of power generation thermodynamics, in *Advanced Gas Turbine Cycles*, J. H. Horlock, Ed. Oxford: Pergamon, pp. 1–11.

[6] **E. Benini**, (2011). *Advances in gas turbine technology*. Rijeka: InTech.

[7] **A. Advanced Metallurgical Group N.V. - Innovation**, "Titanium Aluminide." http://www.amg-nv.com/Innovation/Titanium-Aluminide/default.aspx.

[8] **C. Soares,** (2008). 3 - Gas Turbine Configurations and Heat Cycles, in *Gas Turbines*, C. Soares, Ed. Burlington: Butterworth-Heinemann, pp. 67–118.

[9] **Department of Energy**, How Gas Turbine Power Plants Work, http://energy.gov/fe/how-gas-turbine-power-plants-work

[10] **M. P. Boyce,** (2012), Gas turbine engineering handbook, 4th ed. Amsterdam ; Boston: *Elsevier/Butterworth-Heinemann*.

[11] **J. Arnold and W. Blake,** (2005)"Method for forming a wear-resistant hard-face contact area on a workpiece, such as a gas turbine engine part," US20050152805 A1.

[12] **P.W. Schilke,** (2004)"Advanced Gas Turbine Materials and Coatings, Handbook of tribology: materials, coatings, and surface treatments," GE Energy General Electric Company, Schenectady, NY, GER-3569G.

[13] **R. Zimmerman, J. Evans, and R. Viguie,** (2007)"Bond coat process for thermal barrier coating," US20070207339 A1.

[14] **R. Darolia**, (2006)"Bond coat for a thermal barrier coating system," EP0985745 B1.

[15]Turbine Blade Alloys. http://www.grc.nasa.gov/WWW/StructuresMaterials/AdvMet/research/turbine_blades.html

[16] M. Konter and H.-P. Bossmann, (2013)"9 - Materials and coatings developments for gas turbine systems and components," in *Modern Gas Turbine Systems*, P. Jansohn, Ed. Woodhead Publishing, pp. 327–381e.

[17] C. T. Sims, N. S. Stoloff, and W. C. Hagel, (1987) "*Superalloys II"*, 2 edition. New York: Wiley-Interscience.

[18] B. Geddes, H. Leon, and X. Huang, (2010) *Superalloys alloying and performance*. Materials Park, Ohio: ASM International.

[19] P. M. L. Weaver, (2007) "MTE585-High Temperature Coating-Iron and Nickel Based Superalloys." Department of Metallurgical and Materials Engineering, The University of Alabama.

[20] J. E. Watson, (2011) *Superalloys production, properties, and applications*. New York: Nova Science Publishers.

[21] M. J. Donachie, (2002) *Superalloys: a technical guide*, 2nd ed. Materials Park, OH: ASM International.

[22] S. Wöllmer, S. Zaefferer, M. Göken, T. Mack, and U. Glatzel, (2003)"Characterization of phases of aluminized nickel base superalloys," *Surf. Coat. Technol.*, vol. 167, no. 1, pp. 83–96.

[23] J. R. Davis, (2001) *Alloying understanding the basics*. Materials Park, OH: ASM International.

[24] D. Coutsouradis, A. Davin, and M. Lamberigts, (1987)"Cobalt-based superalloys for applications in gas turbines," *Mater. Sci. Eng.*, vol. 88, pp. 11–19.

[25] J. R. Davis, Ed., (2001) *Alloying: understanding the basics*. Materials Park, OH: ASM International.

[26] P. M. L. Weaver, (2007) "MTE585-High Temperature Coating- Cobalt based Superalloys." Department of Metallurgical and Materials Engineering, The University of Alabama.

[27] I. Dul, (2013) "Application and processing of nickel alloys in the aviation industry," *Weld. Int.*, vol. 27, no. 1, pp. 48–56.

[28] R. C. Reed, (2006)*The superalloys fundamentals and applications*. Cambridge, UK; New York: Cambridge University Press.

[29] R. DidomizioO, J. S. Marte, and P. R. Subramanian, (2012)"Nickel alloy and articles," EP2412833 A2.

[30] R. E. Smallman and A. H. W. Ngan, (2007)"Chapter 8 - Advanced alloys," in *Physical Metallurgy and Advanced Materials Engineering (Seventh Edition)*, R. E. Smallman and A. H. W. Ngan, Eds. Oxford: Butterworth-Heinemann, pp. 447–480.

[31]Nickel Alloy Inconel 718 "Properties and Applications by United Performance Metals." http://www.azom.com/article.aspx?ArticleID=4459.

[32] F. Farinia Group, "Why choosing Inconel 718 for Aerospace Additive Manufacturing| Farinia Group." http://www.farinia.com/additive-manufacturing/3d-materials/inconel-718-aerospace-additive-manufacturing

[33] S.-H. Chang, S.-C. Lee, T.-P. Tang, H.-H. Ho, and others, (2006) "Influences of soaking time in hot isostatic pressing on strength of Inconel 718 superalloy," *Mater. Trans.*, vol. 47, no. 2, pp. 426–432.

[34] J. R. Davis, (1997) *ASM Specialty Handbook: Heat-Resistant Materials*. ASM International.

[35] X. Zhao, J. Chen, X. Lin, and W. Huang, (2008) "Study on microstructure and mechanical properties of laser rapid forming Inconel 718," *Mater. Sci. Eng. A*, vol. 478, no. 1–2, pp. 119–124, Apr. .

[36] V. L. Tellkamp, M. L. Lau, A. Fabel, and E. J. Lavernia, (1997) "Thermal spraying of nanocrystalline inconel 718," *Nanostructured Mater.*, vol. 9, no. 1–8, pp. 489–492.

[37]INCONEL alloy 718, *http://www.specialmetals.com*, http://www.specialmetals.com/documents/Inconel%20alloy%20718.pdf.

[38] C. Söderström and L. Almström, (2010) "Alternative materials for hightemperature and high-pressure valves," Karlstads universitet, 651 88 Karlstad.

[39] J. R. Davis, (2000) *Nickel, Cobalt, and Their Alloys*. ASM International.

[40] P. W. Schilke, (2004)"ADVANCED GAS TURBINE MATERIALS AND COATING," Schenectady, NY, GER-3569G.

[41] F. C. Campbell, (2006) Manufacturing technology for aerospace structural materials. Amsterdam; Boston: Elsevier.

[42] W. Tabakoff, (1992). High temperature erosion resistance of coatings for use in gas turbine engines, *Surf. Coat. Technol.*, vol. 52, no. 1, pp. 65–79.

[43] D. R. Clarke, M. Oechsner, and N. P. Padture, (2012).Thermal-barrier coatings for more efficient gas-turbine engines,*MRS Bull.*, vol. 37, no. 10, pp. 891–898.

[44] B. Nagaraj, B. Boutwell, and R. Baur, (2005) Thermal barrier coating protected by alumina and method for preparing same, US20050129862 A1.

[45] J. Pfaendtner, J. Rigney, R. Darolia, R. Corderman, and R. Nardi, (2003). Protective overlay coatings of superalloy substrates for use in high-temperature environments comprising a beta-phase nickel aluminide intermetallic with 1-4% hafnium; gas turbine engine components; spalling, oxidation and heat resistance, US20030134139 A1.

[46]Wadley Research Group - UVA.http://www.virginia.edu/ms/research/wadley/high-temp.html. [Accessed: 07-Dec-2014].

[47] Z. Yu, D. D. Hass, and H. N. G. Wadley, (2005). NiAl bond coats made by a directed vapor deposition approach, *Mater. Sci. Eng. A*, vol. 394, no. 1–2, pp. 43–52, Mar. .

[48] S. Sōmiya, (2013). Handbook of advanced ceramics*: materials, applications, processing, and properties.*

[18] **Committee on Coatings for High-Temperature Structural Materials** (1996). Coatings for High-Temperature Structural Materials: Trends and Opportunities, *National Academy Press.*

[50] J. R. Nicholls, K. A. Long, and N. J. Simms, (2010). 4.05 - Diffusion Coatings, in *Shreir's Corrosion*, B. C. G. L. L. R. S. Stott, Ed. Oxford: Elsevier, , pp. 2532–2555.

[51] R. Pflumm, S. Friedle, and M. Schütze, (2015). Oxidation protection of γ-TiAl-based alloys – A review, *Intermetallics*, vol. 56, pp. 1–14.

[52] R. Chattopadhyay, (2004) Advanced thermally assisted surface engineering processes, *Boston: Kluwer Academic.*

[53] N. Voudouris, C. Christoglou, and G. N. Angelopoulos, (2001). Formation of aluminide coatings on nickel by a fluidised bed CVD process, *Surf. Coat. Technol.*, vol. 141, no. 2–3, pp. 275–282.

[54] C.-J. Wang and S.-M. Chen, (2006) Microstructure and cyclic oxidation of hot dip aluminized coating on Ni-base superalloy Inconel 718, *Surf. Coat. Technol.*, vol. 201, no. 7, pp. 3862–3866.

[35] Prof. Mark L. Weaver, (2007) MTE585 Coatıngs For Superalloys, *The University of Alabama (Tuscaloosa, AL).*

[56] J. J. Liang, H. Wei, Y. L. Zhu, T. Jin, X. F. Sun, and Z. Q. Hu, (2012) Phase stabilities in a NiCrAlYRe coating alloy, *Surf. Coat. Technol.*, vol. 206, no. 11–12, pp. 2746–2750.

[57] J. R. Nicholls, N. J. Simms, W. Y. Chan, and H. E. Evans, (2002) Smart overlay coatings—concept and practice, *Surf. Coat. Technol.*, vol. 149, no. 2, pp. 236–244.

[58] E. Bahadori, S. Javadpour, M. H. Shariat, and F. Mahzoon, (2013) Preparation and properties of ceramic Al2O3 coating as TBCs on MCrAly layer applied on Inconel alloy by cathodic plasma electrolytic deposition, *Surf. Coat. Technol.*, vol. 228, pp. S611–S614.

[59] S. Bose, (2007) Chapter 7 - Thermal Barrier Coatings, in *High temperature coatings*, Amsterdam ; Boston: Elsevier Butterworth-Heinemann.

[60] G. . Goward, (1998) Progress in coatings for gas turbine airfoils, *Surf. Coat. Technol.*, vol. 108–109, pp. 73–79, Oct. .

[61] K. J. Hemker, B. G. Mendis, and C. Eberl, (2008) "Characterizing the microstructure and mechanical behavior of a two-phase NiCoCrAlY bond coat for thermal barrier systems," *Mater. Sci. Eng. A*, vol. 483–484, pp. 727–730.

[62] C. B. Meher-Homji and G. A. Gabriles, (1998) Gas Turbine Blade Failures—Causes, Avoidance, and Troubleshooting, in *Twenty-Seventh Turbomachinery Symposium, Houston, TX*, pp. 22–24.

[63] R. C. Reed, (2006) 5. Environmental Degradation The Role of Coatings," in *The superalloys fundamentals and applications*, Cambridge, UK; New York: Cambridge University Press.

[64] M. Zielińska, M. Zagula-Yavorska, J. Sieniawski, and R. Filip, (2013) Microstructure and Oxidation Resistance of an Aluminide Coating on the Nickel Based Superalloy Mar M247 Deposited by the CVD Aluminizing Process, *Arch. Metall. Mater.*, vol. 58, no. 3.

[65] Stephen J. Balsone, (2010) 4.4.1 Buckets and Nozzles," GE Gas Turbines LLC, P.O. Box 648; GTTC 174D Greenville, SC 29602.

[66] N. Saunders, (1996) Phase diagram calculations for Ni-based superalloys," *ROLLS ROYCE PLC-Rep.-PNR*.

[67]Al-Ni phase diagram, (2008) *The University of Western Ontario Department of Physics and Astronomy*.

[68] W. Huang and Y. A. Chang, (1998) A thermodynamic analysis of the Ni-Al system," *Intermetallics*, vol. 6, no. 6, pp. 487–498.

[69] H. Y. Kim, D. S. Chung, and S. H. Hong, (2005) Reaction synthesis and microstructures of NiAl/Ni micro-laminated composites, *Mater. Sci. Eng. A*, vol. 396, no. 1–2, pp. 376–384.

[70] D. Gupta, Ed., (2005) Diffusion Processes in Advanced Technological Materials, 2005 edition. Norwich, N.Y.: Springer.

[71] K. Fujiwara and Z. Horita, (2002) Measurement of intrinsic diffusion coefficients of Al and Ni in Ni3Al using Ni/NiAl diffusion couples," *Acta Mater.*, vol. 50, no. 6, pp. 1571–1579.

[72] G. W. Goward and D. H. Boone, (1971) Mechanisms of formation of diffusion aluminide coatings on nickel-base superalloys, *Oxid. Met.*, vol. 3, no. 5, pp. 475–495.

[73] M. Zielińska, J. Sieniawski, M. Yavorska, and M. Motyka, (2011) Influence of Chemical Composition of Nickel Based Superalloy on the Formation of Aluminide Coatings, *Arch. Metall. Mater.*, vol. 56, no. 1.

[74] X. Montero, M. C. Galetz, and M. Schütze, (2013) Low-activity aluminide coatings for superalloys using a slurry process free of halide activators and chromates," *Surf. Coat. Technol.*, vol. 222, pp.

[75] M. Kutz, (2012) Handbook of environmental degradation of materials. Waltham, MA: William Andrew, .

[76] A. K. Koul, (1994) Advances in High Temperature Structural Materials and Protective Coatings, *National Research Council of Canada.*

[77] M. F. Smith, (2007) 3 - Comparing cold spray with thermal spray coating technologies, in *The Cold Spray Materials Deposition Process*, V. K. Champagne, Ed. Woodhead Publishing, pp. 43–61.

[78] A. P. Alkhimov, A. N. Papyrin, V. F. Kosarev, N. I. Nesterovich, and M. M. Shushpanov, (1994) Gas-dynamic spraying method for applying a coating, US5302414 A.

[79] J.R. Davis & Associates, ASM International, and Thermal Spray Society Training Committee, (2004) Handbook of thermal spray technology. *Materials Park, OH: ASM International.*

[80] Yu Zou, (2010) Microstructural Studies of Cold Sprayed Pure Nickel, Copper And Aluminum Coatings, *Department of Mining and Materials Engineering*, McGill University, Montreal.

[81] K. Ogawa and D. Seo, (2011) Repair of turbine blades using cold spray technique," *Adv. Gas Turbine Technol. Benini E*.

[82] A. Gouldstone, W. B. Choi, W. Chi, Y. Wu, and S. Sampath, (2007) 13 - Mechanical, thermal and electrical properties of cold sprayed coatings," in *The Cold Spray Materials Deposition Process*, V. K. Champagne, Ed. Woodhead Publishing, pp. 245–263.

[83] V. K. Champagne, (2007) The Cold Spray Materials Deposition Process: Fundamentals and Applications. *Elsevier*.

[84] A. Papyrin, (2007) 2 - The development of the cold spray process, in *The Cold Spray Materials Deposition Process*, V. K. Champagne, Ed. Woodhead Publishing, pp. 11–42.

[85] A. Papyrin, V. Kosarev, S. Klinkov, A. Alkhimov, and V. M. Fomin, (2006) Cold spray technology. *Elsevier*.

[86] Y. Li, C.-J. Li, G.-J. Yang, and L.-K. Xing, (2010) Thermal fatigue behavior of thermal barrier coatings with the MCrAlY bond coats by cold spraying and low-pressure plasma spraying, *Surf. Coat. Technol.*, vol. 205, no. 7, pp. 2225–2233.

[87] F. J. Brodmann, (2007) 6 - Cold spray process parameters: powders," in *The Cold Spray Materials Deposition Process*, V. K. Champagne, Ed. Woodhead Publishing, pp. 105–116.

[88] D. K. Das, S. V. Joshi, and V. Singh, "Evolution of aluminide coating microstructure on nickel-base cast superalloy CM-247 in a single-step high-activity aluminizing process," *Metall. Mater. Trans. A*, vol. 29, no. 8, pp. 2173–2188, Aug. 1998.

[89] Z. Balogh and G. Schmitz, "5 - Diffusion in Metals and Alloys," in *Physical Metallurgy (Fifth Edition)*, D. E. L. Hono, Ed. Oxford: Elsevier, 2014, pp. 387–559.

[90] W. D. Callister, *Materials science and engineering: an introduction*. New York: John Wiley & Sons, 2007.

[91] H. Dinc, A. Motellabzadeh, H. Cimenoglu, and M. Baydogan, (2013). Thermochemical Boriding of Inconel 718 Superalloy, *Academic Journal of Science*

CURRICULUM VITAE

Name Surname: Selda NAYIR

Place and Date of Birth: Konya 02.01. 1985

E-Mail:snayir@itu.edu.tr

EDUCATION:

B.Sc.: Anadolu University Materials Science and Engineering